



Alejandra Daniela Delgado Vallejo

**Electrokinetic remediation for sediments of
Camorim Lagoon**

Tese de Doutorado

Thesis presented to the Programa de Pós-graduação em Engenharia Civil of PUC-Rio in partial fulfillment of the requirement for the degree of Doutor em Engenharia Civil

Advisor: Jose Tavares Araruna Junior
Co-advisor: Rodrigo Fernandes de Magalhães de Souza

Rio de Janeiro
October 2024



Alejandra Daniela Delgado Vallejo

**Electrokinetic remediation for sediments of
Camorim Lagoon**

Thesis presented to the Programa de Pós-graduação em Engenharia Civil of PUC-Rio in partial fulfillment of the requirement for the degree of Doutor em Engenharia Civil. Approved by Examination Committee.

Prof. Jose Tavares Araruna Junior
Advisor

Departamento de Engenharia Civil-PUC-Rio

Prof. Rodrigo Fernandes de Magalhães de Souza
Co-advisor

Departamento de Engenharia Química e de Matérias-PUC-Rio

Prof. Patricio José Moreira Pires
Departamento de Engenharia Civil-UFES

Prof. André Bezerra dos Santos
Departamento de Engenharia Ambiental e Sanitária-UFC

Prof. Elvis Carissimi
Departamento de Engenharia Sanitária e Ambiental-UFSM

Prof. Rodrigo Araújo Gonçalves
Departamento de Química-PUC-Rio

Rio de Janeiro, October 16th, 2024

All rights reserved. The reproduction, in whole or in part, of this work is prohibited without the authorization of the university, the author, and the advisor.

Alejandra Daniela Delgado Vallejo

Graduated in Petroleum Engineering at the Universidad Nacional de Colombia in 2015 and obtained her M.Sc Degree in Environment and Development from the Universidad Nacional de Colombia in 2018

Delgado Vallejo, Alejandra Daniela

Electrokinetic remediation for sediments of Camorim Lagoon / Alejandra Daniela Delgado Vallejo; advisor: Jose Tavares Araruna Junior; co-advisor: Rodrigo Fernandes de Magalhães de Souza. – 2024.

96 f. : il. color. ; 30 cm

Tese (doutorado)–Pontifícia Universidade Católica do Rio de Janeiro, Departamento de Engenharia Civil e Ambiental, 2024.

Inclui bibliografia

1. Engenharia Civil e Ambiental - Teses. 2. Remediação eletrocinética. 3. Elementos potencialmente tóxicos. 4. Sedimento dragado. 5. Controle de pH. I. Araruna Junior, Jose Tavares. II. Souza, Rodrigo Fernandes de Magalhães de. III. Pontifícia Universidade Católica do Rio de Janeiro. Departamento de Engenharia Civil e Ambiental. IV. Título.

CDD:

624

To my parents, brother, husband and friends, for their support and
encouragement

Acknowledge

This study was financed in part by the Coordenação de Aperfeiçoamento de Pessoal de Nível Superior - Brasil (CAPES) - Finance Code 001.

This is a tribute to the numerous people who have helped me evolve in my research and personal life.

I would like to express my sincere gratitude to CAPES for awarding me the scholarship that made this research possible.

I would like to express my gratitude to the Graduate Program in Civil Engineering at PUC-Rio for the opportunity to conduct this research. I am also deeply thankful to all the professors of university.

I would also like to thank all the staff members in the departments of Civil Engineering and Chemical for their constant attentiveness and patience. I am especially grateful to Edson, Amaury, Carlos, Josué, Mauricio, Luana, and Sandra.

I would like to express my deepest gratitude to my advisor, José Araruna, for his invaluable guidance throughout my doctoral studies and personal journey. His advice, encouragement, and insightful conversations have been instrumental in my development. I am particularly grateful for his calm demeanor and objective perspective, which have been invaluable in guiding my research.

I am grateful to my co-advisor, Rodrigo Souza, for his knowledge and expertise.

To my dear friends who shared this incredible journey: Cristian, Melissa, Bárbara, Paula, Alex, Lara, Gabrielle, Julia.

I would like to express my deepest gratitude to my family, Manuel Delgado, Amparo Vallejo, Manuel F Delgado, Cristhian Morales for their unwavering support throughout this journey. Your sacrifices, love, and investments have fueled my determination.

I am also thankful to everyone who has been a part of this experience.

Abstract

Delgado Vallejo, Alejandra Daniela; Araruna, Junior Jose Tavares (advisor). **Electrokinetic remediation for sediments of Camorim Lagoon**. Rio de Janeiro, 2024. 96p. Doctoral thesis. Postgraduate Program in Civil Engineering, Pontifical Catholic University of Rio de Janeiro

Electrokinetic remediation, effective for low-permeability sediments, can simultaneously remove both organic and inorganic contaminants. This study investigated its application to dredged sediments from Camorim Lagoon (Jacarepaguá lagoon complex, Rio de Janeiro), known to be contaminated with potentially toxic metals (chromium, copper, lead, zinc, and nickel). A buffer solution-controlled pH changes, while the complexing agent ethylenediaminetetraacetic acid (EDTA) and humic substances facilitated metal desorption and removal. Treatments utilizing EDTA (EK2 and EK3) achieved lower final concentrations of zinc and lead. Notably, EK1 (freshwater only) achieved the lowest nickel concentration observed in the anodic section. EK1 also achieved the lowest copper concentration; however, none of the treatments reached regulatory limits for copper. Chromium, being the least mobile metal, accumulated in the middle section for all treatments. Electrokinetic remediation demonstrated significant variability in the effectiveness of the evaluated electrolytes, depending on the specific contaminant element present in the dredged sediments.

Keywords

Electrokinetic remediation; potentially toxic elements; dredged sediment; pH control

Resumo

Delgado Vallejo, Alejandra Daniela; Araruna, Junior Jose Tavares (orientador). **Remediação eletrocinética de sedimentos da Lagoa de Camorim**. Rio de Janeiro, 2024. 96p. Tese de doutorado. Programa de pós-graduação em engenharia Civil, Pontifca Universidade Católica do Rio de Janeiro.

A remediação eletrocinética, eficaz para sedimentos de baixa permeabilidade, pode remover simultaneamente contaminantes orgânicos e inorgânicos. Este estudo investigou sua aplicação em sedimentos dragados da Lagoa de Camorim (complexo lagunar de Jacarepaguá, Rio de Janeiro), conhecido por estar contaminado com metais potencialmente tóxicos (cromo, cobre, chumbo, zinco e níquel). Uma solução tampão controlou as mudanças de pH, enquanto o agente complexante ácido etilenodiaminotetraacético (EDTA) e substâncias húmicas facilitaram a dessorção e remoção de metais. Tratamentos utilizando EDTA (EK2 e EK3) alcançaram concentrações finais mais baixas de zinco e chumbo. Notavelmente, EK1 (apenas água) alcançou a menor concentração de níquel observada na seção anódica. EK1 também alcançou a menor concentração de cobre; no entanto, nenhum dos tratamentos atingiu os limites regulatórios para cobre. O cromo, sendo o metal menos móvel, acumulou-se na seção do meio para todos os tratamentos. A remediação eletrocinética demonstrou uma variabilidade significativa na eficácia dos eletrólitos avaliados, dependendo do elemento contaminante específico presente nos sedimentos dragados.

Palavras-chave

Remediação eletrocinética; elementos potencialmente tóxicos; sedimento dragado; controle de pH.

Summary

1. Introduction	14
2. Study site	17
3. Theoretical framework	34
3.1. Electrokinetic remediation	34
4. Methodology	44
4.1. Sediments physical and chemical characterization tests	44
4.2. Electrokinetic materials	45
4.3. Electrokinetic treatments	48
4.3.1. Nomenclature of electrolytes	48
4.3.2. Sediment nomenclature	49
5. Results and discussion	51
5.1. Sampling location	51
5.2. Geotechnical characterization	52
5.3. Chemical characterization	54
5.4. Mineral characterization	55
5.5. Electrokinetic test	57
5.5.1. pH	57
5.5.2. Electric conductivity	61
5.5.3. Concentration of potentially toxic substance	66
5.5.4. Electric current	79
6. Conclusions and recommendations for futures studies	80
6.1. Conclusions	80
6.2. Recommendations for futures studies	81
7. References	81

List of figures

Figure 1 - Overview of the technology readiness level scale	16
Figure 2 - Jacarepaguá Lagoon complex	17
Figure 3 - Sediment Sampling Points, Camorim Lagoon	18
Figure 4 - Map of Jacarepaguá lagoon system	20
Figure 5 - The concentration of potentially toxic elements in the mobile fraction from Camorim lagoon in the year 1994	21
Figure 6 - Sampling stations in the Jacarepaguá lagoon system	22
Figure 7 - Jacarepaguá lagoon system	23
Figure 8 - The concentration of potentially toxic elements in sediments of the Camorim lagoon in the year 1996	24
Figure 9 - Location of the sampling points in rivers and lagoons of the Jacarepaguá basin	25
Figure 10 - Potentially toxic elements (Pb, Cu, Zn, Ni, Cr, and Ba) in fluvial and lagoon environments	26
Figure 11 - Location of sampling points in the Camorim lagoon	27
Figure 12. The concentration of potentially toxic elements from Camorim lagoon sediments in the year 2011	27
Figure 13 - Results of verified test of analysis of the concentration of potentially toxic elements from Camorim lagoon sediments in the year 2011	28
Figure 14 - Location of sampling stations	29
Figure 15 - The concentration of potentially toxic elements from Camorim lagoon sediments in the year 2011	29
Figure 16 - Location of sampling stations in Camorim lagoon	30
Figure 17 - Levels of concentration of potentially toxic elements evaluated in sediment samples from Camorim lagoon in the year 2015	31
Figure 18 - Sampling points distribution of surface sediments in the Tijuca Lagoon (Rio de Janeiro, RJ, Brazil)	32
Figure 19 - The concentration of potentially toxic elements in surface sediments collected in the Tijuca Lagoon	32
Figure 20 - Electrokinetic phenomena	36
Figure 21 - Diagram of leaching as a function of pH	37
Figure 22 - Molecular structure of EDTA	40
Figure 23 - Metals retention mechanism and processes faced by EDTA on soil	41
Figure 24 - Schematic of humic substances structure.	42
Figure 25 – Workflow	44
Figure 26 - Jacarepaguá lagoon system and Camorim lagoon	46

Figure 27 - Electrokinetic cell	47
Figure 28 - Example of electrolyte samples from an electrokinetic treatment	49
Figure 29 - Example of sediment samples from an electrokinetic treatment	50
Figure 30 - Sampling station	51
Figure 31 - Sampling collection. A) Van Veen sampler before sampling B) Van Veem sampler after sampling.	52
Figure 32 - Grain size distribution	53
Figure 33: FTIR spectra of sediment	55
Figure 34 - TG of sediment before thermal treatment	56
Figure 35 - Electrokinetic test with electrolytes. A) EK1 treatment 1. B) EK2 treatment 2. C) EK3 treatment 3. D) EK4 treatment 4	57
Figure 36 - pH variation in catholytes during treatment	59
Figure 37 - pH variation in anolytes during treatment	59
Figure 38 - pH of sediment	61
Figure 39 - Electric conductivity variation in electrolytes during EK1 treatment	63
Figure 40: Electric conductivity variation in electrolytes during EK2 treatment	64
Figure 41 - Electric conductivity variation in electrolytes during EK3 treatment	64
Figure 42 - Electric conductivity variation in electrolytes during EK4 treatment	65
Figure 43 - Electric conductivity of sediment	66
Figure 44 - Zinc concentration at the end of electrokinetic treatments	69
Figure 45 - Lead concentration at the end of electrokinetic treatments	72
Figure 46 - Nickel concentration at the end of electrokinetic treatments	74
Figure 47 - Copper concentration at the end of electrokinetic treatments	77
Figure 48 - Chromium concentration at the end of electrokinetic treatments	79
Figure 49 - Electric current variation in electrolytes during treatment	80
Figure 49 - The electric charge for EK1	81
Figure 49 - The electric charge for EK2	82
Figure 49 - The electric charge for EK3	82
Figure 49 - The electric charge for EK4	83

List of tables

Table 1 - Percentage values of the main granulometric classes in the sediments of the Camorim lagoon	18
Table 2 - Concentration of potentially toxic elements in the background stations	19
Table 3 - Potentially toxic elements concentration from Camorim lagoon in dredged sediments in the year 1996	22
Table 4 - Summary of research on concentrations of potentially toxic elements exceeding levels 1 and 2 as defined by CONAMA Resolution No. 454 of 2012	33
Table 5 - Electrokinetic test	48
Table 6 - Nomenclature of electrolytic samples and sediment samples	50
Table 7 - Physical characterization of sediments	52
Table 8 - Chemical characterization of sediments and water	54
Table 9 - Initial concentration of potentially toxic metals in sediments	54

List of equations

Equation 1	35
Equation 2	35
Equation 3	35
Equation 4	37
Equation 5	37
Equation 6	38
Equation 7	38
Equation 8	38

1. Introduction

The Jacarepaguá lagoon complex has suffered from anthropogenic contamination for decades due to rapid industrial and urban growth. This has led to silting, reduced water surface area, and degraded water quality in rivers and lagoons (Masterplan, 2013).

According to research by Almeida et al. (2001b), Benedetti (2011), and Fernandes et al. (1994), the lagoon system has become a recipient of domestic and industrial effluents, raising concerns about potentially toxic elements. Hortellani et al. (2008) also suggested that sediment contamination is linked to upstream water contamination, which is transported to lagoons and the ocean, ultimately reducing sediment quality.

It is necessary to highlight the importance of sediments for various reasons, including environmental, ecological, economic, and social ones. Therefore, Masi (2017) mentioned that they should be considered a crucial component of coastal areas and river basins.

Instituto Estadual do Ambiente – INEA conducted an environmental impact assessment for a project to extending breakwater at the entrance of the Joatinga Canal and improve water circulation within the Jacarepaguá Lagoon Complex. This project involves dredging the Jacarepaguá, Camorim, Tijuca, and Marapendi lagoons, as well as the Marapendi and Joatinga canals. Its aim is to improve water quality (physical, chemical, and biological aspects), restore the aquatic space, lagoon ecosystem, and environment. Dredging activities are commonly employed worldwide to remove sediments from lagoons, rivers, ports, and the sea (Çevikbilen et al., 2020; Kim et al., 2011).

According to Amar et al. (2021), dredging generates a large volume of dredged material annually. International conventions, such as the London Convention (1972), Barcelona Convention (1976), Helsinki Convention (1992), and OSPAR Convention (1992), have promoted the concept of dredged sediment as a potential resource. Today, the reuse of these materials is encouraged for sustainable development.

Dredged sediments have garnered significant interest in the construction industry due to their potential applications. Beddaa et al. (2020) discussed their use in road construction, cement production, and as an aggregate replacement for mortar or concrete manufacturing. This potential is further supported by the wide range of civil engineering projects where the feasibility of utilizing dredged material has been investigated (Bortali et al., 2023).

However, Agostini et al. (2007), Akcil et al. (2015), and Çevikbilen et al. (2020) point out that sediment pollution can be a global economic and environmental problem.

Strategies exist for managing contaminated sediments, including landfill disposal, confined disposal facilities, and sediment treatment. However, landfill disposal requires significant space and long-term monitoring. Additionally, Agostini et al. (2007), Masi (2017), and Pal and Hogland (2022) warn that landfill disposal can create secondary environmental issues including greenhouse gases emissions and polluted leachates disposal.

Detzner et al. (2007) and Rulkens (2005) described various sediment treatment techniques, such as thermal, chemical, physical, and biological methods. However, these strategies were primarily developed for highly permeable soils compared to fine-grained sediments. Consequently, their effectiveness is lower when applied to low-permeability materials. Electrokinetic remediation, in contrast, has proven effective for low-permeability materials with fine-grained matrices (Virukyte et al., 2002), minimally invasive (Cercato & De Donno, 2020). It can also remove organic (Gidudu & Chirwa, 2020) and inorganic contaminants simultaneously while dewatering the sediment to reduce its volume (Ammami et al., 2020).

The presence of potentially toxic elements in the sediments of Camorim Lagoon has been documented by research such as Fernandes et al. (1994). Since then, other investigations have been carried out. Comparing the current concentration levels with the standards established in the COMANA Resolution of 2012, elements like nickel, zinc, and copper exceed Level 1, which indicates a low probability of adverse effects on the biota. Thus, developing strategies to address or solve pollution issues is crucial for environmental protection.

This doctoral research evaluates different strategies for applying remedial electrokinesis in contaminated sediments in Camorim Lagoon.

An electrokinetic process is used to minimize potentially toxic elements (zinc, lead, nickel, copper and chromium) in the sediments to meet the threshold limits set by CONAMA Resolution No. 454 of (2012).

In this work, electrokinesis with EDTA (Ethylenediaminetetraacetic acid) and humic substances is used to reduce the concentration of metals (zinc, lead, nickel, copper and chromium) in the sediments of the Camorim lagoon together with buffer solution to control the change in pH during the process.

This research falls within the scope of the project "*Estudos e Estratégias para Utilização de Sedimentos Acumulados por Ações Antrópicas no*

Complexo Lagunar da Baixada de Jacarepaguá” (Chamada CNPQ/Finep/MCTIC/BRICS-STI N° 03/2019)”

The following work, in Chapter 2, presents the study site. This chapter also reviews previous research on the concentration of potentially toxic elements in Camorim Lagoon. Chapter 3 explores the theoretical framework of electrokinetic remediation. Chapter 4 details the materials and methods used in the development of the research. Chapter 5 presents the results and discussion. Finally, Chapter 6 lists the references used.

The work is framed within the Technological Readiness Levels (TRL) (Mankins, 2009; Moura Ribeiro, 2019), in which level 4 is targeted. Figure 1 shows an overview of the technology readiness level scale

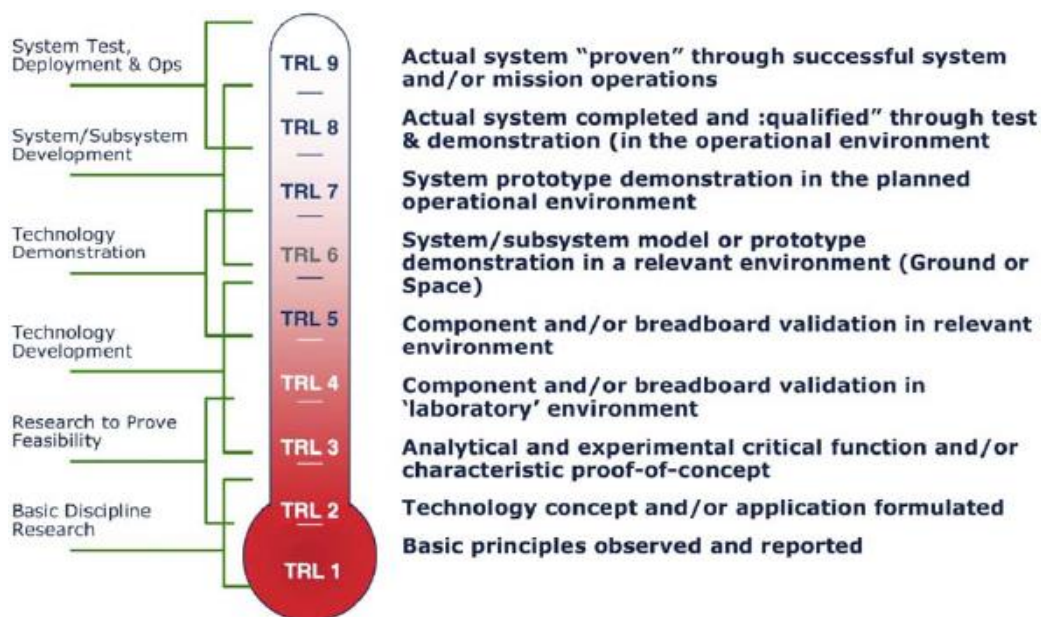


Figure 1 - Overview of the technology readiness level scale Mankins (2009)

2. Study site

The Jacarepaguá lagoon system is comprised of three main lagoons: Tijuca, Jacarepaguá, and Marapendi. Located between Jacarepaguá and Tijuca lagoons (as shown in Figure 2), the Camorim lagoon resembles a canal in shape despite its significant role in the survival of system (FUNDAÇÃO COPPETEC-UFRJ, 1998; INEA, 2020).

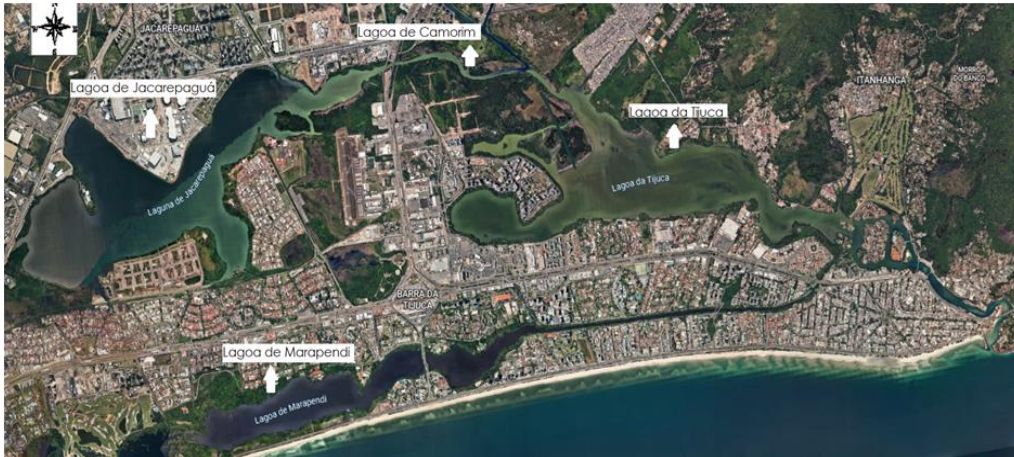


Figure 2 - Jacarepaguá Lagoon complex
Google Earth

Fine sediments predominate in the lagoon sediments, as shown in Table 1 and the sampling stations were characterized as Dredging Characterization Units (DCUs) are shown in Figure 3. Borma et al. (2003) analyzed sediment samples from Jacarepaguá and Camorim lagoons and reported the following minerals: kaolinite (low crystallinity) as the main clay mineral, along with quartz, orthoclase feldspar, biotite, ilmenite, and magnetite (in smaller quantities). The researchers also mentioned that sediments have a low buffering capacity and high content of iron sulfides.

Almeida et al. (2001b) found similar composition in Jacarepaguá lagoon sediments. These sediments contained kaolinite, micas, iron sulfides, large quantities of sodium chloride crystals, and a smaller quantity of quartz and carbonate. Meanwhile, tributary rivers sediments were quartz, micas, kaolinites, and potassium feldspar predominate.

de Magalhães et al. (2017) obtained comparable results for Jacarepaguá lagoon sediment and the banks of the Funil Reservoir. Kaolinite was again the most abundant mineral, followed by goethite and mica.



Figure 3 - Sediment Sampling Points, Camorim Lagoon

Modified from Masterplan (2015)

The sampling stations were characterized as Dredging Characterization Units (DCUs), a technique recommended in CONAMA Resolution No. 454/201.

● 1 ● 2 ● 3 ● 4 ● 5 ● 6

Table 1 - Percentage values of the main granulometric classes in the sediments of the Camorim lagoon

Sampling station		Gravel ($\geq 2\text{mm}$)	Sand (2-0.0625 mm)	Silt (0.0625-0.0039 mm)	Clay (0.0039-0.00195 mm)
C01	S	5.2	18.6	69.7	6.5
C01	B	4.1	10.5	47.0	38.3
C02	S	0.5	7.1	81.5	10.9
C02	B	0.2	14.0	65.3	20.5
C03	S	0.2	14.4	31.1	54.4
C03	B	0.2	13.4	20.7	65.7
C04	S	0.3	20.6	48.6	30.5
C04	B	1.2	22.0	49.0	27.9
C05	S	3.5	41.6	54.5	0.5
C05	B	0.3	18.8	68.9	12.1
C06	S	0.5	44.0	52.8	2.6
C06	B	8.3	20.1	64.0	7.6

Modified from Masterplan (2015)

The names of the sampling stations are the same as in the original document.

S and B indicated surface and bottom, respectively.

Soil fraction according to CONAMA n° 454 de 2012.

The lagoon system has suffered from anthropogenic contamination due to the rapid growth industrial and urban areas without adequate infrastructure in the drainage basin. Consequently, as Almeida et al. (2001b), Benedetti (2011), and Fernandes et al. (1994) mention, the lagoon system has become a recipient of domestic and industrial effluents. Fernandes et al. (1994), highlight that potentially toxic elements are of particular concern.

According to FUNDAÇÃO COPPETEC-UFRJ (1998), *Arroio Pavuna*, *Arroio Fundo*, and *Rio do Anil* are the main contributors of potentially toxic elements. Barcellos et al. (2019) further state that the *Arroio Pavuna* is “the most important anthropogenic heavy-metals source to that system; they arrived at values of 85 000 g day⁻¹ of iron, 600 g day⁻¹ of manganese, 400 g day⁻¹ of lead, 840 g day⁻¹ of copper, 2300 g day⁻¹ of zinc, 130 g day⁻¹ of nickel and 80 g day⁻¹ of chromium.”

Azevedo et al (1988) studied the variation of several potentially toxic elements, including chromium, lead, nickel, and zinc, in the mobile fraction of sediments from tributaries of the Jacarepagua and Camorim lagoons. Additionally, background samples were collected at stations not influenced by industrial effluents but potentially impacted by domestic waste.

Table 2 presents the concentration ranges and the mean values of these potentially toxic elements in the background stations: Pavuninha (RP), Rio Camorim (RC), Rio Papagaio, and Rio Caçambe (RC), which receive domestic effluents.

Table 2 - Concentration of potentially toxic elements in the background stations

	Potentially toxic elements concentration mg Kg⁻¹				
	Chromium	Lead	Nickel	Copper	Zinc
Range	2.8 and 5.6	6.4 and 43	1.7 and 4.7	7.0 and 40	26 and 194
Mean values	4.4 ± 1.0	27 ± 13	2.6 ± 0.9	19 ± 11	-

Data obtained from Azevedo et al (1988)

Research by FUNDAÇÃO COPPETEC-UFRJ (1998) identified Camorim lagoon as the area within the Jacarepaguá lagoon system experiencing the most negative environmental impacts from potentially toxic elements, sewage, and increased sedimentation. These impacts likely arise because aforementioned tributaries (*Arroio Pavuna*, *Arroio Fundo*, and *Rio do Anil*) discharge their waters into the Jacarepaguá lagoon and the Camorim lagoon.

Currently, Resolution 454/2012 defines the general guidelines and minimum procedures for evaluating and classifying dredged material in Brazilian jurisdictional waters.

Fernandes et al. (1994) analyzed the concentration of chromium, copper, nickel, lead, and zinc in 18 samples collected from both Jacarepaguá and Camorim lagoons. The lagoons were chosen for this study because they are located in areas likely to receive the highest impact from river discharge.

However, only the results for the Camorim Lagoon samples are presented here. The sampling stations are shown in Figure 4.

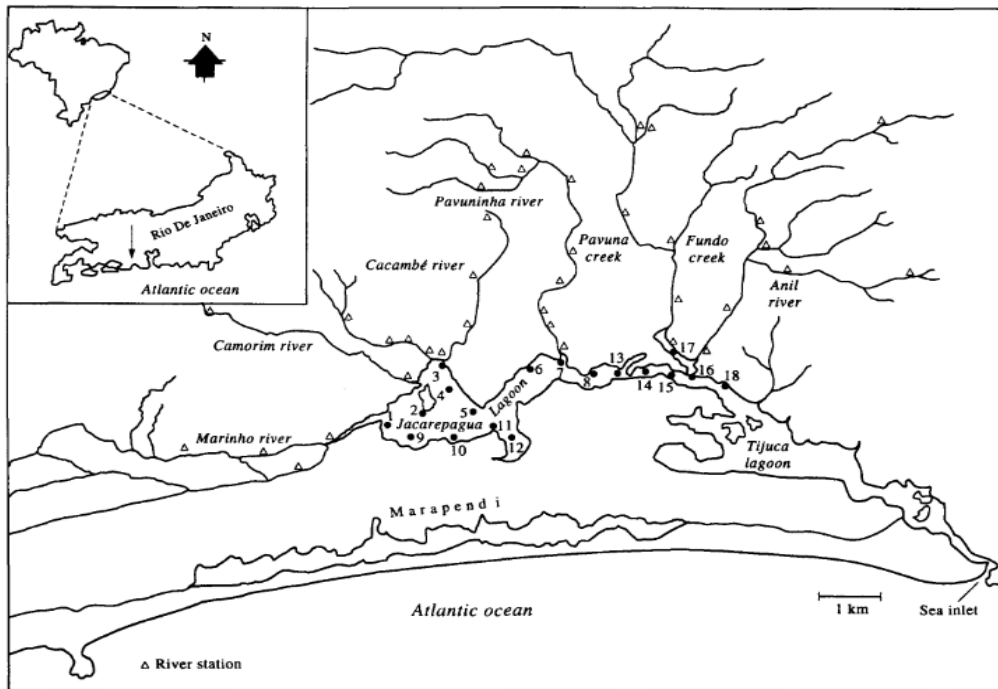


Figure 4 - Map of Jacarepaguá lagoon system
Fernandes et al. (1994)

Unfortunately, at that time, the results were not compared to any established threshold limits because no such legislation existed in Brazil. CONAMA Resolution No. 344/2004 was later introduced to provide guidelines for metal concentrations in dredged material. However, this resolution was subsequently revoked by Resolution No. 454 of 2012.

Figure 5 compares the concentration of mobile fractions of potentially toxic elements in the Camorim Lagoon sediment with the threshold limits established by CONAMA Resolution No. 454 of 2012.

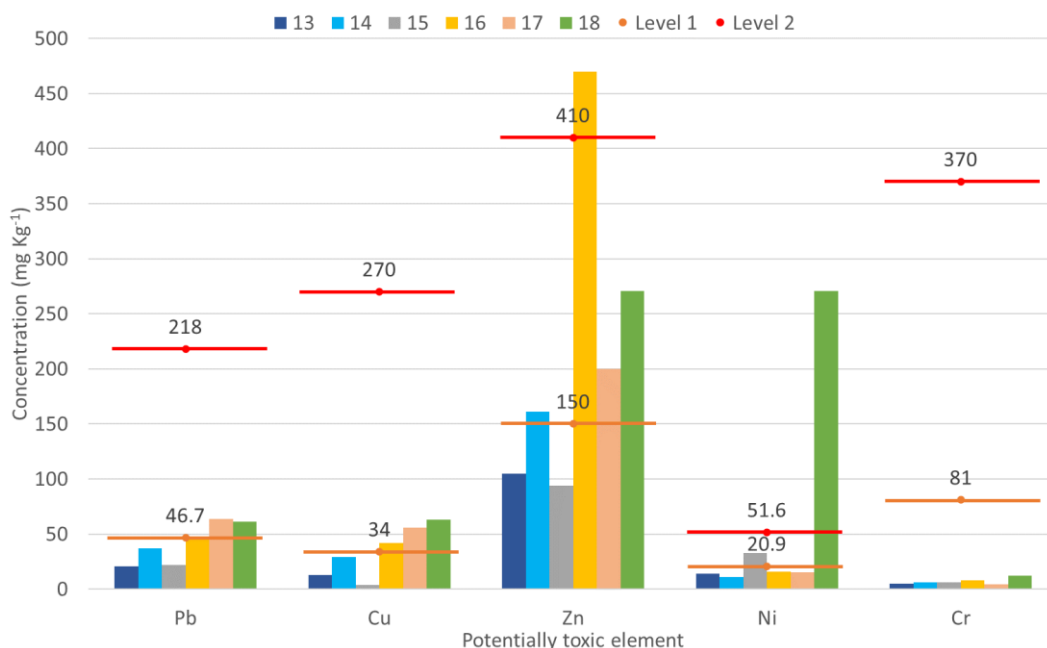


Figure 5 - The concentration of potentially toxic elements in the mobile fraction from Camorim lagoon in the year 1994

Modified from Fernandes et al. (1994).

Level 1 - the threshold below which there is a lower probability of adverse effects on the biota; Level 2 - the threshold above which there is a higher probability of adverse effects on the biota. CONAMA Resolution No. 454 of 2012.

The names of the sampling stations are the same as in the original document.

This study revealed the highest concentration of lead, copper, zinc, nickel, and chromium, at various sampling points: 64 mg kg⁻¹ at point 17 (lead), 63 mg kg⁻¹ at point 18 (copper), 470 mg kg⁻¹ at point 16 (zinc), 271 mg kg⁻¹ at point 18 (nickel), and 7.9 mg kg⁻¹ at point 16 (chromium).

Points 16 to 18 exceed CONAMA Resolution No. 454 of 2012 level 1 for lead and copper concentrations. Additionally, points 14, 17, and 18 exceed level 1 for zinc, while point 16 exceeds level 2 for the same metal. Finally, points 15 and 18 exceed levels 1 and 2 for nickel, respectively.

FUNDAÇÃO COPPETEC-UFRJ (1996) conducted a sediment analysis of the Jacarepaguá Lagoon system as part of a project by *Secretária Municipal de Meio Ambiente da Prefeitura da Cidade do Rio de Janeiro (SMAC)*. It is important to note that this investigation did not focus on determining the overall contamination of the lagoon system.

Only results from samples collected in the Camorim Lagoon are presented here. The sampling station locations are shown in Figure 6.

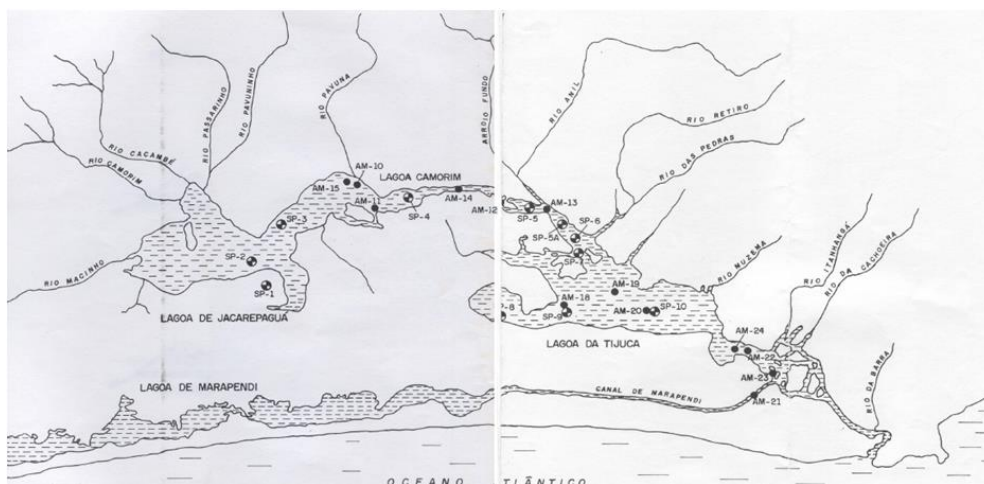


Figure 6 - Sampling stations in the Jacarepaguá lagoon system FUNDAÇÃO COPPETEC-UFRJ (1996)

The research investigated the concentration of eight metals in the lagoon sediments: chromium, copper, nickel, lead, and zinc. To simulate dredging conditions and reflect potential metal mobilization during the process, the collected sediment samples were allowed to mix with water. Table 3 presents the concentration of these metals in Camorim Lagoon sediments collected at different depths, alongside the corresponding threshold limits established by CONAMA Resolution No. 454 of 2012.

Table 3 - Potentially toxic elements concentration from Camorim lagoon in dredged sediments in the year 1996

Sampling station	Depth (m)	Potentially toxic elements concentration (mg kg ⁻¹)				
		Pb	Cu	Zn	Ni	Cr
AM-12A	1.30-1.60	500	103	500	0	0
AM-12B	1.80-2.10	500	94	500	0	0
AM-13A	0.15-0.45	56-82.5	61-80	223-297	19-25	0-37
AM-13B	1.15-1.45	29.5-73	51-71.5	181-233	12-23	0-31
Level 1 (mg kg ⁻¹)		46.7	34	150	20.9	81
Level 2 (mg kg ⁻¹)		218	270	410	51.6	370

Modified from FUNDAÇÃO COPPETEC-UFRJ, (1996).

The names of the sampling stations are the same as in the original document.

Level 1 - the threshold below which there is a lower probability of adverse effects on the biota. Level 2 - the threshold above which there is a higher probability of adverse effects on the biota. CONAMA Resolution No. 454 of 2012. Values that exceeded the Level 1 and Level 2 limits are in orange and red, respectively.

Lead and zinc concentrations in sampling stations AM-12A and AM-12B were particularly high (500 mg/kg). However, the original document lacks a laboratory report detailing the analytical method used for these samples.

Similar concentration ranges were observed for other metals. All stations exceeded Level 1 of CONAMA Resolution No. 454 of 2012 for lead, chromium, and zinc, except AM-12A and AM-12B, which had lead and zinc exceeding

Level 2. Additionally, nickel concentration surpassed Levels 1 at sampling stations AM-13A.

Fernandes (1997) analyzed chromium, copper, nickel, lead, and zinc. However, only six sediment samples were collected, and only one was located within the Camorim Lagoon, corresponding to point 16 from prior investigation. The sampling station locations for this study are shown in Figure 7.

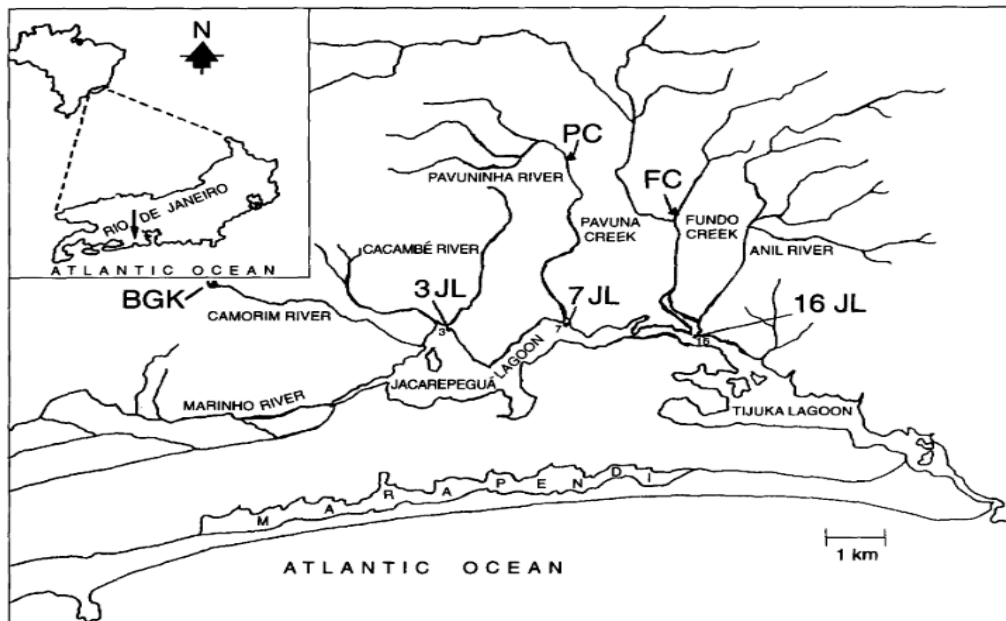


Figure 7 - Jacarepaguá lagoon system
Fernandes (1997)

Figure 8 illustrates the concentration of potentially toxic elements in the Camorim Lagoon sediment compared to the threshold limits set by CONAMA Resolution No. 454 of 2012.

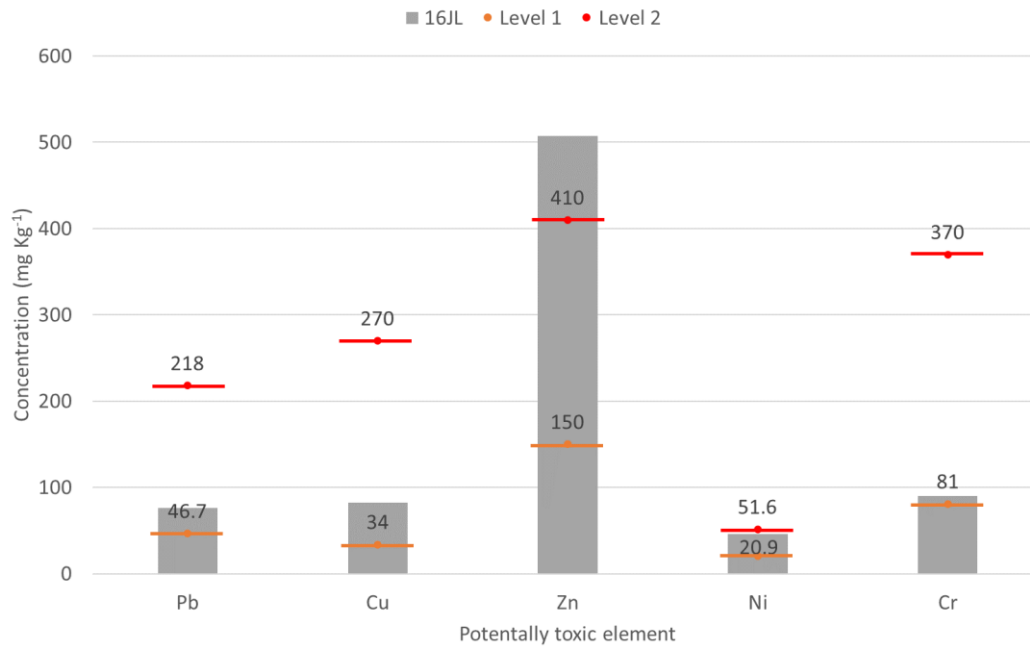


Figure 8 - The concentration of potentially toxic elements in sediments of the Camorim lagoon in the year 1996

Modified from Fernandes (1997).

Level 1 - the threshold below which there is a lower probability of adverse effects on the biota. Level 2 - the threshold above which there is a higher probability of adverse effects on the biota. - CONAMA Resolution No. 454 of 2012.

The names of the sampling stations are the same as in the original document.

Compared to the previous study by Fernandes et al. (1994) all metal concentrations increased at point 16. Furthermore, lead, copper, nickel, and chromium exceed Level 1 of CONAMA Resolution No. 454 of 2012, while zinc surpasses Level 2 of the same resolution.

Almeida et al. (2001b) present the results of a research carried out in 1998.

This research collected samples from lagoons, rivers, and streams, but only the results for samples collected in the Camorim Lagoon are presented here. The analyzed metals in the sediments included chromium, copper, nickel, lead, and zinc. The sampling station locations are shown in Figure 9.

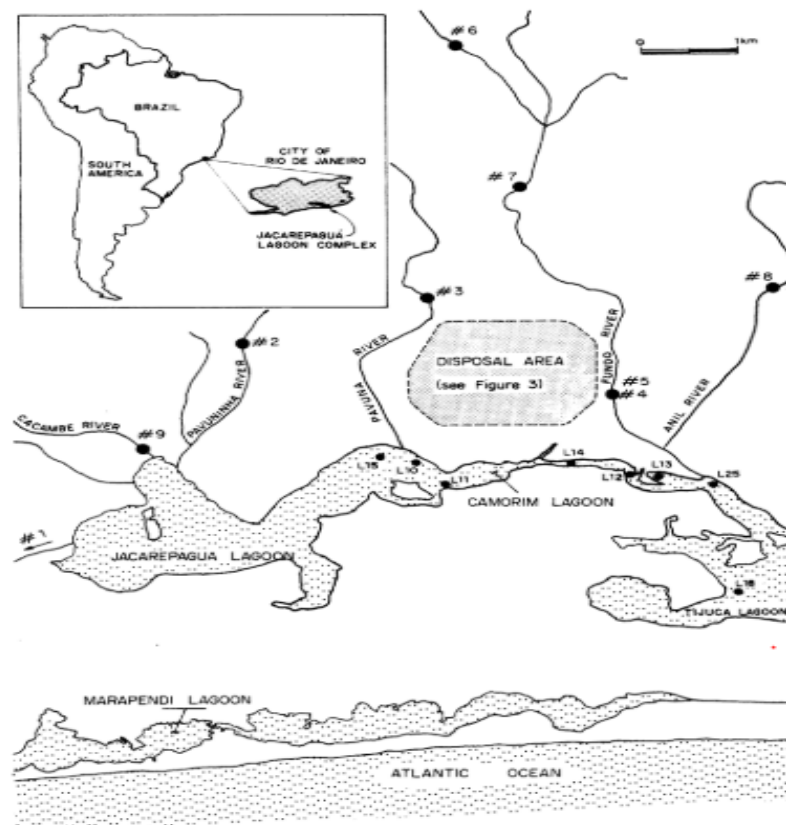


Figure 9 - Location of the sampling points in rivers and lagoons of the Jacarepaguá basin
 Modified from Almeida et al. (2001)

Figure 10 illustrates the concentration of potentially toxic elements in the Camorim Lagoon sediment compared to the threshold limits established by CONAMA Resolution No. 454 of 2012.

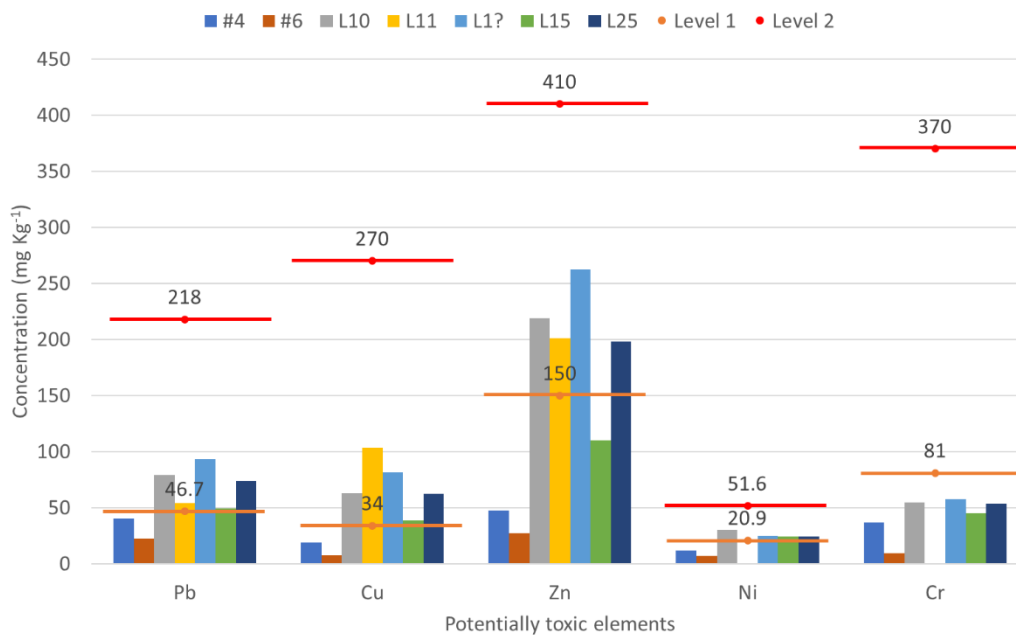


Figure 10 - Potentially toxic elements (Pb, Cu, Zn, Ni, Cr, and Ba) in fluvial and lagoon environments

Modified from Almeida et al (2001).

Level 1 - the threshold below which there is a lower probability of adverse effects on the biota. Level 2 - the threshold above which there is a higher probability of adverse effects on the biota. CONAMA Resolution No. 454 of 2012.

The names of the sampling stations are the same as in the original document.

Figure 10 shows that lead, copper, zinc, and nickel concentrations in both sampling stations exceed Level 1 of CONAMA Resolution No. 454 of 2012. While this indicates a low probability of adverse effects, it is important to consider potential ecological risks.

PROJCONSULT in 2011 evaluated the sediment quality within the Jacarepaguá Lagoon system. Their results are also included in the Relatório Ambiental Simplificado – RAS das Obras de Recuperação Ambiental do Complexo Lagunar de Jacarepaguá. The objective of this investigation was to assess the feasibility of obtaining environmental licenses for the restoration work.

The sampling station locations (AD 11, AD 12, AD 13, AD 14, and AD15) are shown in Figure 11. Samples were collected at two depths: upper samples (S) at 0.75 meters and bottom samples (F) between 1.0 and 2.50 meters.



Figure 11 - Location of sampling points in the Camorim lagoon Masterplan (2013a)

Figure 12 shows the results of potentially toxic elements concentration in the Camorim lagoon.

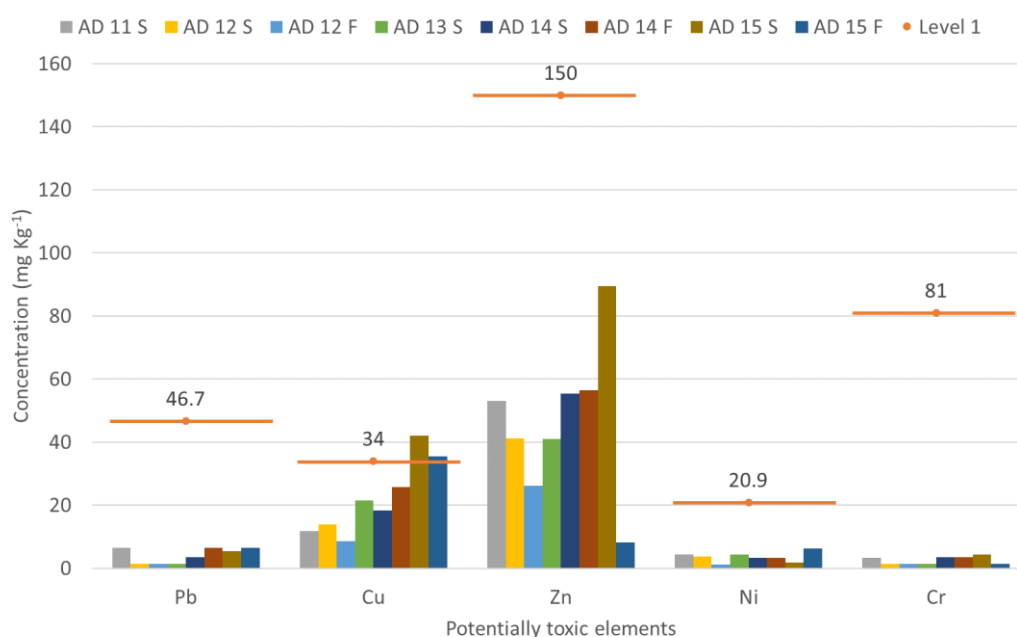


Figure 12. The concentration of potentially toxic elements from Camorim lagoon sediments in the year 2011

Modified from Masterplan, (2013b)

Level 1 - the threshold below which there is a lower probability of adverse effects on the biota. Level 2 - the threshold above which there is a higher probability of adverse effects on the biota. - CONAMA Resolution No. 454 of 2012.

The names of the sampling stations are the same as in the original document.

Lead and chromium concentrations were also below the detection limit at stations AD 12 (both surface and bottom samples), and AD 13 (surface sample only). Conversely, copper concentrations exceeded Level 1 of CONAMA Resolution No. 454 of 2012 at stations AD 15 (both surface and bottom samples).

Further tests were conducted to verify these low concentrations, but for the Camorim Lagoon, only results for station AD 13 (surface sample) were confirmed. These results are presented in Figure 13.

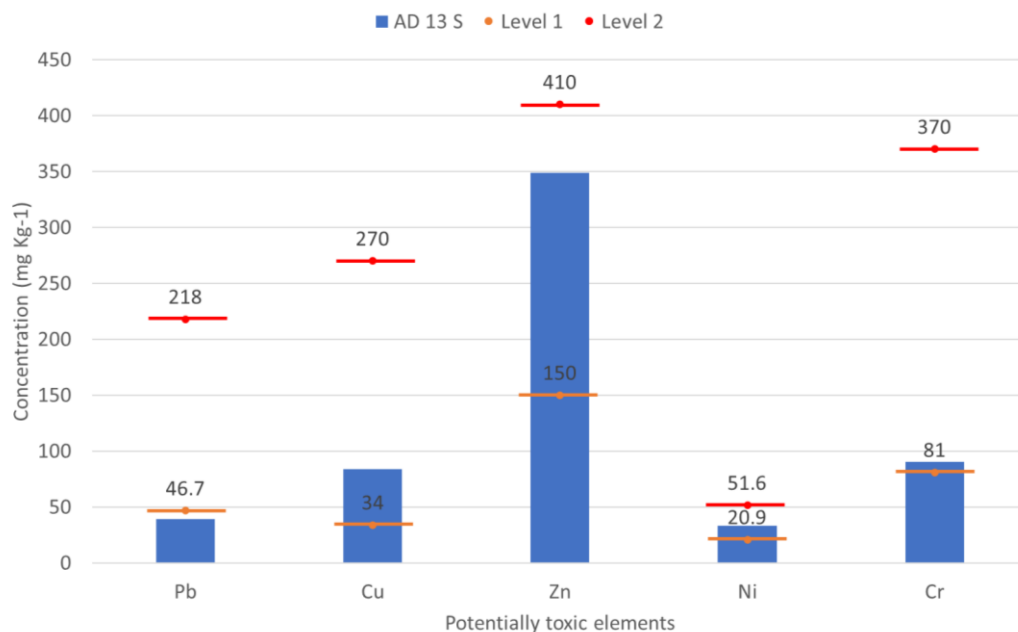


Figure 13 - Results of verified test of analysis of the concentration of potentially toxic elements from Camorim lagoon sediments in the year 2011
Modified from Masterplan (2013b)

Level 1 - the threshold below which there is a lower probability of adverse effects on the biota. Level 2 - the threshold above which there is a higher probability of adverse effects on the biota. CONAMA Resolution No. 454 of 2012.

The names of the sampling stations are the same as in the original document.

The retests revealed that copper, zinc, nickel, chromium, and cadmium concentrations exceeded Level 1 of CONAMA Resolution No. 454 of 2012. Lead, mercury, and arsenic also showed increased concentrations compared to the initial investigation.

Araruna Júnior et al. (2012) conducted a study to obtain a bathymetry chart of the lagoon bottom's relief, characterize the sediment type, and assess sediment quality regarding contamination within the Jacarepaguá Lagoon system. While 13 sampling stations were defined for this investigation, only one

station (LC) was located within the Camorim Lagoon. The sampling station locations are shown in Figure 14.

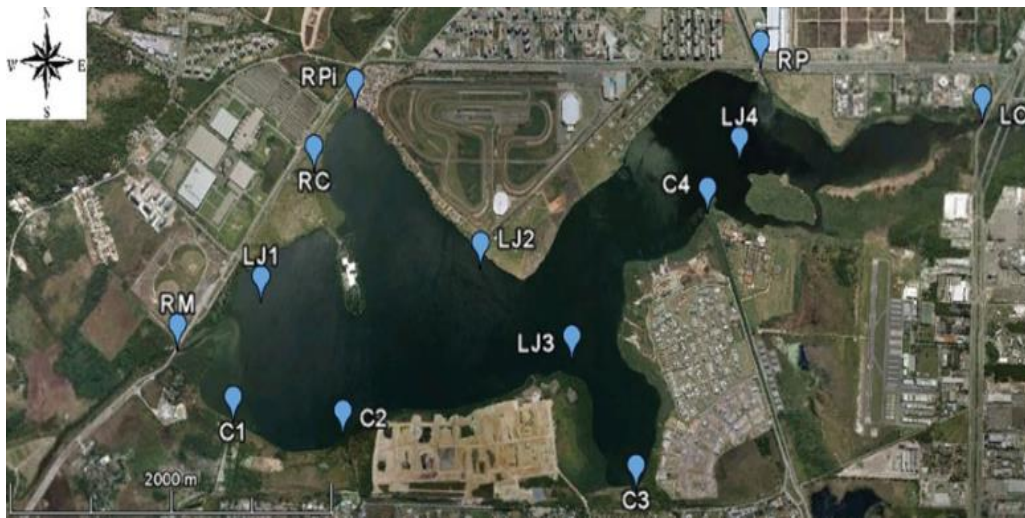


Figure 14 - Location of sampling stations
Araruna Júnior et al. (2012)

Figure 15 shows the results of potentially toxic elements concentration in the Camorim lagoon.

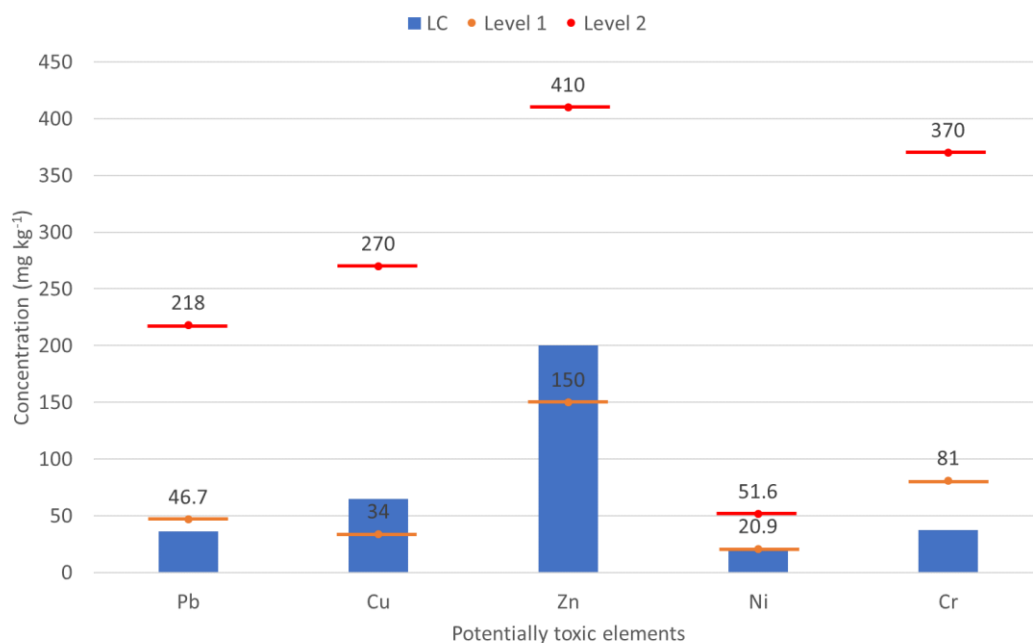


Figure 15 - The concentration of potentially toxic elements from Camorim lagoon sediments in the year 2011

Modified from Araruna Júnior et al. (2012)

Level 1 - the threshold below which there is a lower probability of adverse effects on the biota. Level 2 - the threshold above which there is a higher probability of adverse effects on the biota. CONAMA Resolution No. 454 of 2012.

The names of the sampling stations are the same as in the original document.

This investigation revealed that zinc and copper concentrations exceed Level 1 of CONAMA Resolution No. 454 of 2012. Nickel concentrations (19.7 mg/kg) were close to Level 1 of the same resolution (20.9 mg/kg).

In 2014, the Masterplan commissioned an environmental impact study conducted by *Instituto Estadual do Ambiente – INEA* and *Secretaria do Ambiente*. This study analyzed the quality of sediments in the Jacarepaguá Lagoon complex, including the concentration of potentially toxic elements.

The research employed a sampling approach called "Dredging Characterization Units." This means that the final analyzed samples were homogenized collections from three individual sampling stations. The locations of these sampling stations are shown in Figure 16.

Sediment samples were collected from two layers: surface layers (S) between 0.0 m and 0.5 m depth, and bottom layers (F) between 0.5 m and 3.00 m depth.



Figure 16 - Location of sampling stations in Camorim lagoon
Modified from Masterplan (2015)

Figure 17 illustrates the concentration of potentially toxic elements in the surface layer (S) and bottom layer (B) of the Camorim Lagoon sediments compared to the threshold limits established by CONAMA Resolution No. 454 of 2012.

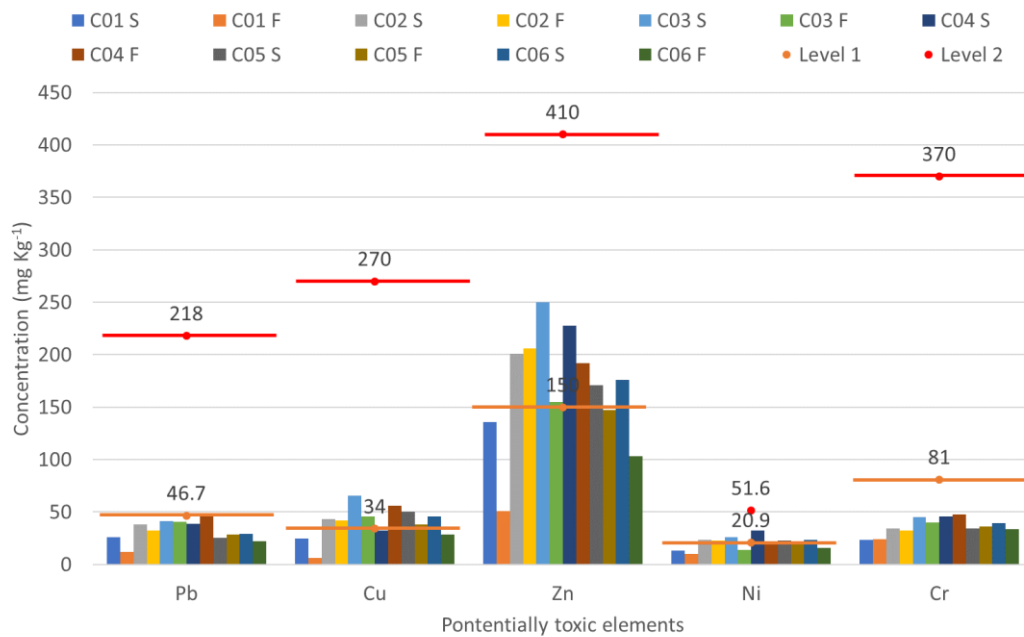


Figure 17 - Levels of concentration of potentially toxic elements evaluated in sediment samples from Camorim lagoon in the year 2015

Modified from Masterplan (2015)

Level 1 - the threshold below which there is a lower probability of adverse effects on the biota. Level 2 - the threshold above which there is a higher probability of adverse effects on the biota. CONAMA Resolution No. 454 of 2012.

The names of the sampling stations are the same as in the original document.

Copper, nickel, and zinc concentrations exceeded Level 1 of CONAMA Resolution No. 454 of 2012 in at least one layer at all sampling stations except C01.

For copper, nickel, and zinc, surface layer concentrations exceeding Level 1 were distributed along the watercourse towards the Tijuca Lagoon, with the highest levels found in the Camorim Lagoon's central meander (detailed data not shown).

Copper and zinc concentrations in the bottom layer were also elevated, exceeding Level 1 throughout the lagoon, although to a lesser extent than the surface layer (detailed data not shown). Nickel in the bottom layer was found in two regions: the westernmost meander and just beyond the central meander (Masterplan, 2015).

Teixeira et al. (2022) conducted a separate study in the Tijuca Lagoon to systematically map metal, PAH (polycyclic aromatic hydrocarbon), and toxicity levels in surface sediments.

Their investigation used 23 sampling stations distributed throughout the lagoon, as shown in Figure 18. Figure 19 specifically show the concentrations of potentially toxic elements in sampling stations P13 and P14, which are

closest to the Camorim Lagoon. The sediment samples for this study were collected in August 2019.

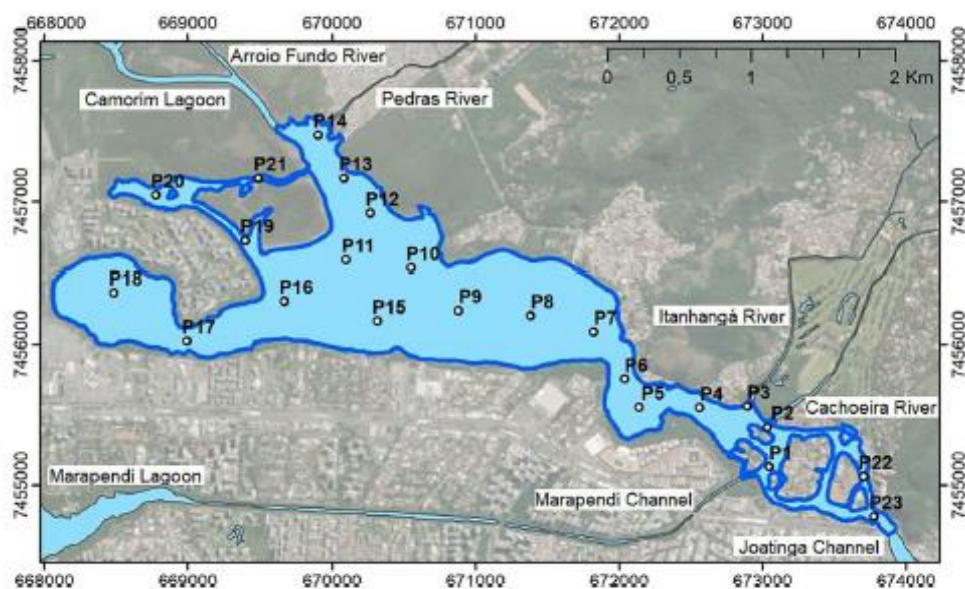


Figure 18 - Sampling points distribution of surface sediments in the Tijuca Lagoon (Rio de Janeiro, RJ, Brazil)
Modified from Teixeira et al. (2022)

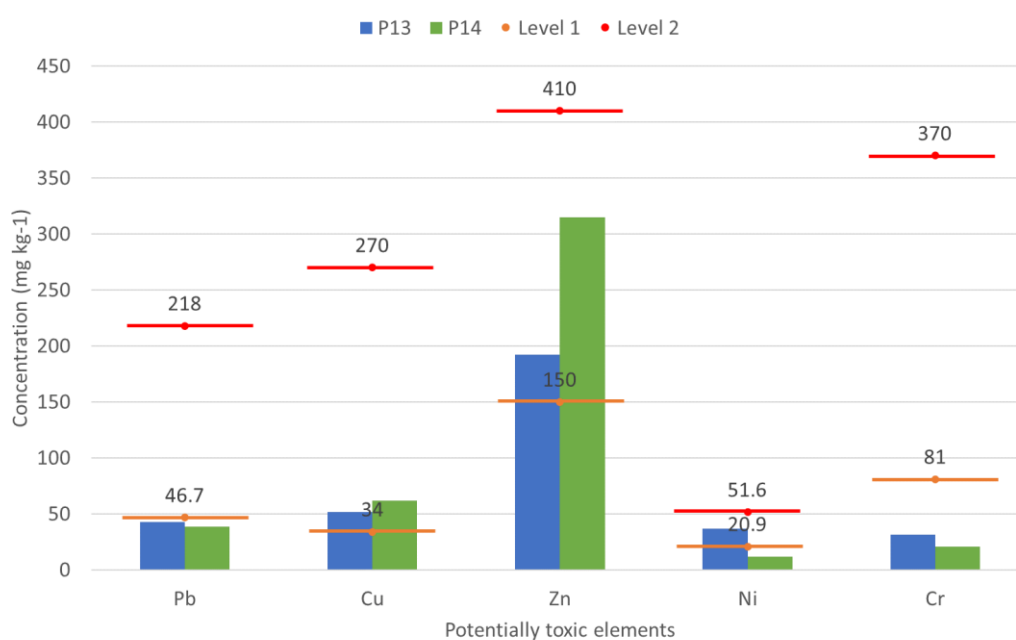


Figure 19 - The concentration of potentially toxic elements in surface sediments collected in the Tijuca Lagoon
Modified from Teixeira et al. (2022)

The results indicate that copper (Cu), zinc (Zn), and nickel (Ni) concentrations in the Tijuca Lagoon sediment exceed Level 1 of CONAMA Resolution No. 454 of 2012 in at least one sampling station. Notably, the nickel

concentration at station P14 (20.5 mg/kg) is very close to the established threshold limit (20.9 mg/kg).

Elevated Zn and Cu levels in the Tijuca Lagoon sediment are likely associated with untreated sewage and potential clandestine discharges entering the lagoon system. These metals are known as good indicators of domestic sewage contamination.

Table 4 summarizes the potentially toxic elements (Cr, Cu, Ni, and Zn) for each study. Elements exceeding Level 1 of CONAMA Resolution No. 454 of 2012 are highlighted in orange, while those exceeding Level 2 are highlighted in red.

All studies indicate that concentrations of all elements exceed Level 1 of the CONAMA resolution, except for zinc in the Fernandes (1997) study, which exceeds Level 2 of the same resolution.

Table 4 - Summary of research on concentrations of potentially toxic elements exceeding levels 1 and 2 as defined by CONAMA Resolution No. 454 of 2012

Author	Elements				
Fernandes et al. (1994)	Pb	Cu	Zn	Ni	
Fernandes (1997)	Pb	Cu	Zn	Ni	Cr
Almeida et al. (2001)	Pb	Cu	Zn	Ni	
Araruna Júnior et al. (2012)		Cu	Zn		
Masterplan (2013b)		Cu	Zn	Ni	Cr
Masterplan (2015)		Cu	Zn	Ni	
Teixeira et al. (2022)	Pb	Cu	Zn	Ni	

Level 1 - Orange - The threshold below which there is a lower probability of adverse effects on the biota. Level 2 - Red - the threshold above which there is a higher probability of adverse effects on the biota. CONAMA Resolution No. 454 of 2012.

3. Theoretical framework

3.1. Electrokinetic remediation

Electrokinetic (EK) remediation, as noted by Ribeiro & Mateus (2016), is considered an environmentally friendly technology. However, it remains under development due to inconsistencies between laboratory and field results. Initially designed for treating soils contaminated with heavy metals and organic pollutants, EK can also be applied to sediments, sludge, and porous materials (Han et al., 2021; Osman, 2014, 2018). Osman (2014) and Rahman et al. (2021) further highlight its applicability in both in-situ and ex-situ scenarios.

According to Osman (2014) and Ribeiro & Mateus (2016), the key advantages of this method include its effectiveness in low-permeability soils, heterogeneous media, and fine-grained materials.

Despite its advantages, the technology has limitations. Changes in pH can occur, leading to the precipitation of species that may affect the solubility or corrode the anode. Several factors influence its efficacy, as pointed out by Han et al. (2021), Saini et al. (2020), and Virkutyte et al. (2002). These factors include soil type, contaminant type, pollutant concentration and extent, the presence of rocks or buried objects, and the spacing between electrodes.

Principles of electrokinetic (EK)

Electrokinetic remediation consists of inserting at least two electrodes into the polluted porous medium and applying a direct low-intensity electric current (DC) (Asadollahfardi et al., 2021; Baudhdh et al., 2017; Osman, 2018; Ribeiro & Mateus, 2016; Sharma et al., 2018). It generates an electric field that causes the mobilization and transportation of pollutants, nutrients, and microorganisms.

Transport under electric field

Electrokinetic (EK) remediation relies on an electric field to mobilize and transport various species, including pollutants, within the contaminated medium (Osman, 2018; Sharma et al., 2018). Four key mechanisms govern this movement: electro-osmosis, electromigration, electrophoresis, and diffusion (Figure 20).

Additionally, as Ribeiro & Mateus (2016) point out, contaminant migration in the soil is also influenced by sorption/desorption and precipitation/dissolution processes. The dominant transport mechanisms and

overall mass flux will ultimately depend on the specific composition of the medium and environmental conditions (Acar & Alshawabkeh, 1993).

Electro-osmosis

Osman (2018) defines electro-osmosis as the bulk movement of pore fluid through the electrical double layer in clayey soils, typically occurring from the anode towards the cathode. This phenomenon is most significant in materials with fine pores and is the dominant transport process for non-polar organic compounds (Ottosen et al., 2008).

Electro-osmotic flow (EOF) can be described with the Helmholtz–Smoluchowski theory, which is used when the pores are large compared to the size of the electrical double layer. The electro-osmotic flow rate is described by Equation 1 and “depends on the balance between the electrical force on the liquid and the friction between the liquid and the surface of the soil particles.”(Page & Page, 2002).

$$q_A = -\frac{\varepsilon\zeta EnA}{\eta} \quad \text{Equation 1}$$

Where ε is the permittivity of the liquid, ζ is the zeta potential, n is the porosity of the medium, η is the viscosity of the liquid, E is the electric field strength or negative potential gradient and A is the total cross-sectional area normal to the flow direction. Equation 1 can be expressed as shown in Equation 2.

$$q_A = -k_e EA \quad \text{Equation 2}$$

k_e is the coefficient of electro-osmotic permeability.

$$k_e = \frac{\varepsilon\zeta n}{\eta} \quad \text{Equation 3}$$

The equations shown above do not consider the effect of tortuosity. Experimental investigations determined that k_e does not depend on the type of soil (Mitchell, 1993; A. Yeung, 1994). Additionally, Helmholtz–Smoluchowski expresses that k_e does not depend on pore size, contrary to k_h (hydraulic permeability) (Page & Page, 2002). The electro-osmotic and hydraulic permeability values are between $10^{-9} - 10^{-8} \text{ m}^2\text{V}^{-1}\text{s}^{-1}$ and $10^{-13} - 10^{-5} \text{ m s}^{-1}$, respectively. According to the above, the electrical gradient is more effective than a hydraulic gradient for transporting liquids in fine-grained soils (Page & Page, 2002).

Electromigration

Electromigration, as described by Ottosen et al. (2008), involves the transport of ions within the pore fluid towards electrodes with opposite charges. This mechanism is considered the main transport process for ionic compounds, with its rate depending on the pore volume, geometry, and water content.

Furthermore, during electrokinetic remediation processes, electromigration is influenced by several factors, including the strength of the electric field, the concentration of ions, and their charge (Acar & Alshwabkeh, 1993).

Electrophoresis

Electrophoresis is a phenomenon where an electric field induces movement of charged particles within the diffuse layer surrounding a colloid. This movement creates slip at the interface between the particle and the liquid, causing the particle to migrate in the direction opposite the overall slip velocity (Lockwood, 2012). This mechanism can transport bacterial cells and micelles.

While studies like capillary electrophoresis demonstrate the ability to move particles within capillaries, electrophoresis is generally considered negligible in porous materials due to the complex and winding nature of the pores, also known as tortuosity (Ottosen et al., 2008).

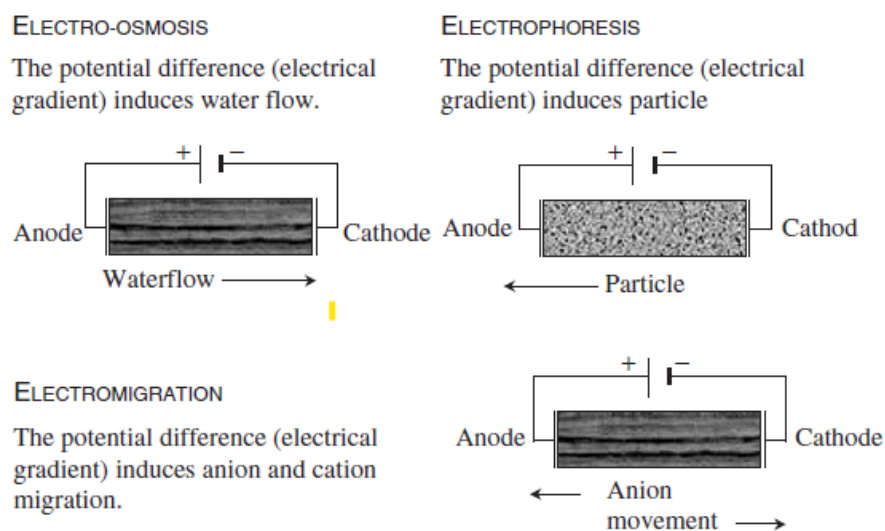


Figure 20 - Electrokinetic phenomena
Glendinning et al (2015)

Diffusion

The application of an electric field during mass transport can generate chemical and pressure gradients. These gradients, particularly near the electrodes (Osman, 2018; Ottosen et al., 2008; Sharma et al., 2018), contribute

to diffusion. As Ottosen et al. (2008) explain, when desorption processes release ions into the pore water, a concentration gradient develops between the pore solution and the electrolyte solution at the electrode. This gradient drives the diffusion of ions.

Factors affecting electrokinetic remediation

pH is a critical factor in electrokinetic remediation, influencing the direction of electro-osmotic flow, degree of sorption and desorption of contaminants, formation of complexes, precipitation of chemical species, and dissociation of organic acids (Reddy & Cameselle, 2009).

(Reddy & Cameselle, 2009) highlight that pH significantly impacts contaminant mobility. For instance, elements like Cu and Zn become mobile under acidic conditions (Siegel, 2002). Król et al. (2020) observed a thousand-fold increase in Ni and Cu concentration under acidic conditions compared to alkaline environments. Conversely, Pb concentration decreases with decreasing pH. This difference arises due to the varying chemical speciation of cations and anions at different pH levels, as illustrated in Figure 21.

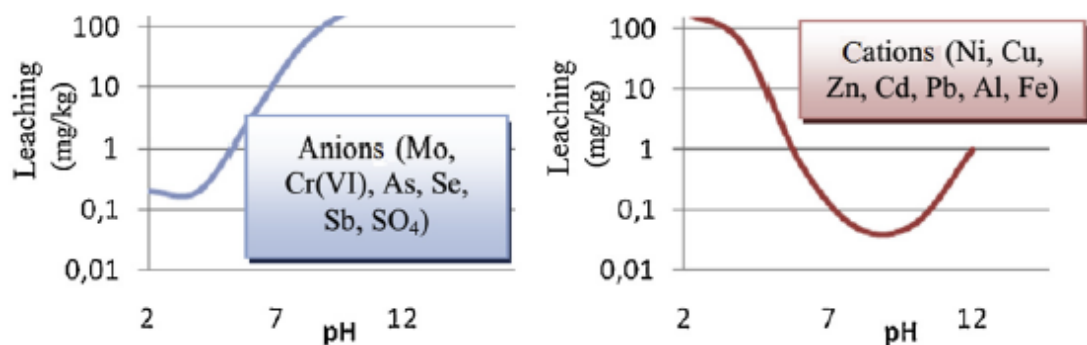
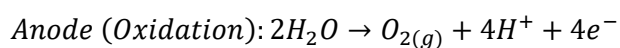
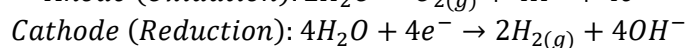


Figure 21 - Diagram of leaching as a function of pH
Król et al. (2020)

In addition to changes in the bulk soil, chemical reactions occur directly at the electrodes. The primary reaction is the electrolysis of water, generating hydrogen gas and hydroxyl ions at the cathode, and oxygen and hydrogen ions at the anode (Gregolec et al., 2005; Ribeiro & Mateus, 2016). These reactions, represented by Equation 4 and Equation 5, respectively, significantly alter the pH near the electrodes. The anode side can become highly acidic (pH 2.0-3.0), while the cathode side can reach a very high pH (up to 12.0) (Acar & Alshwabkeh, 1993; Alshwabkeh, 2009; Ramadan et al., 2018).



Equation 4



Equation 5

At the anode, the hydrogen ions produce an acid medium or acid front in which pollutants and or some ions such as Mg, Al, and Fe from the soil can dissolve in pore solution, allowing their recovery. On the other hand, the cathode produces an alkaline medium or basic front that can precipitate the ionic contaminants, making their recovery difficult. However, the concentration of ions as *Si* and *Al* increases with alkalinity conditions (Arbai et al., 2014; Page & Page, 2002; Ribeiro & Mateus, 2016; Sapsford et al., 2017). The acid front advances in the opposite direction by migration, pore fluid advection, hydraulic potential differences, and diffusion (Acar & Alshawabkeh, 1993), and the basic front moves towards the anode. When both fronts meet, there is a sudden change in pH, which produces changes in adsorption and solubility of contaminants. It was reported that ions such as Pb^{2+} , Zn^{2+} , Cd^{2+} , and Cu^{2+} precipitated as metal hydroxides when this happened (Page & Page, 2002).

When the medium treated with electrokinetic remediation does not have the buffering capacity, the chemistry will be dominated by the transport of hydrogen ions. Otherwise, some salts, organic species, and cation exchange capacity increases the buffering capacity (Acar & Alshawabkeh, 1993).

Besides, the secondary reactions can be present as described by Equation 6 to Equation 8, and they will depend on the concentration of available species (Acar & Alshawabkeh, 1993).



Where M_e refers to metals

Electrolysis-induced pH changes alter the electrolyte concentration, impacting soil properties (Arbai et al., 2014; Ribeiro & Mateus, 2016; Sapsford et al., 2017).

Several methods can be employed to control pH during electrokinetic remediation, including injection of appropriate solutions, switching electrode positions (fixing the cathode and moving the anode), electrolyte circulation, and application of non-uniform electric fields (Ma et al., 2018).

Zeta potential: The zeta potential, which is generally negative in soils due to isomorphic substitution and broken bonds, significantly influences the direction and rate of electro-osmotic flow (EOF). Zeta potential and EOF exhibit an inverse relationship: as the zeta potential decreases, the magnitude of the

electro-osmotic flow increases (F. Chen et al., 2019; Reddy & Cameselle, 2009; Virkutyte et al., 2002).

According to Wang et al. (2021), two main factors can influence the zeta potential during electrokinetic remediation: pH and ionic strength. As they explain, a decrease in pH (increasing acidity) can cause the zeta potential to become less negative or even positive. Conversely, an increase in ionic strength tends to make the zeta potential more positive. However, the sensitivity of zeta potential to these factors varies depending on the specific clay type.

Soil chemistry: Several characteristics influence the rate of contaminant removal during electrokinetic remediation, including adsorption, ion exchange, and the buffer capacity of the soil. Effective remediation of ionic contaminants relies on desorption, the process of removing them from soil particles. Page & Page (2002) observed that higher initial contaminant concentrations can facilitate faster decontamination, exceeding the ion exchange capacity of soil.

Electrokinetic processes can alter soil pH, impacting its adsorption capacity for contaminants. The electrolysis of water generates hydrogen (H^+) and hydroxyl (OH^-) ions, promoting the mobilization of metal cations and anions. Viadero et al. (1998) highlight that the availability of these H^+ and OH^- ions is linked to the soil's buffering capacity. Soil composition plays a crucial role in buffering capacity: the presence of calcium (Ca^{2+}), magnesium (Mg^{2+}), sodium carbonate (Na_2CO_3), or impurities like iron oxides, quartz, and titanium oxides contribute to a high buffering capacity, which can influence the soil's affinity for potentially toxic elements. Furthermore, as noted by Reddy & Cameselle (2009), buffering capacity itself is also dependent on the prevailing pH.

Electrical conductivity and field strength: During the electrokinetic remediation process, there are changes in the pH and ionic strength. These changes cause the electrical conductivity to be uneven and the voltage profiles to develop rapidly. The most notable changes occur near the cathode (Page & Page, 2002).

Water content: Eykholt (1997) points out that electrokinetic remediation can lead to uneven moisture distribution and consolidation zones within the soil. These phenomena are caused by negative pore pressure. Additionally,

the overall soil saturation level can significantly impact the electro-osmotic flow rate, ultimately affecting contaminant removal efficiency.

Coordination compound

Electrokinetic remediation can be enhanced by the addition of coordination compounds, which can increase the removal of contaminants. Coordination compounds, also called complexes, consist of two key components: (a) an electron donor (ligand or Lewis base) with lone-pair electrons, and (b) an electron acceptor (metal atom, cation, or Lewis acid) with empty orbitals (Kettle, 1996). As Yeung & Gu (2011) stated, contaminants can only be removed when they are mobile. Coordination compounds are employed to solubilize contaminants (e.g., metals) and keep them in a mobile chemical state, facilitating their removal. Recently, ligands such as EDTA have shown promise in improving remediation effectiveness (Song et al., 2016).

Ethylenediaminetetraacetic acid (EDTA): EDTA, a polyaminocarboxylic acid, finds applications in various fields according to Zhang et al. (2021), including chemical analysis, synthetic detergents, the paper industry, biology, and, particularly relevant here, metal ion remediation. This molecule possesses six potential binding sites for metal ions, consisting of two ammonia groups and four carboxyl groups, as illustrated in Figure 22.

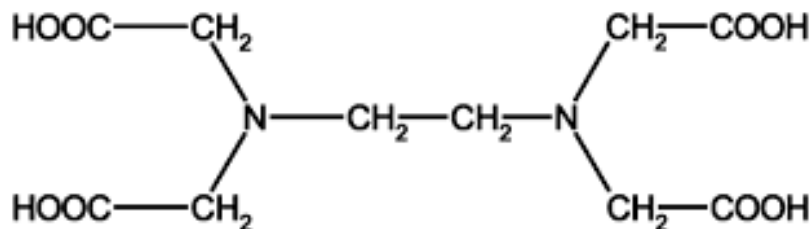


Figure 22 - Molecular structure of EDTA
Oviedo and Rodríguez (2003)

The lone pair electrons on EDTA's binding sites can fill in the electron vacancies of metal ions, forming complexes (Zhang et al., 2021). This complexation process promotes the solubilization of metals from the soil. Effectiveness of EDTA as a chelating agent stems from its strong complexing ability and minimal acidification of the medium, making it preferable to some alternatives (Gidaracos & Giannis, 2006). As GARVAN (1964) mentions, EDTA can form stable water-soluble chelates with many metal ions in a 1:1 ratio. According to Y. Chen et al. (2022), EDTA employs two removal mechanisms: desorbing potentially toxic elements from the soil through H⁺ input and

complexation. They further suggest that EDTA can form complexes with metal cations such as Pb^{2+} , Cu^{2+} , and Ni^{2+} . Figure 23 illustrates the metal retention mechanisms and processes involved in EDTA's interaction with soil, as described by Y. Chen et al. (2022).

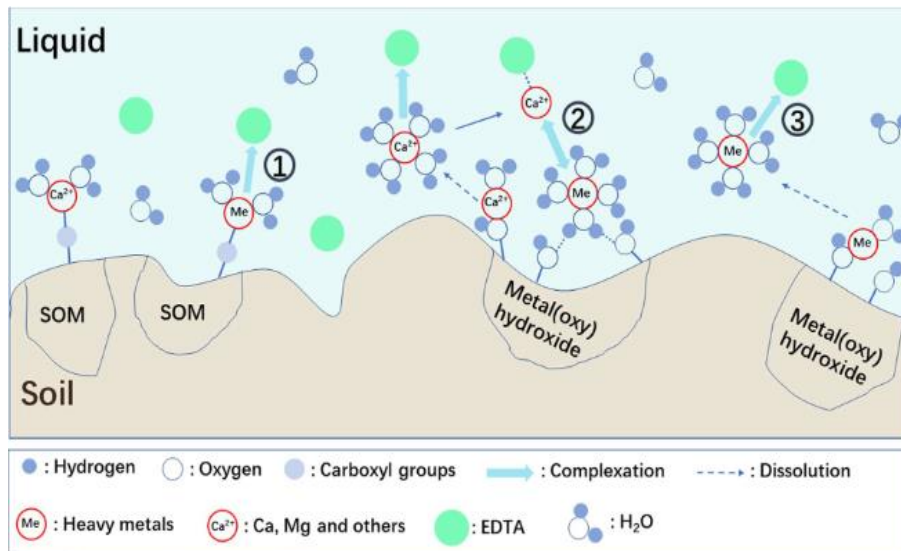


Figure 23 - Metals retention mechanism and processes faced by EDTA on soil (1) EDTA chelation of metal linked to organic matter/surface metal(oxy)hydroxide; (2) Ion exchange due to the main cation competition at low EDTA concentration; (3) Soluble metal complexation by EDTA (SOM: soil organic matter. Taken from Chen et al. (2022)

Humic substances are a ubiquitous component of soil and water environments, as De Boodt & Hayes (1990) explain. They arise from the decomposition of organic matter and transformations that occur in sediments. Humic substances are part of a broader category called humus, which also includes non-humic substances.

Non-humic substances are well-defined organic molecules with known structures and characteristics. These can be synthesized by microbes or result from modifications of existing organic materials in soil or waste. Examples include polysaccharides, polypeptides, and altered lignin De Boodt & Hayes (1990).

In contrast, humic substances are a complex and heterogeneous group of organic molecules with high molecular weights. They are resistant to degradation (refractory) and lack a single, well-defined structure. Unlike non-humic substances, humic substances cannot be easily categorized based on their chemical structure De Boodt & Hayes (1990).

Classification of humic substances and structure

Stevenson (1994) classified humic substances into three main fractions based on their solubility in water at different pH levels: humic substances, fulvic acids, and humin.

Humic substances: Insoluble in water at acidic pH (below pH 2) but become soluble under alkaline conditions.

Fulvic acids: Remain soluble in water at all pH values.

Humin: Insoluble in water regardless of pH.

It is important to note that this classification scheme categorizes humic substances based on solubility, not on their chemical composition. Each fraction (humic substances, fulvic acid, and humin) is a complex and heterogeneous mixture of various organic molecules De Boedt & Hayes (1990). Figure 24 illustrates a possible chemical structure for humic substances.

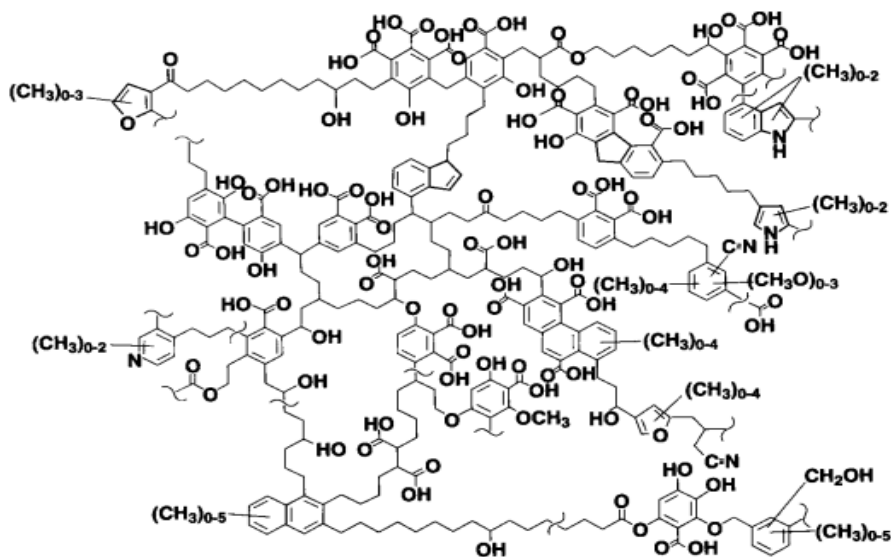


Figure 24 - Schematic of humic substances structure.
Donald (2002)

Humic substances exhibit a unique property called polyfunctionality, enabling them to interact with metals and organic chemicals. Perminova & Hatfield (1993) described the common elements of their structure: the average humic macromolecule consists of a central aromatic core with a high number of functional groups (mainly carboxyl and hydroxyl) and aliphatic side chains. This central aromatic core is surrounded by a periphery of hydrolyzable carbohydrate and protein fragments. As Stevenson (1994) mentioned, the presence of carboxylic and hydroxyl groups allows humic substances to form stable and mobile complexes with metals. These stable complexes can mobilize and transport potentially toxic elements within a porous matrix

(Bahemmat et al., 2016). This property makes humic substances valuable as complexing agents in the remediation process.

4. Methodology

The methodology to be used during the investigation is presented in the Figure 25.

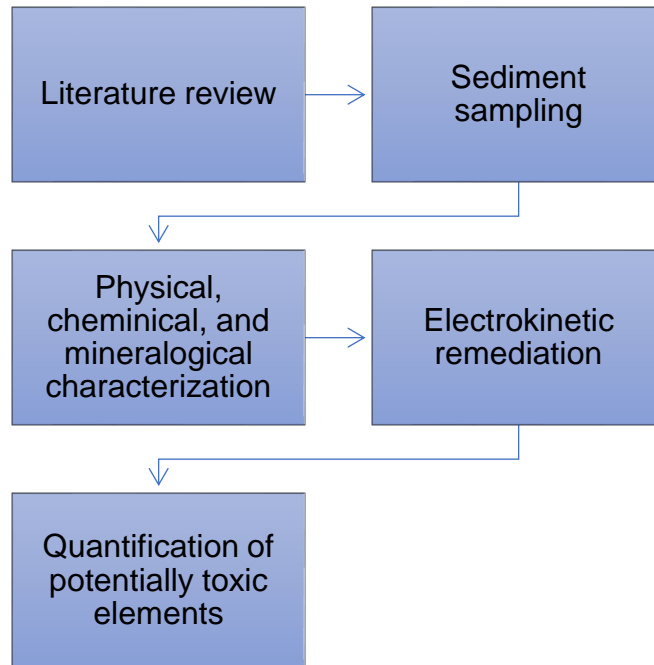


Figure 25 – Workflow
Created by author

4.1. Sediments physical and chemical characterization tests

Sediment samples underwent physical, chemical, and mineralogical characterization using the following standardized test methods.

Particle size distribution: The clay, silt, sand, and gravel fractions in sediment samples were determined through sieving and sedimentation, following the ABNT NBR 7181 (2016) standard. Additionally, a CILAS 1190 Particle Size Analyzer was used. This followed ISO (2020), which specifies that the level of obscuration should lie between 1% and 10%.

The organic matter content: The organic matter content of sediment samples was determined through combustion using a muffle furnace, following the ABNT NBR 13600 (2022) standard.

pH: The pH of sediment samples was determined following D4972-19 (ASTM, 2019b) for soils or D1293 (ASTM, 2018) for water, depending on the sample state.

Electric conductivity (EC): The electrical conductivity of sediment samples was determined following ISO (1994) for soils or D1125 (ASTM, 2014) for water, depending on the sample state.

Moisture content: The moisture content in sediment samples were determined in compliance with D2216-19 (ASTM, 2019a)

Atterberg limits: The determination of liquid limit and plasticity limit was performed in compliance with ABNT NBR 6459 (2017) and ABNT NBR 7180 (2016), respectively.

The concentration of potentially toxic elements: Coupled Plasma Optical Emission Spectrometry (ICP-OES) was used to determine the concentration of potentially toxic elements. This analysis was carried out using a 7300 DV instrument from Perkin Elmer Instruments, located at the *Laboratório de Espectrometria Atômica (LABSPECTRO) PUC-Rio*. The specific elements investigated were copper, zinc, lead and nickel, following the EPA 3051 A standard.

Additional Equipment for Sediment Characterization.

Thermogravimetric analysis (TGA) was performed with a TA Instruments NETZSCH STA 449F3 in the temperature range 25–1300 °C with a heating rate of 10 °C/min under an air stream (80/20). This analysis was carried at the *Laboratório de Departamento de Engenharia Química e de Materiais- PUC-Rio (Casa XXI da Vila dos Diretórios)*.

Fourier-transform infrared spectroscopy (FTIR) The structural-functional groups present in the thermally treated sediments were identified using Fourier-transform infrared spectroscopy (FTIR). This analysis was carried out with a Perkin-Elmer Frontier FTIR spectrometer located at the *Laboratório de Departamento de Engenharia Química e de Materiais- PUC-Rio (Casa XXI da Vila dos Diretórios)*.

4.2. Electrokinetic materials

Sediment

Permission to collect sediments was granted by INEA, whose sampling service assisted with the process. The sediments were collected from Camorim

Lagoon, with the specific location chosen based on a prior investigation by Masterplan (2015). Figure 26 illustrates the sampling station.

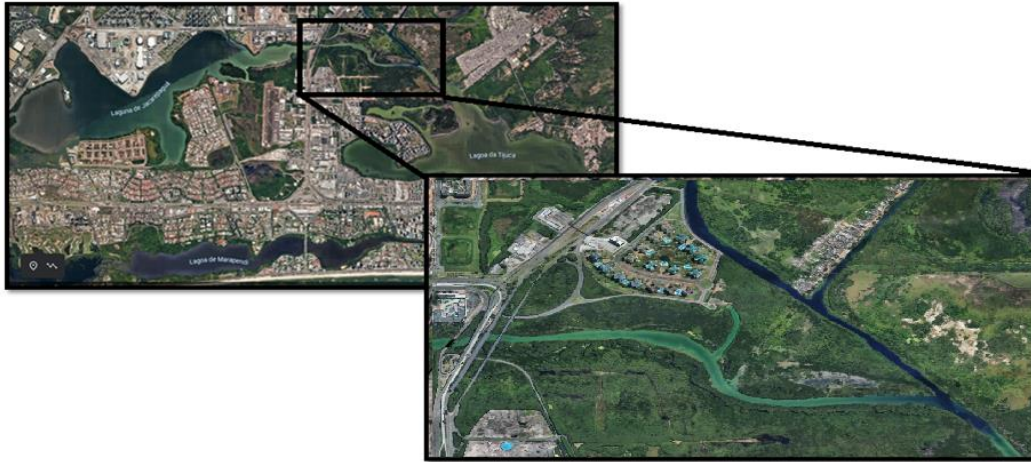


Figure 26 - Jacarepaguá lagoon system and Camorim lagoon
Google Earth

Electrolytic solution

Two electrolyte solutions were prepared to enhance metal removal. The first solution utilized EDTA, while the second employed humic substances. Water Type 1 served as the solvent for both solutions. Additionally, acetic acid and sodium hydroxide were included as a buffer system.

Humic substances: For the electrokinetic treatment, an electrolyte solution was prepared using water Type 1 and Aport Max, a commercial product with a high humic substance (HS) content (55% humic substances and 15% fulvic acid). Therefore, humic substances were chosen due to their complex structure, which enhances various chemical interactions, including the formation of stable complexes with potentially toxic elements (Perminova & Hatfield, 1993). A concentration of 5 g L^{-1} was used, based on the findings of Bahemmat et al. (2016).

EDTA (Ethylenediaminetetraacetic acid): The electrolyte solution was prepared using disodium EDTA and water Type 1. Therefore, EDTA was chosen due to its strong chelating ability, which allows it to form stable water-soluble complexes with many metals, resulting in minimal acidification of the medium (GARVAN, 1964; Gidaracos & Giannis, 2006). A concentration of 0.1 M EDTA was employed in the electrokinetic treatment, based on the research conducted by Rozas & Castellote (2012).

Buffer solution: A buffer solution was prepared using Type 1 water to maintain a stable pH during the electrokinetic treatment. This solution contained both acetic acid (AA) and sodium hydroxide (NaOH). A concentration

of 0.3 M acetic acid was used based on a literature review, and 1.6 M sodium hydroxide was added until a pH of 7 was reached. Due to its effectiveness, acetic acid is a popular choice for pH control in such experiments (F. Chen et al., 2019; Fu et al., 2017; Tian et al., 2017).

Electrokinetic device

The electrokinetic experiments were conducted using a custom-built cell fabricated from Perspex in *the Laboratório de Geotecnia e Meio Ambiente - PUC-Rio* (Figure 27). Consequentially, the cell is designed to accommodate various test conditions and features two electrode holders, two electrodes, two electrolyte reservoirs, and a dedicated sample compartment.

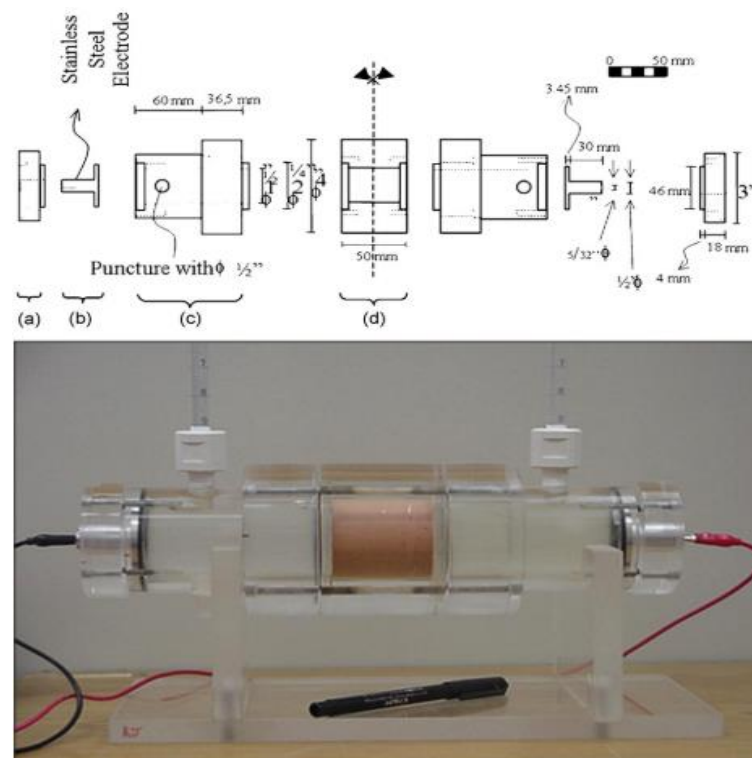


Figure 27 - Electrokinetic cell
da Rocha et al (2009)

Electrodes are fixed on the acrylic plate and connected to the DC power supply. They have no direct contact with the sample to achieve a homogeneous current density over the end surfaces.

Two pipettes are connected to the electrode compartments, which allow the volume variation of solution and exhaust of gasses.

4.3. Electrokinetic treatments

Electrokinetic remediation was employed at *Laboratório de Geotecnia e Meio Ambiente - PUC-Rio* as a method to reduce the concentration of potentially toxic elements in sediment samples.

Experimental Design

Four tests were performed using different electrolyte solutions. Each test was carried out in triplicate and included a control group for comparison, ensuring results were not solely attributed to the passage of time. For the electrolyte solutions, acetic acid (AA), sodium hydroxide (NaOH), and humic substances (HS) were used. A constant electric potential of 1 V cm^{-1} was selected based on a literature review (Song et al., 2016; SONG et al., 2018) for all tests. Table 5 summarizes the details of each test.

Table 5 - Electrokinetic test

Test	Anolyte	Catholyte	Duration (days)
EK1	Fresh water	Fresh water	7.0
EK2	0.01 M NaOH	0.3 AA M+ 0.1 M EDTA	9.0
EK3	Buffer solution	0.3 AA M+ 0.1 M EDTA	11.0
EK4	HS 5 g L^{-1}	HS 5 g L^{-1}	11.0

Created by author

Electrolyte Monitoring: Throughout the electrokinetic treatment process, aliquots of both the anolyte (solution near the anode) and catholyte (solution near the cathode) were collected periodically using a syringe with a 2 mm diameter hose. The collected samples were used to monitor the pH and electrical conductivity (EC) of the solutions. The removed electrolytes were then replaced with fresh solutions to maintain consistent conditions.

4.3.1. Nomenclature of electrolytes

A unique identifier is used to name the electrolyte samples collected during the experiment. The format is "EK#-X", where "#" represents a number identifying the specific electrokinetic treatment. An additional letter suffix is used to differentiate between the anolyte ("A") and catholyte ("C") solutions within each treatment. Control samples, which were not subjected to an electric current, are denoted by "C" at the end of the identifier (e.g., "EK2-C-C"). Therefore, "EK2-A" refers to the anolyte solution from electrokinetic treatment 2, and "EK2-C-C" refers to the catholyte solution from the control group in

electrokinetic treatment 2. Figure 28 exemplified the aliquots of electrolytes and the nomenclature.

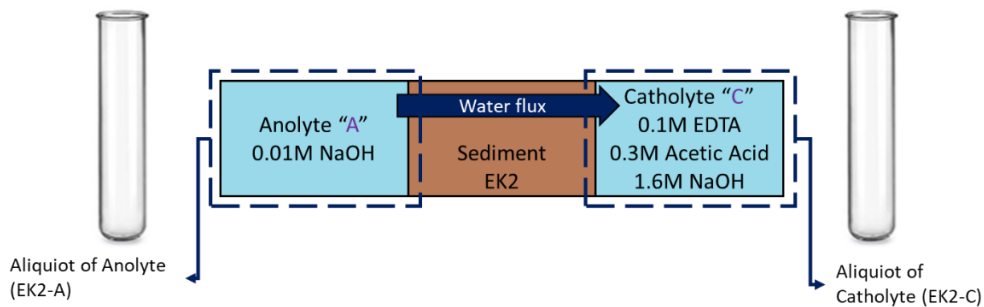


Figure 28 - Example of electrolyte samples from an electrokinetic treatment
Created by author

Post-Treatment Analysis: Following treatment period, the sediment samples were sectioned into three roughly equal portions: anodic (near the anode), middle, and cathodic (near the cathode). These sections were then analyzed for pH, EC, and potentially toxic element concentrations.

4.3.2. Sediment nomenclature

A unique identifier is used to name the sediment samples collected after the electrokinetic treatment. The format is "EK#-XS", where "#" represents a number identifying the specific electrokinetic treatment, and "S" indicates the sample is sediment. An additional letter prefix is used to differentiate between sections of the sample after treatment: "A" for the anodic section, "M" for the middle section, and "C" for the cathodic section. Control samples, which were not subjected to an electric current, are denoted by "C" at the end of the identifier (e.g., "EK2-C-S"). Therefore, "EK3-CS" refers to the sediment sample from the cathodic section of electrokinetic treatment 3, and "EK3-AS-C" refers to the sediment sample from the anodic section of the control group in electrokinetic treatment 3.

The sediment samples were sectioned into approximately three equal portions: anodic, middle, and cathodic, as illustrated in Figure 29. These sections were then assigned unique identifiers based on the naming system described above.

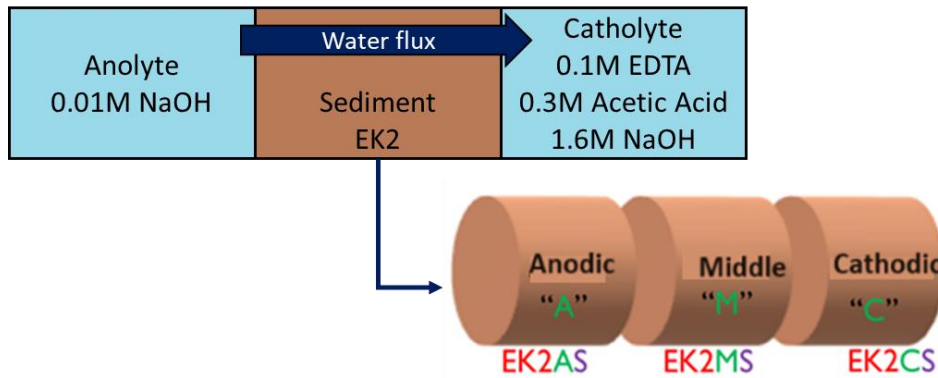


Figure 29 - Example of sediment samples from an electrokinetic treatment
Created by author

Table 6 presents the nomenclature used for electrolytes and sediment samples in test EK1, which is similar to other tests.

Table 6 - Nomenclature of electrolytic samples and sediment samples

Treatment	Nomenclature	Description
EK1	EK1-C	Catholyte for experiment EK1
	EK1-A	Anolyte for experiment EK1
	EK1-C-C	Control catholyte for experiment EK1
	EK1-A-C	Control anolyte for experiment EK1
	EK1-CS	Cathodic sediment for experiment EK1
	EK1-MS	Middle sediment for experiment EK1
	EK1-AS	Anodic sediment for experiment EK1
	EK1-CS-C	Control cathodic sediment for experiment EK1
	EK1-MS-C	Control middle sediment for experiment EK1
EK1-AS-C	Control anodic sediment for experiment EK1	

Created by author

Electrokinetic Parameters: The electric current applied was also monitored throughout the experiment.

5. Results and discussion

5.1. Sampling location

The sediments used in the electrokinetic tests were collected from Camorim Lagoon, Rio de Janeiro, Brazil, in July 2022. The specific sampling station, designated CP1, is located at coordinates 22°58.533'S latitude and 43°21.511'W longitude (Figure 30).

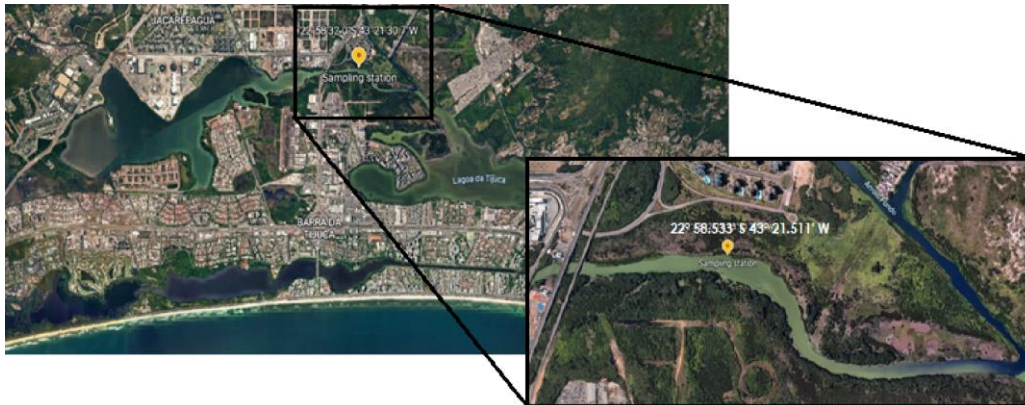


Figure 30 - Sampling station
Google Earth

A Van Veen sampler was used to extract the sediment from the designated sampling station (Figure 30). The collected material, approximately 47 kg in total, was then stored in plastic bags for transport. To maintain cool conditions during transport, the sediment was placed in a thermal box and transported to the laboratory.

Upon arrival at the laboratory, the sediment was homogenized using a mechanical mixer to ensure a representative sample for further testing. Following homogenization, the sediment was stored under refrigeration at 4°C.



Figure 31 - Sampling collection. A) Van Veen sampler before sampling B) Van Veem sampler after sampling.

5.2. Geotechnical characterization

Grain size distribution was determined using the standard NBR 7181 and a particle size analyzer. The results are presented in Figure 32 (distribution) and Table 7 (passing percentage summary).

Table 7 - Physical characterization of sediments

Parameter	Testing method	Results
Particle size distribution	ABNT NBR 7181(2016a)	Medium sand 1.5 %
		Fine sand 6.7 %
		Silt 72.4 %
		Clay 19.4%
Particle size distribution	Particle size analyzer	Medium sand 0.0 %
		Fine sand 1.0 %
		Silt 90.0 %
		Clay 9.0 %
Moisture content	ASTM D2216 (2019).	318.5 %
Liquid limit	ABNT NBR 6459 (2016b)	141.6 %
Plasticity limit	ABNT NBR 7180 (2016c)	56.0 %
Plasticity index	ABNT NBR 7180 (2016c)	85.6 %
Grain density	ABNT NBR 6457 (2016c)	2.54

Created by author

The liquid limit and plasticity limit values obtained were consistent with the findings of Almeida (2001a).

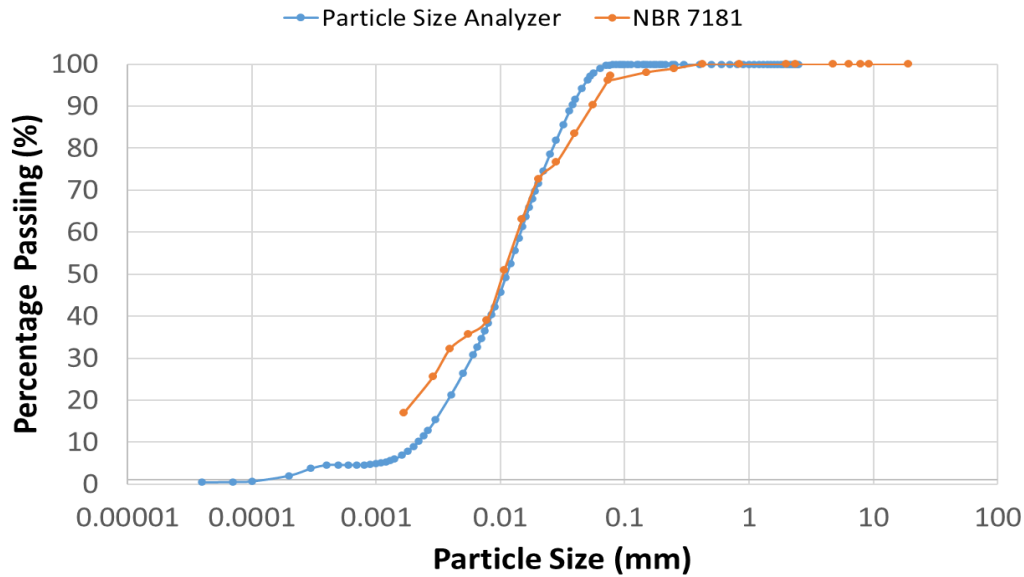


Figure 32 - Grain size distribution
Created by author

The grain size distribution of the sediment was determined using two methods: the NBR 7181 standard and a particle size analyzer. The results are presented in Figure 32 (distribution curve) and Table 7 (summary of percent passing).

A notable difference is observed in the clay content between the two methods (Figure 32). The NBR 7181 standard yielded a higher percentage of clay (19.4%) compared to the particle size analyzer (9.0%). This discrepancy is likely due to the use of sodium hexametaphosphate, a deflocculant, in the NBR 7181 method. Deflocculants break down particle aggregates, potentially leading to an overestimation of clay content in this method. Conversely, the higher percentage of medium and fine sand measured by the particle size analyzer might be attributed to the smaller sample size (0.1 g) compared to the NBR 7181 method (50 g). A larger sample size, as used in the NBR 7181 standard, might provide a more representative picture of the overall grain size distribution.

Despite methodological differences, both analyses in Figure 32 indicate that the sediment is predominantly composed of silt and clay. This finding aligns with previous studies, such as the Masterplan 2015, which reported a similar dominance of fine-grained textures in the top 10 cm of sediments in the area. The shape of Camorim Lagoon, resembling a channel, likely facilitates the accumulation of fine-grained sediments discharged or transported into the lagoon from nearby sources like Arroio Pavuna to the west and Arroio Fundo to the east.

5.3. Chemical characterization

The pH and electrical conductivity (EC) of both the sediment samples and the lagoon water were measured at the *Laboratório de Geotecnia e Meio Ambiente do Departamento de Engenharia Civil da PUC-Rio*. A Hanna Instruments HI11310 pH meter was used to measure pH, while a Hanna Instruments HI763100 conductivity electrode was employed to determine EC. The results of these measurements are presented in Table 8.

Table 9 presents the initial concentrations of potentially toxic metals in the sediment samples.

Table 8 - Chemical characterization of sediments and water

Test characterization	Testing method	Results
pH sediment	ASTM D4972 (2019)	7.11
pH water	ASTM D1293 (2018)	7.73
Electrical conductivity sediment	ISO 11265 (1994)	13.37 mS cm ⁻¹
Electrical conductivity water	ASTM D1125 (2014)	8.48 mS cm ⁻¹

Created by author

Table 9 - Initial concentration of potentially toxic metals in sediments

Parameter	Testing method	Results	Limit quantitation	Limit detection
Zn		287.33 mg kg ⁻¹	0.005	0.0016
Pb	ICP-OES	46.00 mg kg ⁻¹	0.034	0.0104
Ni	EPA 3051A	27.33 mg kg ⁻¹	0.007	0.0022
Cu		76.00 mg kg ⁻¹	0.00002	0.0001
Cr		40.67 mg kg ⁻¹	0.005	0.0016

Created by author

5.4. Mineral characterization

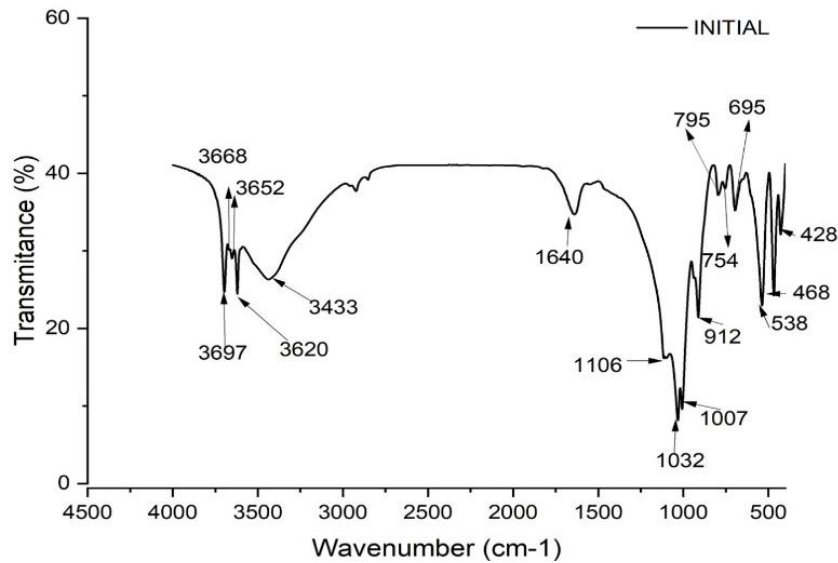


Figure 33: FTIR spectra of sediment
Created by author

Figure 33 shows the Fourier Transform Infrared (FTIR) spectrum of the sediment. The absorption bands indicate the presence of kaolinite and quartz.

Kaolinite Identification:

Pure kaolinite, with aluminum in the octahedral positions, produces four characteristic infrared (IR) absorption frequencies in the stretching region due to hydroxyl groups. These occur at approximately 3695 cm⁻¹, 3669 cm⁻¹, and 3653 cm⁻¹. These hydroxyls reside at the octahedral surface of the layers and form weak hydrogen bonds with the oxygens of the Si-O-Si bonds on the lower surface of the next layer (Madejová, 2003; Pansu & Gautheyrou, 2007; Souri et al., 2015).

The bands at 3697 cm⁻¹, 3668 cm⁻¹, and 3652 cm⁻¹ (stretching) correspond to inner hydroxyl groups, while the band at 3620 cm⁻¹ corresponds to outer hydroxyl groups (Ferone et al., 2015; Linares et al., 2013; Pansu & Gautheyrou, 2007).

FTIR analysis identified bands at 795 cm⁻¹ and 695 cm⁻¹, characteristic of quartz (Ferone et al., 2015; Souri et al., 2015). Additionally, bands at 1106 cm⁻¹, 1032 cm⁻¹, and 1007 cm⁻¹ indicated the presence of siliceous oxide, while a band at 912 cm⁻¹ suggested the presence of inner hydroxyl groups (Linares et al., 2013; Pansu & Gautheyrou, 2007). A band at 1640 cm⁻¹ was

attributed to water hydration (Ferone et al., 2015; Pansu & Gautheyrou, 2007), and a band at 538 cm^{-1} suggested deformation of the siliceous oxide network (Pansu & Gautheyrou, 2007).

The results of the thermogravimetric analysis are presented in Figure 34. An approximate weight loss of 3% was observed in temperature between 30 and 200 °C, likely attributed to the removal of adsorbed water or weakly bound water within the sediment (Božič et al., 2023; Ferone et al., 2015).

A further weight loss of 8% occurred between temperature of 200 and 450 °C, potentially resulting from the oxidation of organic residues (Ferone et al., 2015) or the decomposition of iron oxyhydroxides (Zheng et al., 2022).

Between 450 and 550 °C, a weight loss of 5.3% was observed, associated with the dehydroxylation of clay minerals (Eliche-Quesada et al., 2021; Touhami et al., 2024) and subsequent collapse of the clay structure (Ferone et al., 2015). According to Souri et al. (2015), the well-defined peak of weight loss in this temperature range (450 and 550 °C) is suggested to be associated with kaolinite, indicating the completion of kaolinite the dihydroxylation at approximately 600 °C (Fernandez et al., 2011).

The dehydroxylation of other clay minerals, such as illite and montmorillonite, occurs gradually across a wider temperature range, with the most significant mass loss typically observed between 600 and 900 °C (Dixit et al., 2021).

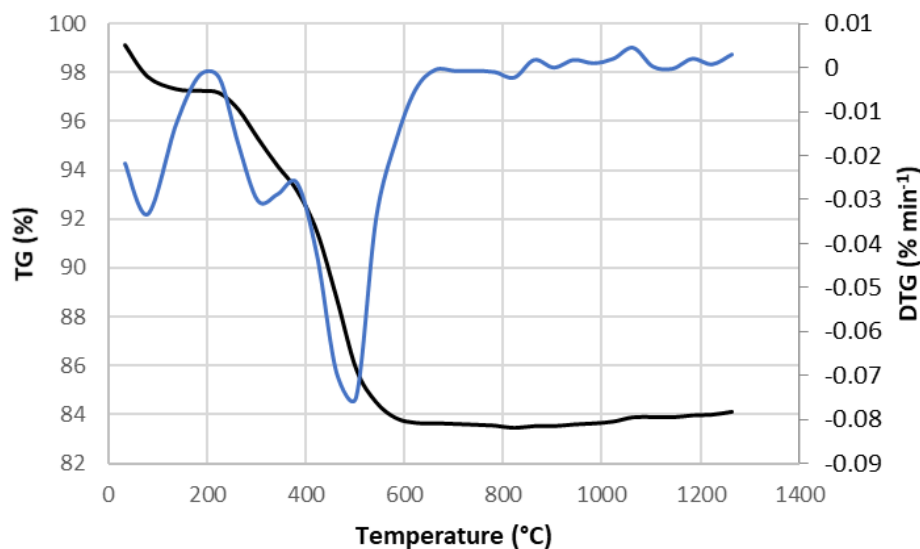


Figure 34 - TG of sediment before thermal treatment
Created by author

5.5. Electrokinetic test

Figure 35 illustrates the four electrokinetic treatments employed in this study, detailing the electrolyte solution used in each chamber (anolyte and catholyte). Additionally, a control treatment was included for each experiment, performed without applying any electrical current.

EK1: Both the anolyte and catholyte chambers contained fresh water.

EK2: The anolyte chamber contained a sodium hydroxide solution, while the catholyte chamber contained a combined solution of EDTA, citric acid, and sodium hydroxide.

EK3: The anolyte chamber contained a solution of citric acid and sodium hydroxide, while the catholyte chamber contained a solution of EDTA, citric acid, and sodium hydroxide.

EK4: Both the anolyte and catholyte chambers contained a solution of humic substances.

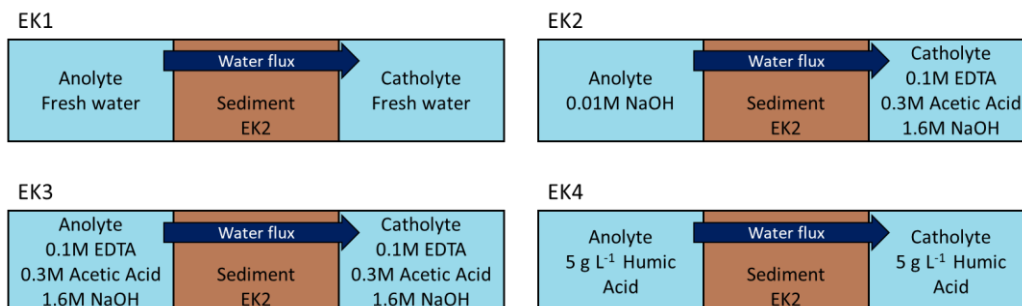


Figure 35 - Electrokinetic test with electrolytes. A) EK1 treatment 1. B) EK2 treatment 2. C) EK3 treatment 3. D) EK4 treatment 4
Created by author

5.5.1. pH

These results analyze the pH behavior of both the electrolytes throughout the experiment and the final pH of the sediment samples. This allows for a comprehensive understanding of how different electrolytes affect the overall pH conditions during electrokinetic treatment.

Electrolytes

Figure 36 and Figure 37 illustrates the pH variations within each electrolyte throughout the experiment. Notably, the catholytes in treatments 1 (EK1-C) and 4 (EK4-C) experienced a rapid rise in pH. This is likely because

fresh water and humic substances solution, neither of which have significant buffering capacity, were used in these treatments. Additionally, humic substances do not form strong complexes that dissociate when an electric current is applied. Therefore, the behavior of humic substance solutions is similar to that of water. Consequently, when subjected to water electrolysis, the pH of these solutions rapidly increased, exceeding 12 within 24 hours. In contrast, the catholytes of treatments 2 (EK2-C) and 3 (EK3-C) remained below pH 6 and 6.5, respectively, despite water electrolysis. This response suggests that the buffer solution composed of acetic acid and sodium hydroxide effectively controlled the pH increase, preventing it from reaching the high values observed in the catholytes without a buffer.

All anolyte exhibited a rapid decline in pH, reaching values below 2 within two days, as shown in Figure 36. These results suggest that neither the buffer solution used in treatment 3 (EK3) nor the sodium hydroxide solution in EK2 was effective in controlling the pH decrease caused by water electrolysis.

The pH of both anolytes and catholytes in the control treatments generally remained constant throughout the experiment. However, the pH of electrolytes in the control for treatment 1 (EK1-C-C and EK1-A-C) exhibited a slight decrease, changing from approximately 7.33 to 6 within the first day. This change stabilized after 24 hours, and the pH remained constant thereafter. This initial variation may be attributed to the interaction between the fresh water and the sediment.

Studies have consistently shown that electrokinetic treatment leads to a rise in catholyte pH due to the generation of hydroxide ions (OH^-) and a decrease in anolyte pH due to the production of hydrogen ions (H^+). Beyrami (2021) and Estabragh et al. (2019) observed similar pH changes during water electrolysis experiments. Interestingly, Kanbar et al. (2023) reported an increase in catholyte pH even with citric acid present.

In contrast, the pH of the electrolytes in the control for treatment 3 (EK3-C-C and EK3-A-C) remained constant from the beginning of the treatment, maintaining a pH of around 4. This stability is likely due to the presence of a buffer solution in both electrolytes, which effectively resisted changes in pH

Both the catholyte and anolyte exhibited a stable pH range between 9.86 and 8.37 throughout the control treatment. Since their composition (5 g L⁻¹ humic substances) was identical and their pH behavior mirrored each other, the observed variations likely stem from interactions with the sediment.

The catholyte maintained a constant pH of around 4, likely due to the buffering capacity of the electrolyte solution. In contrast, the pH of anolyte decreased during the experiment. This decrease is possibly caused by reactions between hydroxyl ions (OH^-) and cations (K^+ , Mg^{2+} , Fe^{2+} , Fe^{3+} , Ca^{2+}) in the sediment, or by the dissolution of silicon (Si^{4+}) and aluminum (Al^{3+}), as reported by Z. Chen et al. (2023).

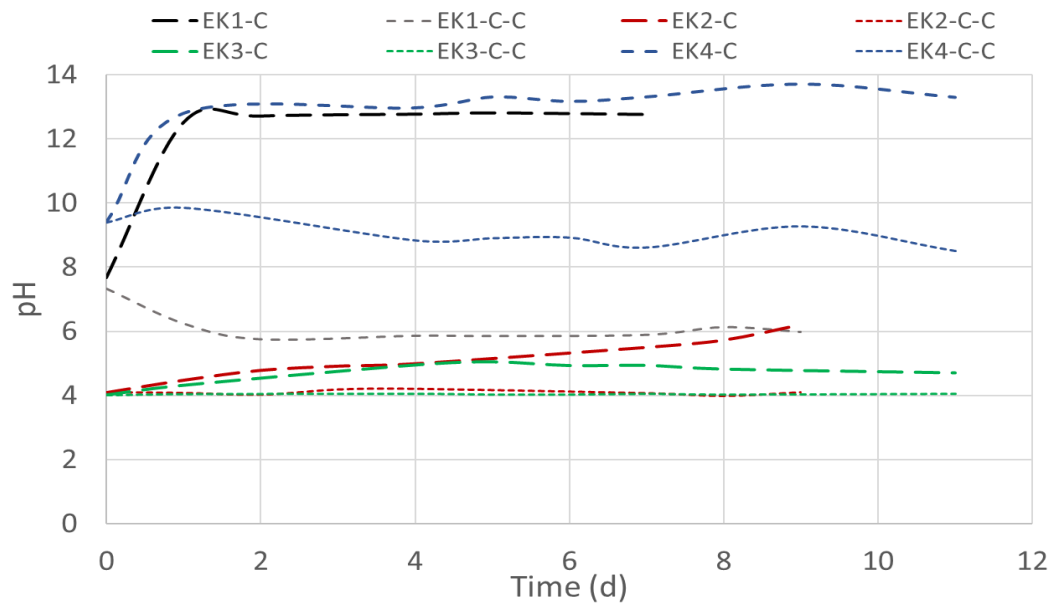


Figure 36 - pH variation in catholytes during treatment
Created by author

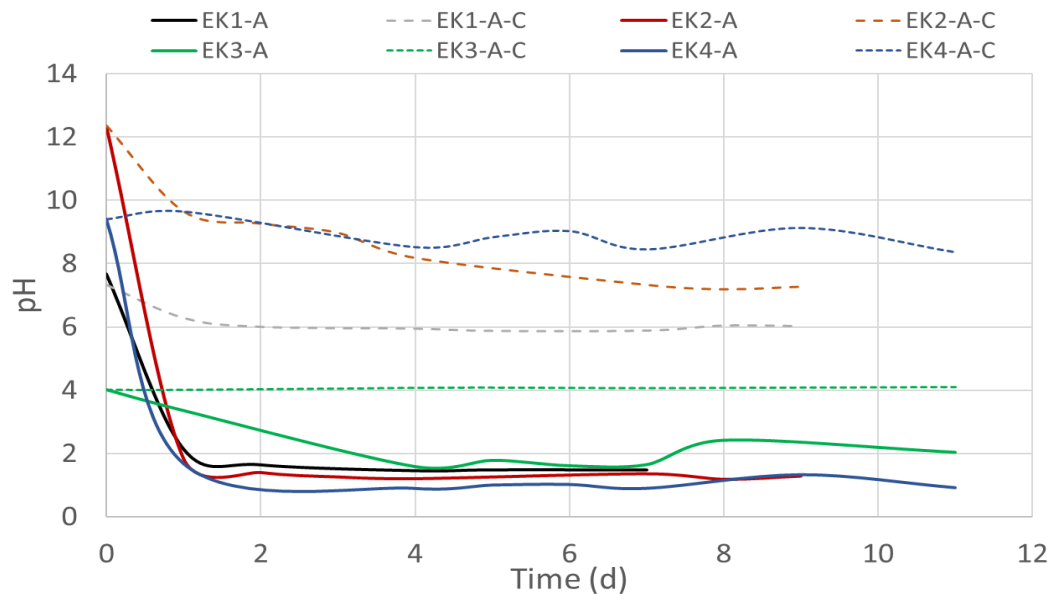


Figure 37 - pH variation in anolytes during treatment
Created by author

Sediment

Figure 38 presents the final pH of the sediment samples after electrokinetic treatment. This data clearly illustrates the influence of both water electrolysis and the selected electrolytes on the overall sediment pH.

The electrolytes of treatments EK1 and EK4, lacking a built-in ability to resist pH changes (buffering capacity), resulted in significant shifts in sediment pH. This is because water electrolysis naturally creates hydroxyl ions (OH^-) near the cathode (negative electrode), which significantly increased the pH of the sediment in that region (reaching 9.1 and 8.4 for EK1 and EK4, respectively, as shown in Figure 38). Conversely, the production of hydrogen ions (H^+) at the anode (positive electrode) caused a sharp decrease in the pH of the sediment near the anode (reaching 2.5 and 1.9 for EK1 and EK4, respectively). This finding aligns with previous research by Fu et al. (2017), Kanbar et al. (2023), and Mohamadi et al. (2019), who observed a similar pattern of low pH near the anode and high pH near the cathode in treated soils.

Treatments EK2 and EK3 incorporated a buffer solution and EDTA in their catholytes, which efficiently countered the pH increase near the cathode. This resulted in significantly lower pH values (5.9 and 4.6 for EK2 and EK3, respectively) compared to treatments without buffer control, as seen in Figure 38. However, while effective for the cathode, the use of sodium hydroxide as the anolyte in EK3 was not as successful in regulating pH near the anode. Consequently, the anodic sediment exhibited lower pH values. This finding highlights the critical role of the anolyte composition in maintaining overall pH balance during electrokinetic remediation.

The pH of the control treatments exhibited minimal changes compared to the electrokinetic treatments. The most notable exception was observed in the catholyte of the control group for treatment EK2, where the pH reached 5.4. This variation likely stems from the use of a catholyte solution with an initial pH of 4.0 in this specific control treatment.

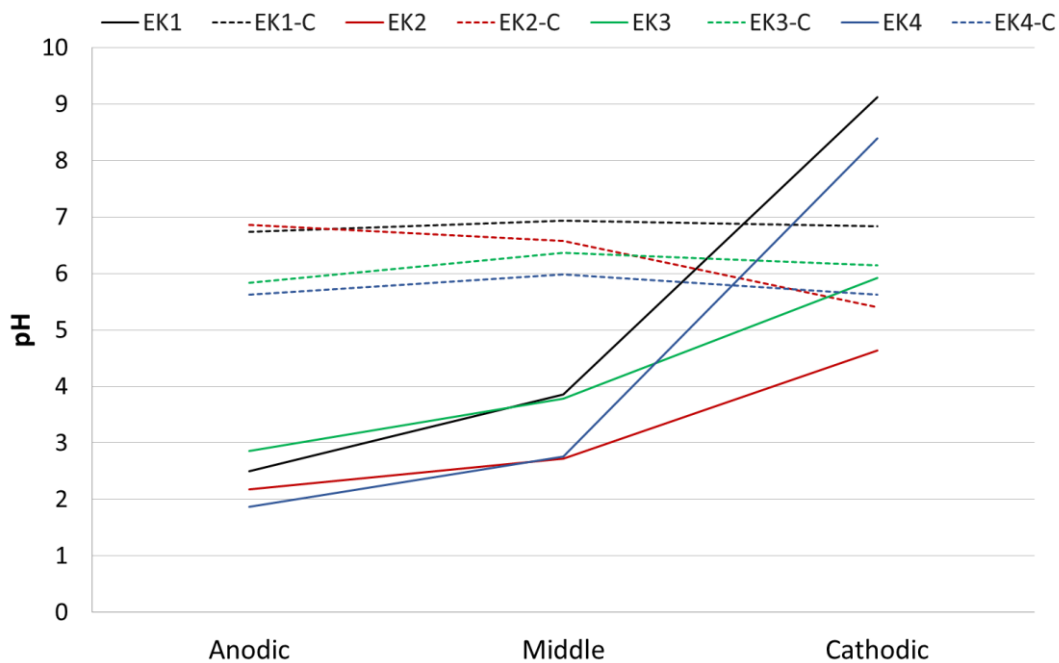


Figure 38 - pH of sediment
Created by author

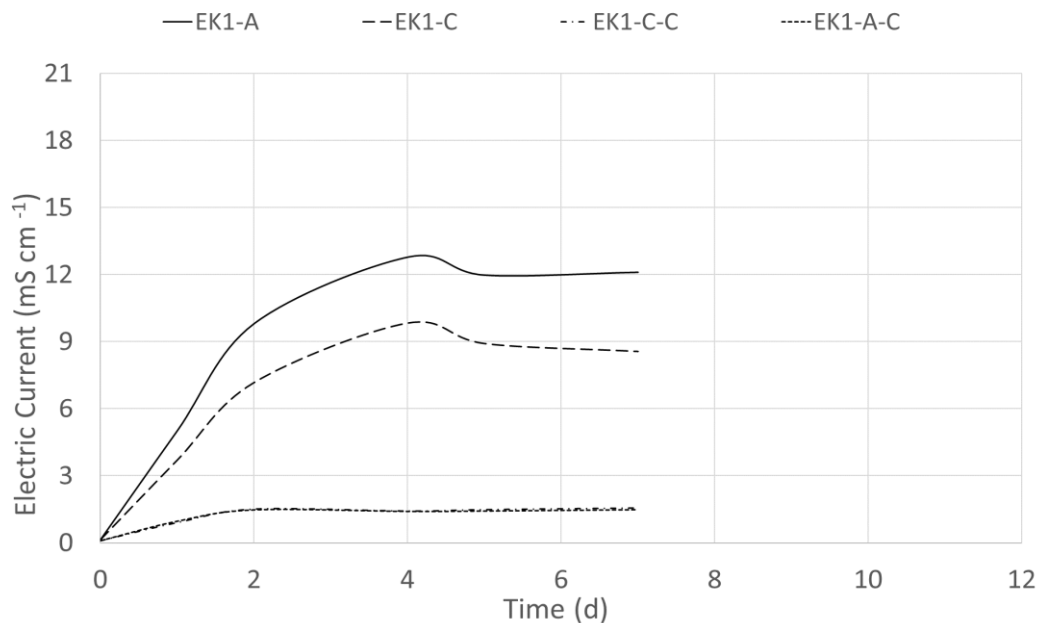
5.5.2. Electric conductivity

These results examine the electrical conductivity (EC) behavior within the electrolytes throughout the experiment. Additionally, they investigate the final EC of the sediment samples, revealing how different electrolytes influence overall EC during electrokinetic treatment.

Electrolytes

Figure

39



to Figure 42 illustrate the varying initial electrical conductivity (EC) values across the different treatments. This variation is due to the use of distinct electrolytes in each treatment, as detailed in Figure 35. Notably, in treatments EK1 and EK4, the initial EC of the anolyte and catholyte solutions is identical. Both EK1 and EK4 begin with an initial EC of 0.104 mS cm⁻¹ (for EK1) and 1.846 mS cm⁻¹ (for EK4), respectively, for both the anolyte and catholyte.

Both anolytes and catholytes exhibited a similar trend in electrical conductivity (EC). Their EC values increased rapidly during the initial days of the experiment, followed by a gradual decrease until reaching a stable state. This behavior aligns with observations by Estabragh et al. (2019), who also reported an increase in EC over time.

However, treatment EK1 displayed a distinct pattern. In this treatment, the anolytes consistently exhibited higher EC compared to the catholytes. This can be attributed to the lower mobility of hydroxyl ions (OH⁻) and cations like Ca²⁺ compared to hydrogen ions (H⁺). This phenomenon is also discussed by Kanbar et al. (2023).

As expected, the electrical conductivity (EC) of the control treatments (without applied electric current) remained relatively constant throughout the experiment. This is because there is no mobilization of charged ions caused by an electric field. However, a slight change in EC was observed during the first day, likely due to the interaction between the electrolytes and the sediment they

were in contact with. Electrolytes can promote the dissolving (solubilization) of ions present in the sediment.

Treatment EK3-C-C, containing a mixture of buffer solution and EDTA, exhibited the most significant change in EC during the first day. Its EC decreased from 12.04 mS cm⁻¹ to 7.91 mS cm⁻¹, but then remained stable throughout the rest of the experiment. This initial decrease in EC for EK3-C-C, along with EK3-A, EK3-C, and EK3-A-C, might be attributed to the precipitation of some of the buffer solution components.

An unexpected finding was observed in the initial EC values of the catholyte solutions for EK2-C and EK2-C-C. These solutions had a higher initial EC (14.57 mS cm⁻¹) compared to EK3-C and EK3-C-C (12.04 mS cm⁻¹). This difference could be due to the fact that the solutions were prepared on separate dates and might have used slightly different reagents. Although both EK2 and EK3 had a similar initial pH (around 4.0 and 4.1, respectively), small variations in pH can influence EC.

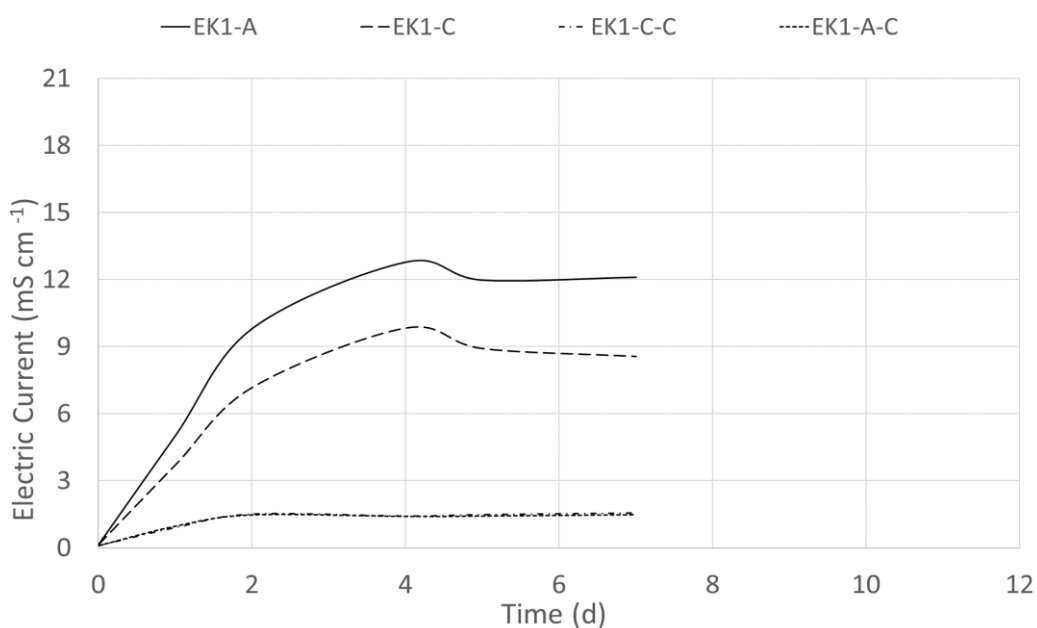


Figure 39 - Electric conductivity variation in electrolytes during EK1 treatment

Created by author

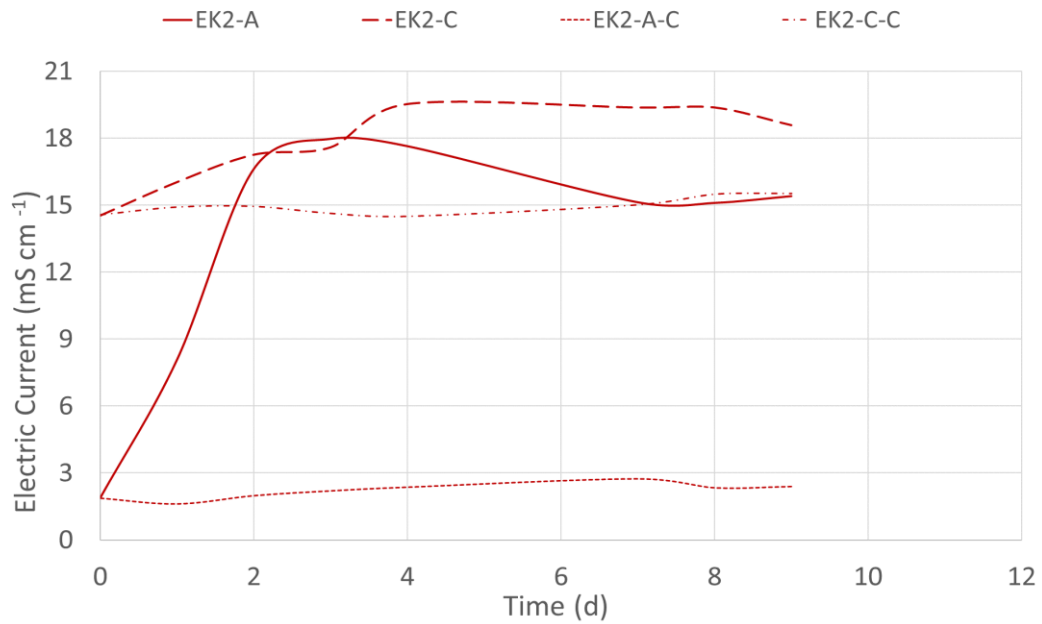


Figure 40: Electric conductivity variation in electrolytes during EK2 treatment
Created by author

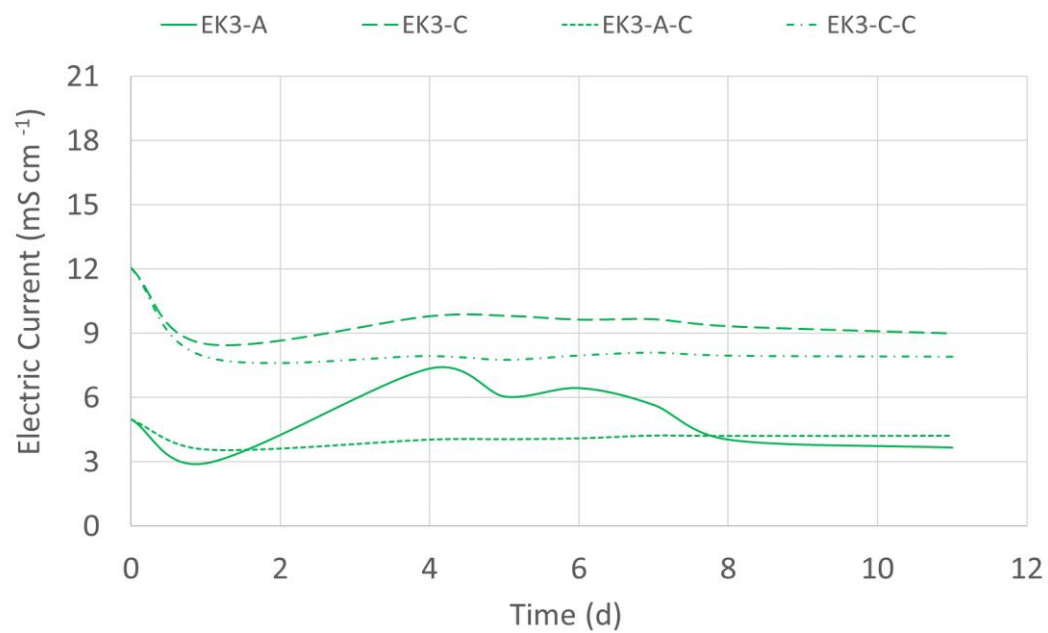


Figure 41 - Electric conductivity variation in electrolytes during EK3 treatment
Created by author

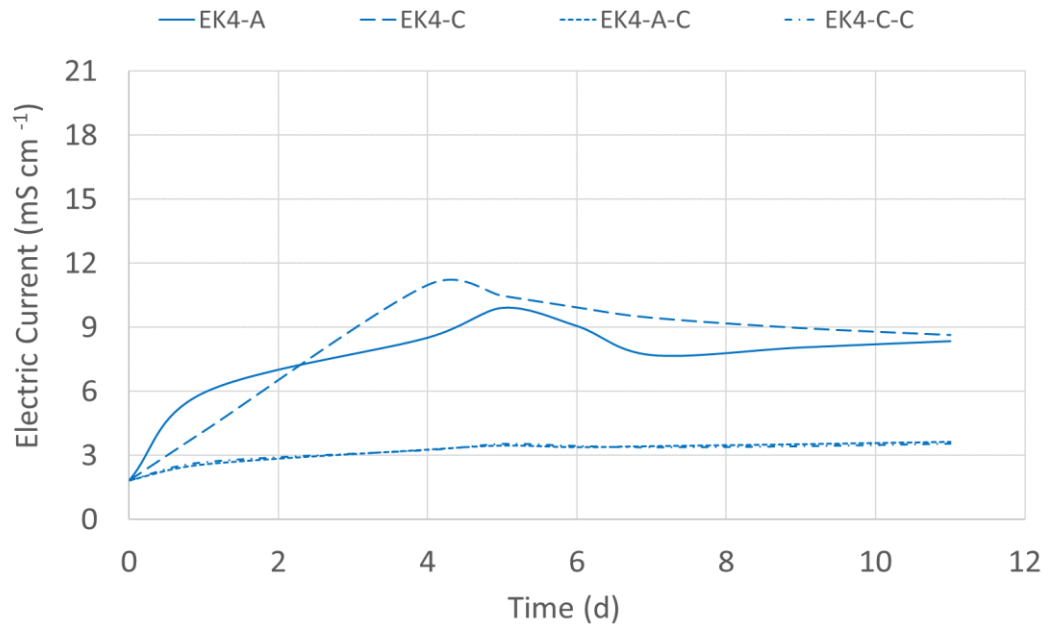


Figure 42 - Electric conductivity variation in electrolytes during EK4 treatment
Created by author

Sediment

As shown in Figure 43, the electrical conductivity (EC) of the sediment samples varied depending on their location within the treatment section (anodic, middle, or cathodic) after electrokinetic treatment. Interestingly, the sediment closest to the anode and cathode (the extremities) had higher EC compared to the central region. This makes sense because these end zones were closer to the electrolytes, which had high starting EC values (in the millisiemens per centimeter range, mS cm^{-1}). Additionally, the electric field applied during treatment likely caused ions to move throughout the sediment, further influencing EC (Kanbar et al., 2023; Tang et al., 2020). Similar findings were reported by Kanbar et al. (2023), who attributed this pattern to the combined effects of ions produced during water electrolysis (like hydrogen ions, H^+ , and hydroxyl ions, OH^-) and ions released from the sediment itself.

When looking at the control treatments (EK2 and EK3 without an electric current), higher EC readings were observed in the cathodic section. This is likely because the catholytes in these treatments contained high concentrations of ions. In contrast, the control treatments for EK1 and EK4 displayed minimal changes in EC throughout the sediment.

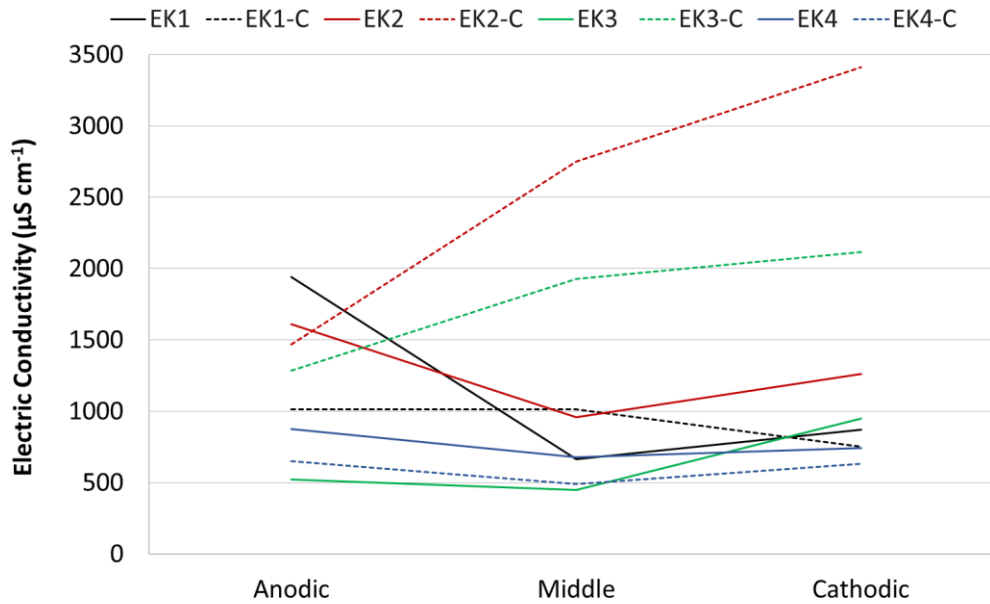


Figure 43 - Electric conductivity of sediment
Created by author

5.5.3. Concentration of potentially toxic substance

Figure 44 to Figure 48 illustrate the concentrations (mg kg^{-1}) of potentially toxic elements in the sediment following electrokinetic treatment. The figures also present the initial concentration, control test results, and the levels 1 and 2 set by CONAMA Resolution N° 454 of 2012. All sections (anodic, middle, cathodic) were analyzed for each treatment.

Sediment

Figure 44 displays the zinc concentration (mg kg^{-1}) measured in each section (anode, middle, cathode) of the treatment zones for all treatments, including the control test. It also presents the initial zinc concentration and the regulatory limits set by CONAMA Resolution N° 454 of 2012.

EK1 treatment

As shown by the blue bars in Figure 44, zinc concentration is lowest at the anode (52.33 mg kg^{-1}), followed by the middle section ($104.50 \text{ mg kg}^{-1}$), and highest at the cathode ($311.00 \text{ mg kg}^{-1}$). This distribution likely reflects the influence of pH, with lower pH at the anode facilitating the desorption of zinc cations. These results suggest electro-osmosis, possibly combined with electromigration, as the primary mechanisms governing zinc transport in EK1. This indicates a potential synergy between these two processes. Notably, the

anode and middle sections fall below the level 1 limit (150 mg kg^{-1}) established by CONAMA Resolution N° 454 of 2012.

In contrast, the light blue bars for the control treatment reveal relatively consistent concentrations (around $286.00 \text{ mg kg}^{-1}$) across all sections. This indicates that water alone, used as the electrolyte in this test, was ineffective in removing zinc.

EK2 treatment

The green bars in Figure 44 show that zinc transport in EK2 was towards the anode side. The highest concentration ($340.50 \text{ mg kg}^{-1}$) was found on this side, while the middle and cathode sections had lower concentrations ($123.00 \text{ mg kg}^{-1}$ and $136.50 \text{ mg kg}^{-1}$, respectively). This suggests electromigration as the primary transport mechanism. This reduction was likely due to the catholyte used, which contained EDTA and a buffer solution. These components facilitated the desorption of zinc and formed negatively charged complexes with it, leading to its transport towards the anode side. Notably, the middle and cathode sections fell below the level 1 limit set by CONAMA Resolution N° 454 of 2012.

The light green bars represent the control for EK2. A considerable reduction in concentration was observed on the cathode side, likely due to the presence of EDTA in the catholyte, which promoted zinc desorption.

EK3 treatment

As shown by the orange bars in Figure 44, EK3 exhibited the lowest zinc concentration across all sections compared to the initial value. Zinc was transported towards the anode side, resulting in the highest concentrations there. This suggests electromigration as the primary transport mechanism, likely promoted by the EDTA and buffer solution in the catholyte. These components facilitated zinc desorption and formation of negatively charged complexes that were then transported by electromigration.

Despite having the lowest overall zinc concentration, only the sediment corresponding to the cathodic section ($124.33 \text{ mg kg}^{-1}$) fell below level 1 ($150.00 \text{ mg kg}^{-1}$) of CONAMA Resolution N° 454 of 2012. However, the middle section was very close, with a concentration of $152.00 \text{ mg kg}^{-1}$, while the anode section remained the highest at $183.00 \text{ mg kg}^{-1}$. Song et al. (2016) achieved

favorable results (~35% removal efficiency) using EDTA as both anolyte and catholyte, suggesting its potential for enhancing zinc removal.

The light orange bars represent the control for EK3. The cathode section exhibited the lowest concentration, likely due to EDTA promoting zinc desorption from the sediment.

EK4 treatment

The purple bars in Figure 44, show the zinc concentration distribution for EK4. The lowest concentration was found in the anode section (87.33 mg kg^{-1}), followed by the middle section ($240.00 \text{ mg kg}^{-1}$), and the highest at the cathode section ($537.33 \text{ mg kg}^{-1}$). This pattern likely reflects the influence of pH, similar to EK1. Therefore, the primary transport mechanisms are likely electro-osmosis, possibly combined with electromigration. Similar to EK3, only one section in EK4 has a zinc concentration below the level 1 limit set by CONAMA Resolution N° 454 of 2012. This was the anode section with 87.33 mg kg^{-1} .

The light purple bars represent the control for EK4. The similar concentration across all three sections suggests that humic substances under these pH conditions (~8.9 in the anolyte and ~9.0 in the catholyte) do not promote zinc desorption, unlike EK2 and EK3 control treatments.

All treatments exhibited a trend of zinc accumulation in either the anode or cathode section, as shown in Figure 44. Despite having the highest concentration in the anode section ($183.00 \text{ mg kg}^{-1}$), EK3 achieved the lowest overall zinc content compared to the initial value. This value remains lower than the peak concentrations observed in EK1 ($311.00 \text{ mg kg}^{-1}$ cathode), EK2 ($340.50 \text{ mg kg}^{-1}$ anode), and EK4 ($537.33 \text{ mg kg}^{-1}$ cathode). Notably, only the cathode section in EK3 fell below the level 1 limit ($150.00 \text{ mg kg}^{-1}$) set by CONAMA Resolution N° 454 of 2012. Extending the treatment duration might be necessary to achieve compliance across all sections in EK3 and potentially other treatments.

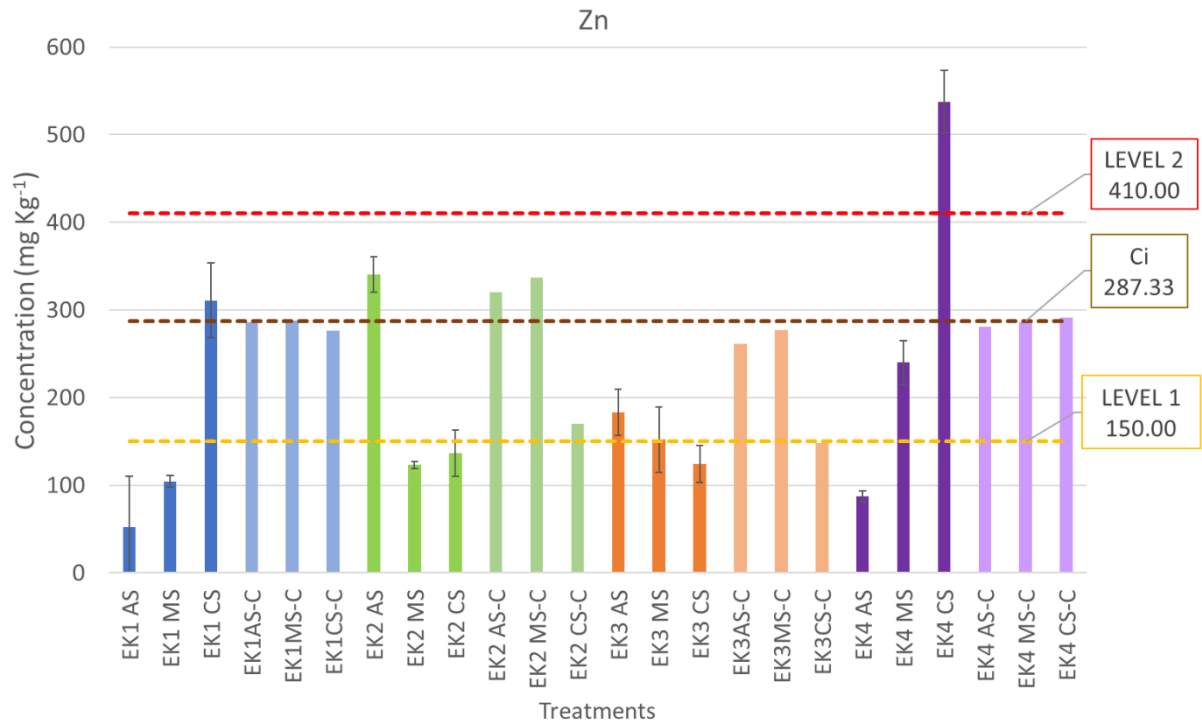


Figure 44 - Zinc concentration at the end of electrokinetic treatments
Created by author

Figure 45 displays the lead concentration (mg kg^{-1}) measured in each section (anode, middle, cathode) of the treatment zones for all treatments, including the control test. It also presents the initial lead concentration and the level 1 limit set by CONAMA Resolution N° 454 of 2012. Due to the high level 2 limit (218 mg kg^{-1}), data for this level is omitted for better visualization.

EK1 treatment

The blue bars in Figure 45, represent the lead concentration for EK1. Lead concentration increased towards the anode, with values of 38.67 mg kg^{-1} , 29.50 mg kg^{-1} , and 26.00 mg kg^{-1} for anode, middle, and cathode sections, respectively. Unlike most metal cations, lead in EK1 (using freshwater as an electrolyte) migrated towards the anode, likely due to the formation of soluble metal hydroxides at the high pH environment. Importantly, all sections were below the level 1 limit (46.70 mg kg^{-1}) set by CONAMA Resolution N° 454 of 2012.

The light blue bars represent the control treatment using water. These sections show a relatively equal concentration around the initial lead level, indicating that water alone was ineffective in removing lead.

EK2 treatment

As shown by the green bars in Figure 45, lead transport in EK2 displayed a clear direction towards the anode side. The highest concentration was observed in the anode section, with lower concentrations in the middle and cathode sections. This suggests electromigration as the primary transport mechanism, potentially facilitated by the EDTA and buffer catholyte, which promoted lead desorption and the formation of negatively charged complexes (EDTA-lead complexes).

The concentration in the anode section (60.50 mg kg^{-1}) exceeded the level 1 limit (46.70 mg kg^{-1}) set by CONAMA Resolution N° 454 of 2012. Interestingly, both the middle and cathode sections had concentrations below the limit, at 25.00 mg kg^{-1} and 24.00 mg kg^{-1} , respectively.

The control for EK2, shown in light green bars, exhibited a minor reduction in lead concentration, primarily in the cathode section. This likely indicates some desorption due to the presence of EDTA in the catholyte.

EK3 treatment

Similar to the zinc results in EK3, the lead concentration across all sections was the lowest compared to the initial value, as shown by the orange bars in Figure 45. The anode and middle sections had equal concentrations (33.67 mg kg^{-1}), while the cathode section had the lowest (23.67 mg kg^{-1}). This is likely due to the catholyte containing EDTA and buffer solution, which promoted lead desorption and the formation of negatively charged complexes that were then transported by electromigration towards the anode side. All sections in EK3 treatment were below the level 1 limit (46.70 mg kg^{-1}) of CONAMA Resolution N° 454 of 2012.

EDTA likely aided lead desorption and complexation for transport towards the anode. Hahladakis et al. (2016) observed similar results with zinc, nickel, and lead, suggesting that potentially toxic metals may have formed complexes with organic matter, facilitating transport towards the anode. Wen et al. (2023) and Song et al. (2016) also found EDTA effective for lead removal.

The control for EK3, shown in light orange bars, displayed the lowest concentration in the cathode section, likely due to EDTA in the catholyte promoting lead desorption from the sediment. While the concentrations in the anode and middle sections were near the initial concentration (46.00 mg kg^{-1}).

EK4 treatment

Unlike other treatments where concentration reduction occurred in a single direction, EK4 (represented by the purple bars in Figure 45) exhibited low lead concentrations in both the anode and cathode sections compared to the middle section. This complexity makes determining a single direction of lead transport difficult.

The concentration in the anode section (45.67 mg kg^{-1}) was very close to the initial concentration (46.00 mg kg^{-1}). The concentrations in the middle and cathode sections were 51.67 mg kg^{-1} and 44.00 mg kg^{-1} , respectively. It appears that the humic substances in the catholyte partially formed negative complexes with lead, which were then transported towards the anode but accumulated in the middle section. This suggests that humic substances are not as efficient at forming strong complexes.

Both the anode (45.67 mg kg^{-1}) and cathode (44.00 mg kg^{-1}) sections in EK4 fell below the level 1 limit set by CONAMA Resolution N° 454 of 2012 (46.70 mg kg^{-1}). The consistent concentration across all sections in the control treatment (light purple bars) suggests humic substances at these pH values (around 8.9 and 9.0) has minimal lead desorption capacity. This contrasts with EK2 and EK3 controls, where EDTA facilitated lead removal.

Figure 45 highlights that EK2 concentrated lead in the anode section, while humic substances in EK4 were ineffective for desorption and complexation. EK1 and EK3 achieved the best results, with all sections falling below the regulatory limit. Extending treatment duration might lead to even lower concentrations in all treatments.

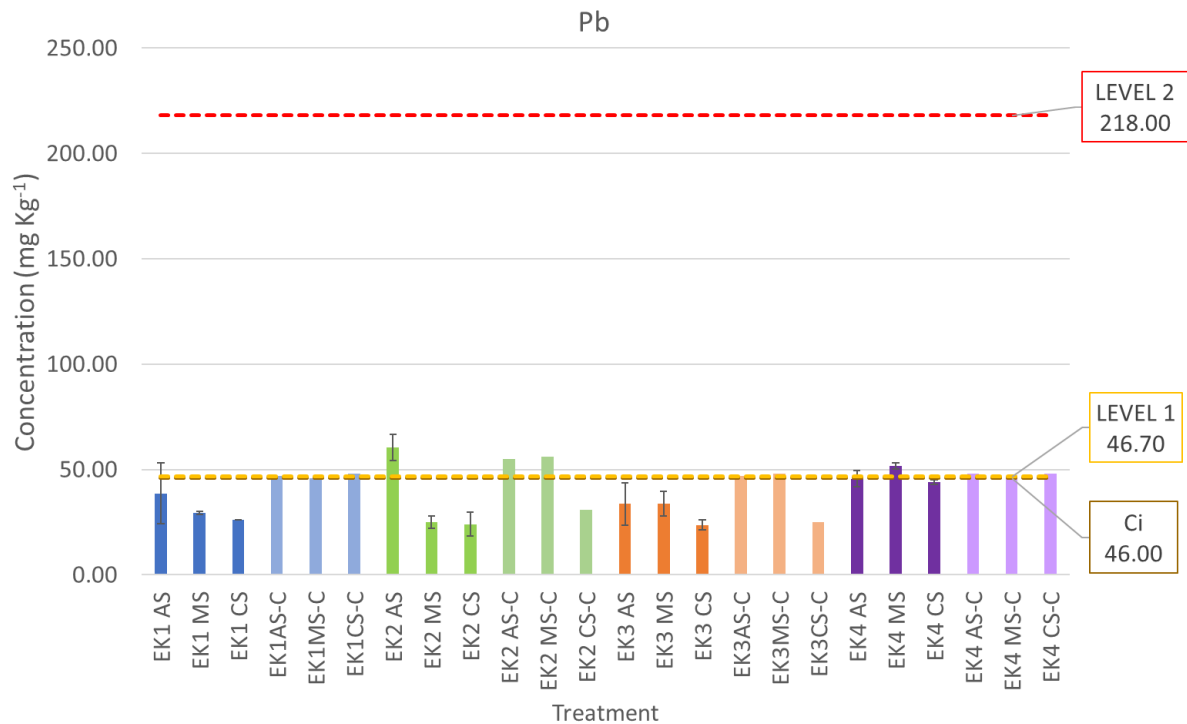


Figure 45 - Lead concentration at the end of electrokinetic treatments
Created by author

Figure 46 displays the nickel concentration (mg kg^{-1}) measured in each section (anode, middle, cathode) of the treatment zones for all treatments, including the control test. It also presents the initial nickel concentration and the level 1 and 2 limits set by CONAMA Resolution N° 454 of 2012.

EK1 treatment

The blue bars in Figure 46 reveal a clear increase in nickel concentration towards the cathode side in EK1. The anode section exhibits the lowest concentration (16.00 mg kg^{-1}), followed by the middle section (17.67 mg kg^{-1}), with the cathode section having the highest (22.33 mg kg^{-1}). This distribution suggests electromigration or electro-osmosis as the likely transport mechanism. Notably, two sections (anode and middle) fall below the level 1 limit (20.90 mg kg^{-1}) established by CONAMA Resolution N° 454 of 2012.

The light blue bars represent the control treatment using water. It shows almost no change in nickel concentration (around 26.00 mg kg^{-1}) across all sections, reflecting the original sediment level. This confirms that water alone was ineffective in removing nickel.

EK2 treatment

EK2 treatment, shown by the green bars in Figure 46, does not exhibit a clear direction of nickel transport. The concentrations across all three sections are quite similar: 26.50 mg kg⁻¹ in the anode, 24.00 mg kg⁻¹ in the middle, and 24.67 mg kg⁻¹ in the cathode. Unfortunately, all sections exceed the level 1 limit set by CONAMA Resolution N° 454 of 2012.

The control for EK2 (light green bars) shows similar results, with a slight reduction in the cathode section. While the middle section has the lowest concentration, the difference compared to the other two sections is negligible. These findings suggest that the chelating agent, EDTA, was not effective in enhancing nickel desorption from the sediment or its transport as a complex under these test conditions.

EK3 treatment

Similar to EK2, EK3 treatment shows almost identical nickel concentrations between all sections (orange bars in Figure 46): 21.33 mg kg⁻¹ in the anode, 22.00 mg kg⁻¹ in the middle, and 21.33 mg kg⁻¹ in the cathode. This makes determining the direction of nickel transport difficult. While all sections exceed the level 1 limit, they also fall below the initial concentration (26.00 mg kg⁻¹). This suggests that the pH control from the buffer solution improved desorption compared to EK2 but remains less effective than EK1. Additionally, the results suggest that EDTA was ineffective in promoting nickel desorption or complexation under these test conditions.

EK4 treatment

EK4 treatment, showcased by the purple bars in Figure 46, reveals a rising nickel concentration towards the cathode. The anode section exhibits the lowest level (23.00 mg kg⁻¹), followed by the middle section (26.00 mg kg⁻¹), and finally, the cathode section with the highest concentration (31.33 mg kg⁻¹). This distribution suggests electromigration or electro-osmosis as the potential transport mechanisms. Similar to EK1, the lower pH in the anode section likely promotes nickel desorption. However, none of the sections in EK4 comply with the level 1 limit.

Under the control conditions with pH values around 8.9 and 9.0 (light purple bars), humic substances exhibit minimal nickel desorption capacity, as evidenced by the consistent concentration across all sections. This contrasts with EK1, where water alone achieved some reduction.

Figure 46 reveals that only EK1 achieved nickel concentrations (all sections) below the level 1 limit set by CONAMA Resolution N° 454 of 2012. The results for EK2 suggest that the electrolytes used were ineffective in promoting nickel desorption. Although EK3 showed a better outcome than EK2, all sections remained above the regulatory limit. While EK4 exhibited a direction of transport towards the cathode, more extended treatment times might be necessary for nickel removal. Notably, none of the treatments except EK1 achieved a significant reduction in nickel compared to the initial concentration. This suggests that the chosen pH values of the electrolytes, especially EK2, were inadequate for effective nickel desorption, and the presence of humic substances might have further hindered its release from the sediment.

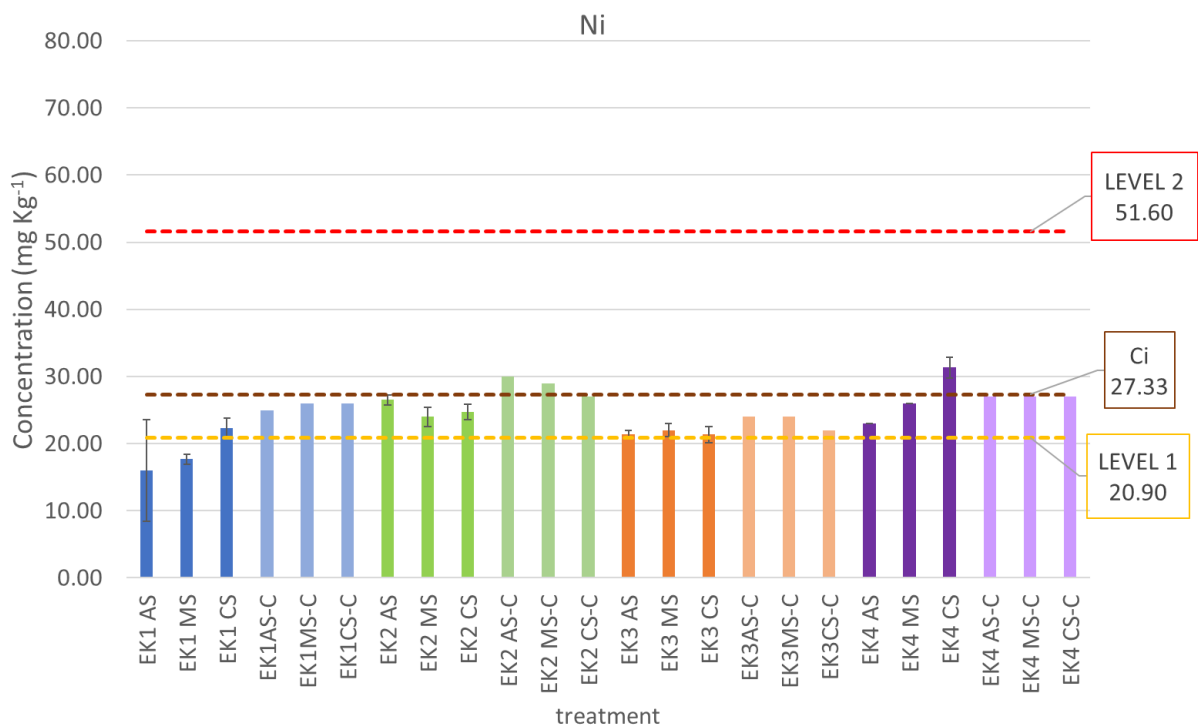


Figure 46 - Nickel concentration at the end of electrokinetic treatments
Created by author

Figure 47 displays the copper concentration (mg kg⁻¹) measured in each section (anode, middle, cathode) of the treatment zones for all treatments and the control test. It also presents the initial copper concentration and the level 1 limit set by CONAMA Resolution N° 454 of 2012. Due to the high level 2 limit (270 mg kg⁻¹), data for sediment is omitted for better visualization.

EK1 treatment

The blue bars in Figure 47 show the copper concentration distribution in EK1. Unlike nickel and zinc, copper migrated towards the anode (52.33 mg kg⁻¹), with lower concentrations in the middle (44.00 mg kg⁻¹) and cathode sections (36.50 mg kg⁻¹). This suggests the formation of soluble copper hydroxides at high pH, which were transported by electromigration. While all sections are below the initial concentration (76.00 mg kg⁻¹), none meet the level 1 limit (34.00 mg kg⁻¹) set by CONAMA Resolution N° 454 of 2012.

The control test (light blue bars) shows minimal change in copper concentration across all sections, indicating water alone is ineffective for copper removal.

EK2 treatment

The green bars in Figure 47 represent the copper concentration results for EK2. The middle section exhibits a slightly higher concentration (79.33 mg kg⁻¹) compared to the anode (72.00 mg kg⁻¹) and cathode (73.67 mg kg⁻¹). While there's a slight decrease in opposing sections, the overall pattern lacks a clear direction of copper transport. All sections exceed the level 1 limit.

The control for EK2 (light green bars) shows a modest reduction in the cathode section, but the change is negligible. This suggests the chelating agent, EDTA, was ineffective in enhancing copper desorption under these test conditions.

EK3 treatment

Similar to EK2, EK3 treatment exhibits almost identical copper concentrations across all sections (orange bars), making it difficult to determine the transport direction. While all sections (70.33 mg kg⁻¹, 73.33 mg kg⁻¹, and 72.00 mg kg⁻¹ for anode, middle, and cathode, respectively) remain above the level 1 limit, they are lower than the initial concentration. This suggests the buffer solution in EK3 might have improved desorption compared to EK2, but EDTA remained ineffective.

The control for EK3 (light orange bars) shows slightly lower copper concentrations in the cathode and middle sections, but the difference is minimal, again suggesting minimal impact from EDTA.

EK3 treatment

EK4 treatment (purple bars) shows a rising copper concentration towards the anode (78.67 mg kg⁻¹), followed by the middle section (77.67 mg kg⁻¹) and

the cathode section (70.00 mg kg^{-1}). This distribution suggests electromigration or electro-osmosis as potential transport mechanisms. However, none of the sections comply with the level 1 limit.

The lower pH in the anode section during EK4 treatment likely promotes copper desorption, but the desorbed copper could then be transported towards the cathode by electro-osmosis or electromigration.

The control conditions with pH values around 8.9 and 9.0 (light purple bars) show minimal copper desorption capacity, as evidenced by the consistent concentration across all sections.

Figure 47 highlights that none of the treatments achieved copper concentrations below the level 1 limit set by CONAMA Resolution N° 454 of 2012. However, EK1 exhibited the lowest overall copper concentration. These results suggest that chelating agents (EDTA) and humic substances were not effective in promoting copper desorption. Increasing the treatment time for EK1 might be necessary to achieve compliance. The lack of significant reduction in other treatments, except EK1, suggests that the chosen electrolyte pH and the presence of humic substances might have hindered copper desorption.

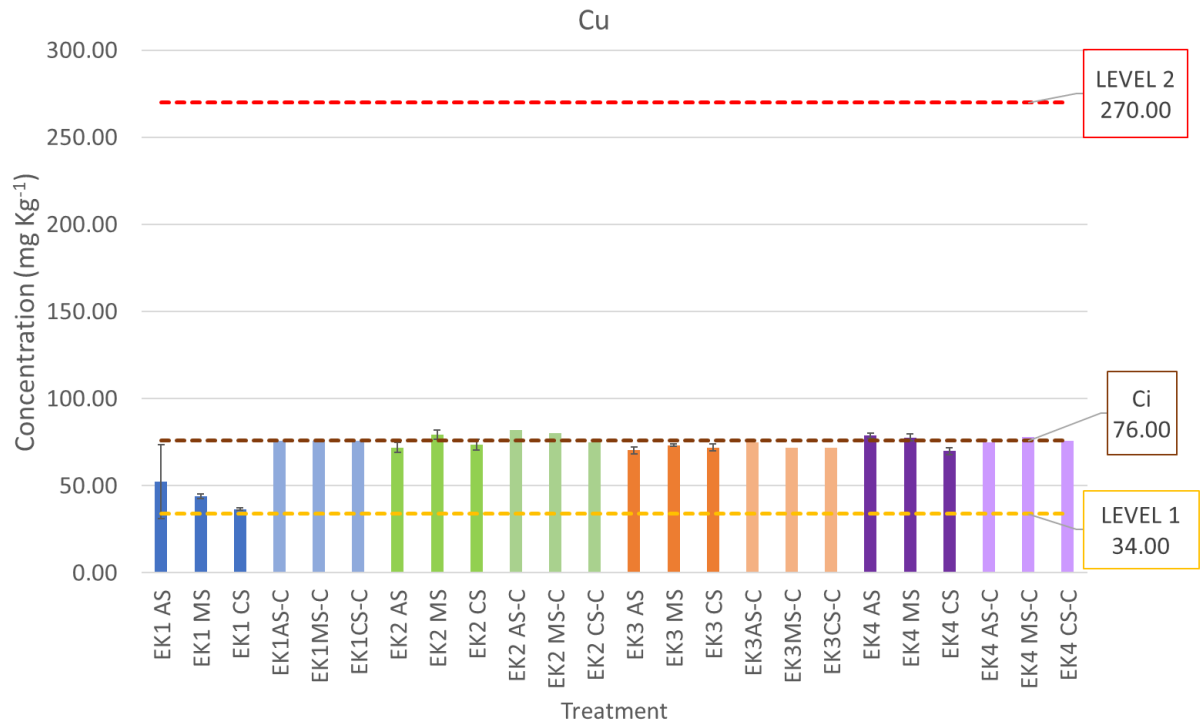


Figure 47 - Copper concentration at the end of electrokinetic treatments
Created by author

Figure 48 displays the chromium concentration (mg kg^{-1}) measured in each section (anode, middle, cathode) of the treatment zones for all treatments and the control test. It also presents the initial chromium concentration and the level 1 limit set by CONAMA Resolution N° 454 of 2012.

EK1 treatment

The blue bars in Figure 48 show the chromium concentration distribution for EK1. Interestingly, the middle section exhibits the highest concentration (33.00 mg kg^{-1}), followed by the anode (27.00 mg kg^{-1}) and cathode sections (26.67 mg kg^{-1}). This pattern makes determining a clear direction of chromium transport difficult.

The lower pH in the anode section likely promotes chromium desorption from the sediment, allowing it to be transported towards the cathode by electro-osmosis or electromigration. Notably, all sections in the EK1 treatment were below the initial concentration (40.67 mg kg^{-1}).

The control results (light blue bars) show minimal change in concentration across all sections, indicating that water alone, without pH adjustments, is ineffective in removing chromium from the sediment.

EK2 treatment

EK2 treatment, shown by the green bars in Figure 48, reveals a rising chromium concentration towards the middle section. The anode section exhibits the lowest concentration (36.00 mg kg^{-1}), followed by the cathode section (40.33 mg kg^{-1}), and finally, the middle section with the highest concentration (42.67 mg kg^{-1}).

The control for EK2 (light green bars) shows a slight decrease in the cathode section compared to the others, but the change is minor. This suggests that EDTA, under these test conditions, may have had a limited effect on promoting chromium desorption.

EK3 treatment

EK3 treatment (orange bars in Figure 48) exhibits the highest chromium concentration in the middle section (40.33 mg kg^{-1}), with the anode and cathode sections showing lower levels (33.67 mg kg^{-1} and 36.67 mg kg^{-1} , respectively). Similar to EK1 and EK2, this distribution makes it difficult to determine the direction of transport. Importantly, no section exceeds the initial concentration of 40.66 mg kg^{-1} .

The control results (light orange bars) reveal slightly lower chromium concentrations in the cathode section compared to the anode and middle sections. However, these differences are minimal (around $5\text{-}6 \text{ mg kg}^{-1}$). This suggests that EDTA was ineffective in promoting significant chromium desorption or complexation under these test conditions.

EK4 treatment

EK4 treatment (purple bars in Figure 48) demonstrates that the anode and cathode sections exhibit chromium concentrations below the initial level: 35.33 mg kg^{-1} in the anode, 43.67 mg kg^{-1} in the middle, and 36.00 mg kg^{-1} in the cathode.

This aligns with Tsang & Hartley (2014), who found synthetic chelating agents to be more effective for metal extraction compared to natural humic substances. The control results (light purple bars) further supports this conclusion. The consistent chromium concentration across all sections in the control demonstrates that humic substances have minimal chromium desorption capacity under these test conditions.

Figure 48 highlights that all treatments and the initial concentration fall below the Level 1 limit of 81 mg kg^{-1} set by CONAMA Resolution N° 454 of

2012. This is noteworthy, but the concentrations in all treatments except EK1 are close to the initial concentration. It is likely that the pH conditions of the electrolytes were not sufficient to promote significant chromium desorption, and the presence of humic substances may have further interfered with the release of this potential toxic metal. Additionally, the consistent presence of the highest concentration in the middle section across all treatments makes it difficult to determine the direction of chromium transport.

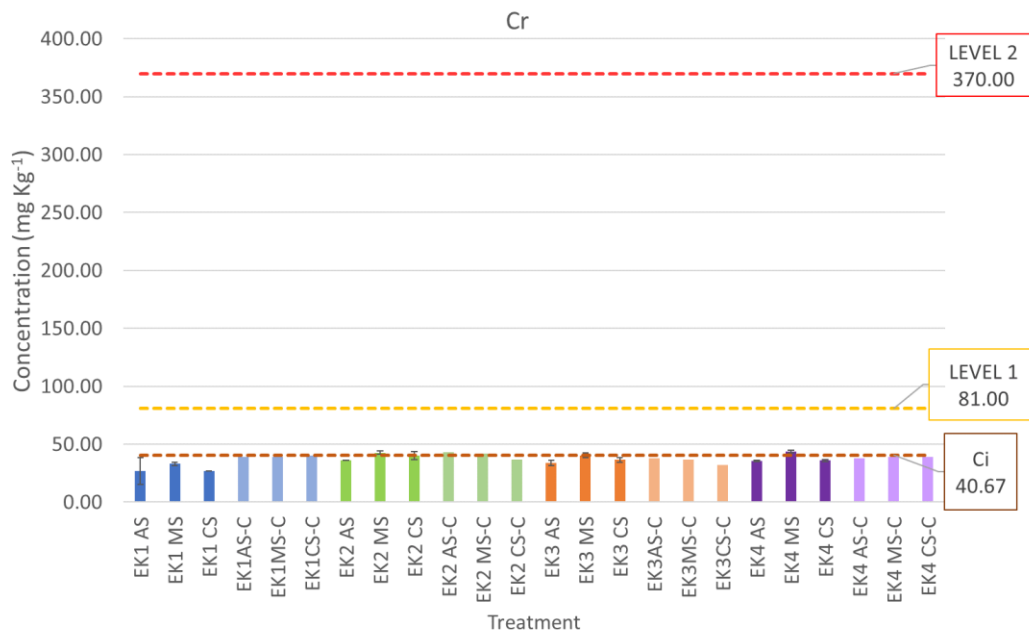


Figure 48 - Chromium concentration at the end of electrokinetic treatments
Created by author.

5.5.4. Electric current

The measured electrical current throughout the experiment differed between the treatments, as illustrated in Figure 49. Treatments EK1 and EK4 exhibited a distinct pattern. They began with low current readings, followed by a rapid rise to peak values (around 7.5 mA and 8.6 mA for EK1 and EK4, respectively). This initial spike in current likely corresponds to ions desorbing from the sediment, as observed by Song et al. (2016). Similar findings were reported by Kanbar et al. (2024), Garcia-Blas et al. (2022), and Song et al. (2016), who also linked this rise to sediment ion desorption.

Following this peak, the current in EK1 and EK4 decreased and stabilized. This suggests a depletion of readily available ions, possibly due to

the formation of electrically resistant compounds through precipitation, as suggested by Falciglia et al. (2017). This decrease aligns with the principles of electromigration and electro-osmosis, which explain the movement of ions away from the electrodes.

In contrast, treatments EK2 and EK3 displayed a unique "U-shaped" pattern in the first few hours. These treatments started with low current values, which then dipped even lower before rising again. This initial decrease might be due to factors specific to the electrolytes used in these treatments, potentially affecting the initial availability of ions for conduction. Masi et al. (2016) observed a similar trend when using EDTA as an electrolyte. Following this initial phase, the current behavior in EK2 and EK3 resembled that of EK1 and EK4, suggesting a similar process of ion depletion and current stabilization. As Maqbool & Jiang (2023) pointed out, the observed electrical current profile is indeed closely linked to ionic migration within the sediment.

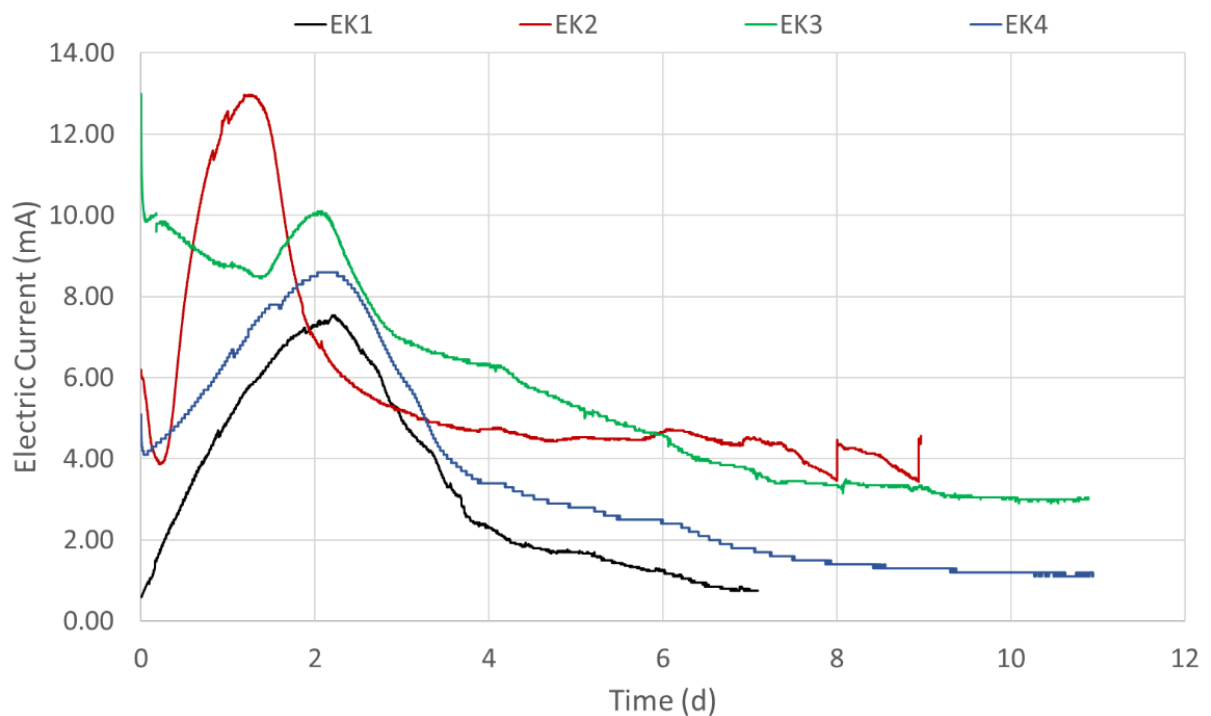


Figure 49 - Electric current variation in electrolytes during treatment
Created by author

The area under the graph of electric current (in mA) versus time (in days) represents the total electric charge that passed through the system. The integral of the current-time curves for all four treatments was calculated using Simpson's numerical integration method to determine the total electric charge passed. The electric charge was calculated over the 7-day period for all treatments.

The results are shown in Figure 50 to Figure 53. As the current is related to the transport processes of electromigration and electro-osmosis, a greater charge indicates greater transport within the sediment. It was observed that treatment EK3, which used a buffer solution as the electrolyte, exhibited the highest electric charge. This observation aligns with the findings of CASCUDO et al. (2022), who stated that a higher electric charge corresponds to greater transport.

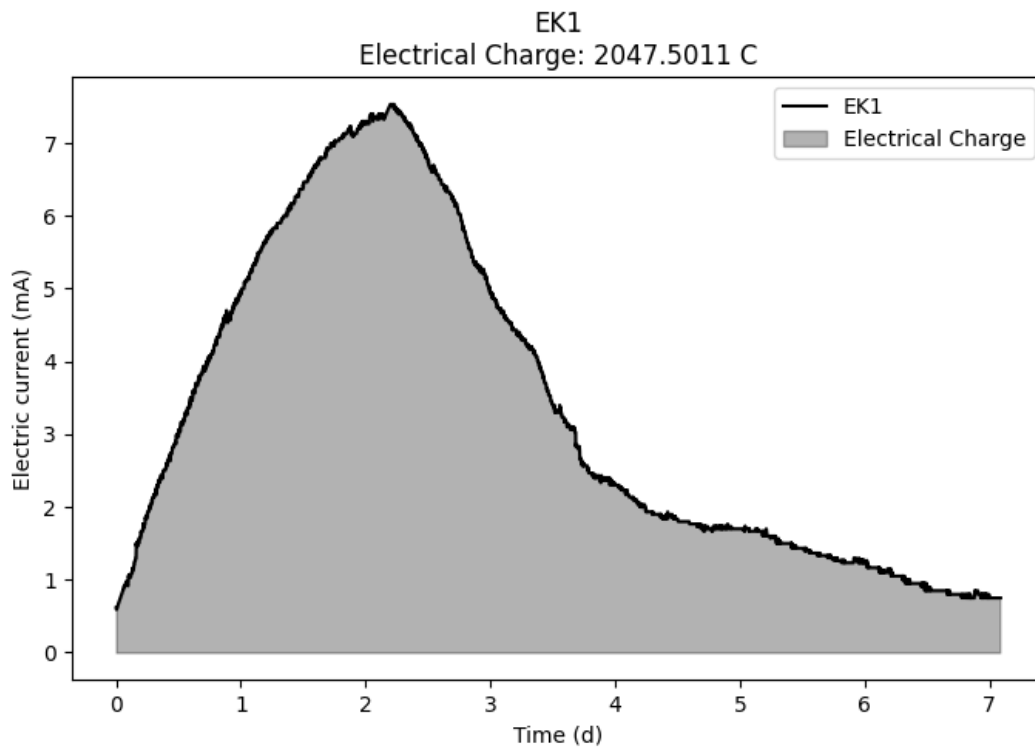


Figure 50 - The electrical charge for EK1
Created by author

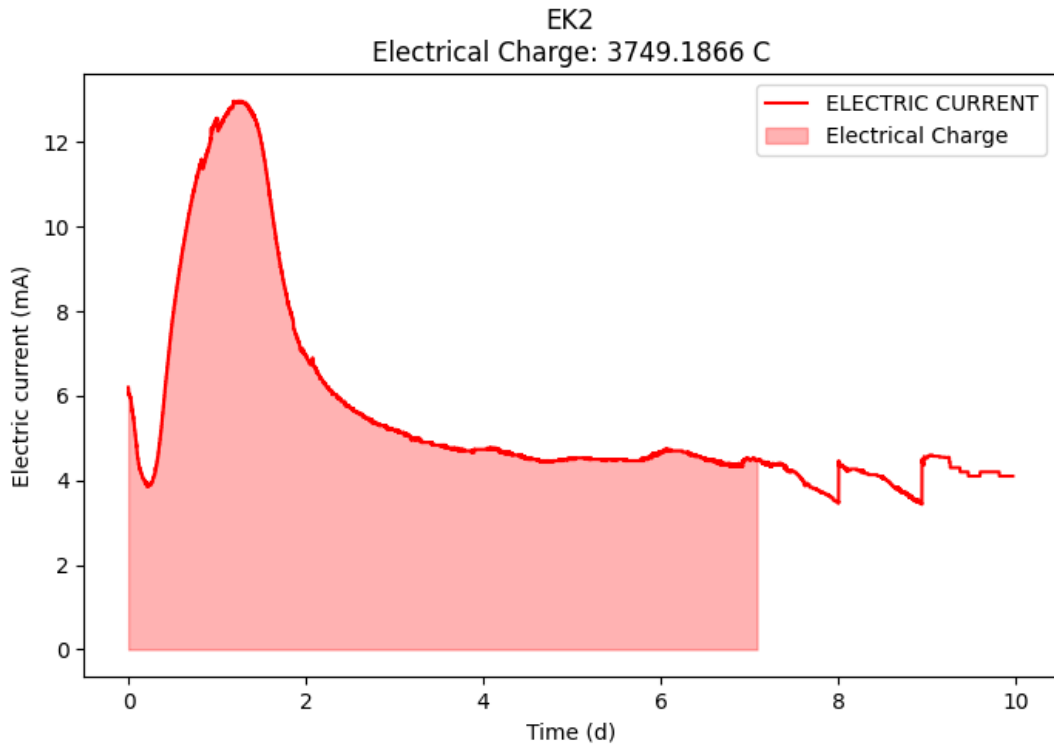


Figure 51 - The electrical charge for EK2
Created by author

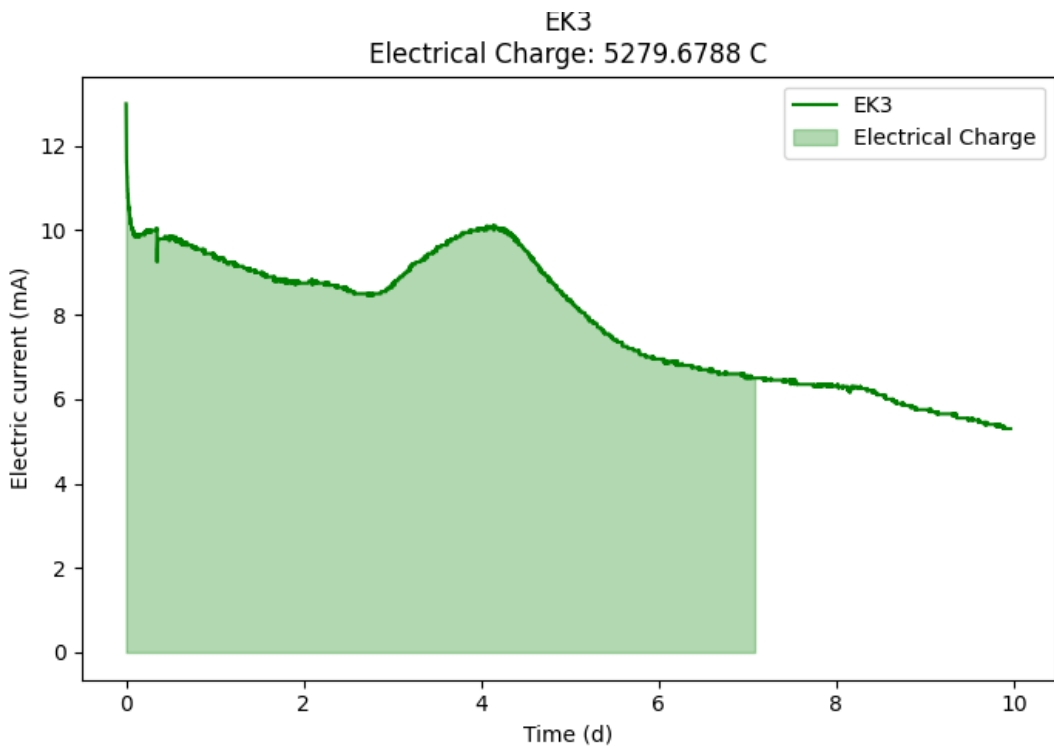


Figure 52 - The electrical charge for EK3
Created by author

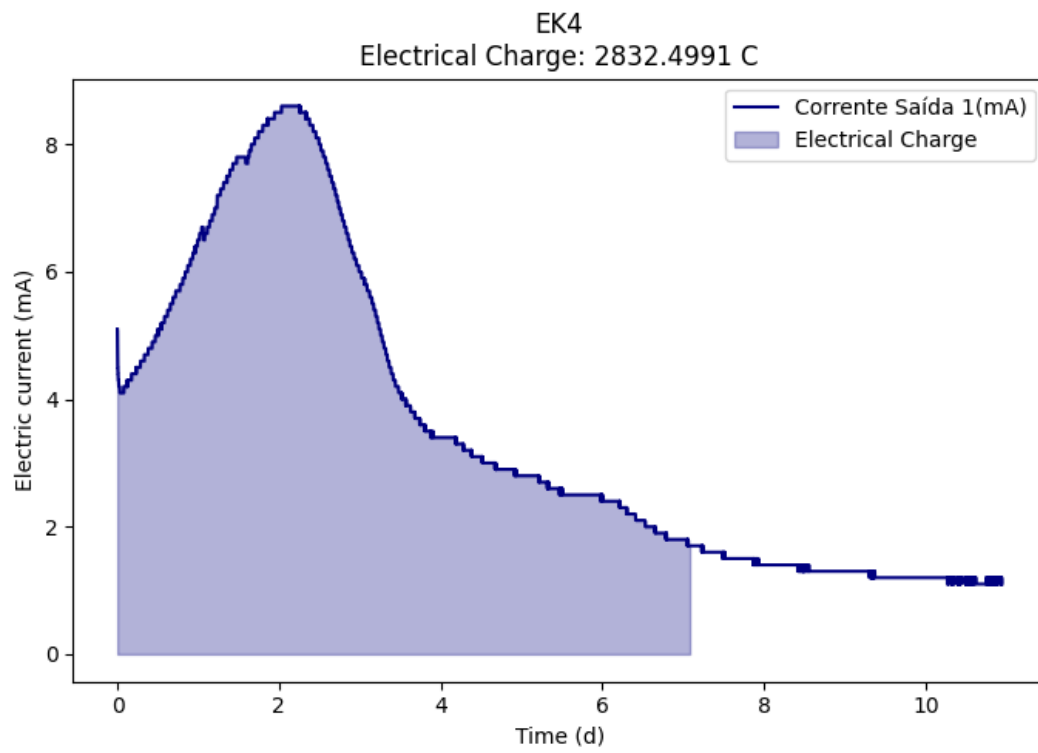


Figure 53 - The electrical charge for EK4
Created by author

6. Conclusions and recommendations for futures studies

6.1. Conclusions

- This study investigated the effectiveness of electrokinetic remediation with various electrolyte compositions for decontaminating sediments from Camorim Lagoon, Rio de Janeiro. While complexing agents (EDTA and humic substances) were expected to enhance the removal of zinc, nickel, lead, copper, and chromium, their effectiveness depended on the specific contaminant present in the dredged sediments, the pH, and the buffer capacity of the solution used.
- The EDTA used in treatments EK2 and EK3 promoted the removal of zinc and lead from the sediment. However, using a buffer as the anolyte also prevented the accumulation of these elements in the anode section. Thus, treatment EK3 resulted in a more uniform reduction in the potentially toxic element concentrations across the entire sediment sample. This suggests that pH affected the mobilization of these potentially toxic metals under the tested conditions.
- Interestingly, treatment EK1 (water) exhibited the lowest overall nickel concentration compared to other treatments, despite a tendency for nickel accumulation in the cathodic section. Likely the low pH near the anode promoted nickel desorption, facilitating transport via electromigration and electroosmosis.
- Under the employed conditions, complexing agents (EDTA and humic substances) were not effective in removing copper and chromium from the sediment. Water (EK1) resulted in the lowest concentration of these metals, suggesting that the high pH environment near the cathode likely induces the formation of soluble metal hydroxides. These charged species can then be transported more readily through the sediment by electromigration, a process driven by the electric field.

6.2. Recommendations for futures studies

- This work could be continued by testing other complexing agents to enhance the removal of copper and chromium from sediment.
- Long-term experiments should be conducted to verify the removal of potentially toxic elements over time and to allow for comparison with the results obtained in this work.
- The study area should be expanded to create a map of the concentration of potentially toxic elements in the Camorim Lagoon.
- Research should be conducted into the reuse of treated sediment in different engineering applications; one potential use could be in the fabrication of mortars

7. References

- ABNT NBR 6459. (2017). *NBR 6459: Determinação do limite de liquidez* (p. 4). www.abntcolecao.com.br
- ABNT NBR 7180. (2016). *NBR 7180: Determinação do limite de plasticidade* (p. 2). www.abntcolecao.com.br
- ABNT NBR 7181. (2016). *NBR 7181: Solo-Análise granulométrica* (p. 2). www.abntcolecao.com.br
- ABNT NBR 13600. (2022). *NBR 13600: Determinação do teor de matéria orgânica por quima a 440°C* (p. 9). www.abntcolecao.com.br
- Acar, Y. B., & Alshawabkeh, A. N. (1993). Principles of electrokinetic remediation. *Environmental Science & Technology*, 27(13), 2638–2647. <https://doi.org/10.1021/es00049a002>
- Agostini, F., Skoczylas, F., & Lafhaj, Z. (2007). About a possible valorisation in cementitious materials of polluted sediments after treatment. *Cement and Concrete Composites*, 29(4), 270–278. <https://doi.org/10.1016/j.cemconcomp.2006.11.012>
- Akcil, A., Erust, C., Ozdemiroglu, S., Fonti, V., & Beolchini, F. (2015). A review of approaches and techniques used in aquatic contaminated sediments: metal removal and stabilization by chemical and biotechnological processes. *Journal of Cleaner Production*, 86, 24–36. <https://doi.org/10.1016/j.jclepro.2014.08.009>
- Almeida, M. S. S., Borma, L. D. S., & Barbosa, M. C. (2001a). Land disposal of river and lagoon dredged sediments. *Engineering Geology*, 60(1–4), 21–30. [https://doi.org/10.1016/S0013-7952\(00\)00085-5](https://doi.org/10.1016/S0013-7952(00)00085-5)
- Almeida, M. S. S., Borma, L. S., & Barbosa, M. C. (2001b). Land disposal of river and lagoon dredged sediments. *Engineering Geology*, 60(1–4), 21–30. [https://doi.org/10.1016/S0013-7952\(00\)00085-5](https://doi.org/10.1016/S0013-7952(00)00085-5)
- Alshawabkeh, A. N. (2009). Electrokinetic Soil Remediation: Challenges and Opportunities. *Separation Science and Technology*, 44(10), 2171–2187. <https://doi.org/10.1080/01496390902976681>
- Amar, M., Benzerzour, M., Kleib, J., & Abriak, N.-E. (2021). From dredged sediment to supplementary cementitious material: characterization, treatment, and reuse. *International Journal of Sediment Research*, 36(1), 92–109. <https://doi.org/10.1016/j.ijsrc.2020.06.002>

- Ammami, M. T., Song, Y., Benamar, A., Portet-Koltalo, F., & Wang, H. (2020). Electro-dewatering of dredged sediments by combined effects of mechanical and electrical processes: Influence of operating conditions. *Electrochimica Acta*, 353, 136462. <https://doi.org/10.1016/j.electacta.2020.136462>
- Araruna Júnior, J. T., Benedetti, P. E., Pires, P. J. M., & de Almeida, R. F. R. (2012). Sediments Quality Assessment of Jacarepaguá Lagoon: The Venue of the 2011 Rock in Rio. *CLEAN - Soil, Air, Water*, 40(9), 906–910. <https://doi.org/10.1002/clen.201100667>
- Arbai, S., Mohamed, Z., Mohamed, K., & Bakar, A. A. (2014). Electrokinetic Remediation to Remove Heavy Metal from Contaminated Soils Using Purging Solution. In R. Hassan, M. Yusoff, Z. Ismail, N. M. Amin, & M. A. Fadzil (Eds.), *InCIEC 2013* (Vol. 265, pp. 531–538). Springer Singapore. https://doi.org/10.1007/978-981-4585-02-6_46
- Asadollahfardi, G., Sarmadi, M. S., Rezaee, M., Khodadadi-Darban, A., Yazdani, M., & Paz-Garcia, J. M. (2021). Comparison of different extracting agents for the recovery of Pb and Zn through electrokinetic remediation of mine tailings. *Journal of Environmental Management*, 279(December 2020), 111728. <https://doi.org/10.1016/j.jenvman.2020.111728>
- ASTM. (2014). *Test Methods for Electrical Conductivity and Resistivity of Water* (Vol. 14, pp. 1–7). ASTM International. <https://doi.org/10.1520/D1125-14>
- ASTM. (2018). *Standard Test Methods for pH of Water* (D1293; pp. 1–10). <https://doi.org/10.1520/D1293-18.2>
- ASTM. (2019a). *Test Methods for Laboratory Determination of Water (Moisture) Content of Soil and Rock by Mass* (ASTM D2216-19; pp. 1–7). ASTM International. <https://doi.org/10.1520/D2216-19>
- ASTM. (2019b). *Test Methods for pH of Soils* (D 4973-19; pp. 1–6). ASTM International. <https://doi.org/10.1520/D4972-19>
- Azevedo, H. L., Monken, H. R., & Melo, V. P. (1988). Study of Heavy Metal Pollution in the Tributary Rivers of the Jacarepagua Lagoon, Rio de Janeiro State, Brazil, Through Sediment Analysis. In *Metals in Coastal Environments of Latin America* (pp. 21–29). Springer Berlin Heidelberg. https://doi.org/10.1007/978-3-642-71483-2_4
- Bahemmat, M., Farahbakhsh, M., & Kianirad, M. (2016). Humic substances-enhanced electroremediation of heavy metals contaminated soil. *Journal of Hazardous Materials*, 312, 307–318. <https://doi.org/10.1016/j.jhazmat.2016.03.038>

- Barcellos, D., Queiroz, H. M., Nóbrega, G. N., de Oliveira Filho, R. L., Santaella, S. T., Otero, X. L., & Ferreira, T. O. (2019). Phosphorus enriched effluents increase eutrophication risks for mangrove systems in northeastern Brazil. *Marine Pollution Bulletin*, 142(January), 58–63. <https://doi.org/10.1016/j.marpolbul.2019.03.031>
- Bauddh, K., Singh, B., & Korstad, J. (2017). Phytoremediation Potential of Bioenergy Plants. In K. Bauddh, B. Singh, & J. Korstad (Eds.), *Phytoremediation Potential of Bioenergy Plants*. Springer Singapore. <https://doi.org/10.1007/978-981-10-3084-0>
- Beddaa, H., Ouazi, I., Ben Fraj, A., Lavergne, F., & Torrenti, J.-M. (2020). Reuse potential of dredged river sediments in concrete: Effect of sediment variability. *Journal of Cleaner Production*, 265, 121665. <https://doi.org/10.1016/j.jclepro.2020.121665>
- Benedetti, P. E. (2011). *Caracterização Geoambiental dos Sedimentos da Lagoa de Jacarepaguá - RJ*. Pontifícia Universidade Católica do Rio de Janeiro.
- Beyrami, H. (2021). Effect of different treatments on electrokinetic remediation of Zn, Pb and Cd from a contaminated calcareous soil. *Chinese Journal of Chemical Engineering*, 38, 255–265. <https://doi.org/10.1016/j.cjche.2020.09.011>
- Borma, L. D. S., Ehrlich, M., & Barbosa, M. C. (2003). Acidification and release of heavy metals in dredged sediments. *Canadian Geotechnical Journal*, 40(6), 1154–1163. <https://doi.org/10.1139/t03-062>
- Bortali, M., Rabouli, M., Yessari, M., & Hajjaji, A. (2023). Assessment of harbor sediment contamination for a path to valorize dredged material. *Arabian Journal of Chemistry*, 16(11), 105208. <https://doi.org/10.1016/j.arabjc.2023.105208>
- Božič, M., Žibret, L., Kvočka, D., Pranjić, A. M., Gregorc, B., & Ducman, V. (2023). Drava river sediment in clay brick production: Characterization, properties, and environmental performance. *Journal of Building Engineering*, 71, 106470. <https://doi.org/10.1016/j.jobbe.2023.106470>
- CASCUDO, O., LOPES, R. C., & OLIVEIRA, A. M. de. (2022). Métodos de transporte de cloretos em concreto uma análise crítica e comparativa. *CONCRETO & Construções*, L(108), 53–59. <https://doi.org/10.4322/1809-7197.2022.108.0002>
- Cercato, M., & De Donno, G. (2020). Time-lapse monitoring of an electrokinetic soil remediation process through frequency-domain electrical

- measurements. *Journal of Applied Geophysics*, 175, 103980. <https://doi.org/10.1016/j.jappgeo.2020.103980>
- Çevikbilen, G., Başar, H. M., Karadoğan, Ü., Teymur, B., Dağlı, S., & Tolun, L. (2020). Assessment of the use of dredged marine materials in sanitary landfills: A case study from the Marmara sea. *Waste Management*, 113, 70–79. <https://doi.org/10.1016/j.wasman.2020.05.044>
- Chen, F., Li, X., Ma, J., Qu, J., Yang, Y., & Zhang, S. (2019). Remediation of soil co-contaminated with decabromodiphenyl ether (BDE-209) and copper by enhanced electrokinetics-persulfate process. *Journal of Hazardous Materials*, 369(January), 448–455. <https://doi.org/10.1016/j.jhazmat.2019.02.043>
- Chen, Y., Jiang, H., Li, Y., Liu, Y., Chen, Y., Chen, L., Luo, X., Tang, P., Yan, H., Zhao, M., Yuan, Y., & Hou, S. (2022). A critical review on EDTA washing in soil remediation for potentially toxic elements (PTEs) pollutants. *Reviews in Environmental Science and Bio/Technology*, 0123456789. <https://doi.org/10.1007/s11157-022-09613-4>
- Chen, Z., You, N., Chen, C., Jia, Z., Zhang, Z., & Zhang, Y. (2023). Observation of dissolution behavior of dredged sediment in NaOH-activated system to evaluate potential activity for precursor usage. *Composites Part B: Engineering*, 263, 110865. <https://doi.org/10.1016/j.compositesb.2023.110865>
- CONAMA. (2012). *RESOLUÇÃO CONAMA N° 454, DE 1° DE NOVEMBRO DE 2012*. (pp. 1–18).
- De Boodt, M. F., & Hayes, M. H. B. (1990). *Soil Colloids and Their Associations in Aggregates* (M. F. De Boodt, M. H. B. Hayes, A. Herbillon, E. B. A. De Strooper, & J. J. Tuck, Eds.; Vol. 214). Springer US. <https://doi.org/10.1007/978-1-4899-2611-1>
- de Magalhães, L., Noyma, N. P., Furtado, L. L., Mucci, M., van Oosterhout, F., Huszar, V. L. M., Marinho, M. M., & Lüring, M. (2017). Efficacy of Coagulants and Ballast Compounds in Removal of Cyanobacteria (*Microcystis*) from Water of the Tropical Lagoon Jacarepaguá (Rio de Janeiro, Brazil). *Estuaries and Coasts*, 40(1), 121–133. <https://doi.org/10.1007/s12237-016-0125-x>
- Detzner, H.-D., Hakstege, A. L., Hamer, K., & Pallemans, I. (2007). Overview on treatment and disposal options. In *Sustainable Management of Sediment Resources* (Vol. 2, pp. 59–67). [https://doi.org/10.1016/S1872-1990\(07\)80015-8](https://doi.org/10.1016/S1872-1990(07)80015-8)

- Dixit, A., Du, H., & Pang, S. D. (2021). Performance of mortar incorporating calcined marine clays with varying kaolinite content. *Journal of Cleaner Production*, 282. <https://doi.org/10.1016/j.jclepro.2020.124513>
- Eliche-Quesada, D., Calero-Rodríguez, A., Bonet-Martínez, E., Pérez-Villarejo, L., & Sánchez-Soto, P. J. (2021). Geopolymers made from metakaolin sources, partially replaced by Spanish clays and biomass bottom ash. *Journal of Building Engineering*, 40, 102761. <https://doi.org/10.1016/j.jobbe.2021.102761>
- Estabragh, A. R., Lahoori, M., Javadi, A. A., & Abdollahi, J. (2019). Effect of a surfactant on enhancing efficiency of the electrokinetic method in removing anthracene from a clay soil. *Journal of Environmental Chemical Engineering*, 7(5), 103298. <https://doi.org/10.1016/j.jece.2019.103298>
- Eykholt, G. R. (1997). Development of pore pressures by nonuniform electroosmosis in clays. *Journal of Hazardous Materials*, 55(1–3), 171–186. [https://doi.org/10.1016/S0304-3894\(97\)00022-8](https://doi.org/10.1016/S0304-3894(97)00022-8)
- Falciglia, P. P., Malarbì, D., Greco, V., & Vagliasindi, F. G. A. (2017). Surfactant and MGDA enhanced – Electrokinetic treatment for the simultaneous removal of mercury and PAHs from marine sediments. *Separation and Purification Technology*, 175, 330–339. <https://doi.org/10.1016/j.seppur.2016.11.046>
- Fernandes, H. M. (1997). Heavy metal distribution in sediments and ecological risk assessment: The role of diagenetic processes in reducing metal toxicity in bottom sediments. *Environmental Pollution*, 97(3), 317–325. [https://doi.org/10.1016/S0269-7491\(97\)00004-3](https://doi.org/10.1016/S0269-7491(97)00004-3)
- Fernandes, H. M., Bidone, E. D., Veiga, L. H. S., & Patchineelam, S. R. (1994). Heavy-metal pollution assessment in the coastal lagoons of Jacarepaguá, Rio de Janeiro, Brazil. *Environmental Pollution*, 85(3), 259–264. [https://doi.org/10.1016/0269-7491\(94\)90046-9](https://doi.org/10.1016/0269-7491(94)90046-9)
- Fernandez, R., Martirena, F., & Scrivener, K. L. (2011). The origin of the pozzolanic activity of calcined clay minerals: A comparison between kaolinite, illite and montmorillonite. *Cement and Concrete Research*, 41(1), 113–122. <https://doi.org/10.1016/j.cemconres.2010.09.013>
- Ferone, C., Liguori, B., Capasso, I., Colangelo, F., Cioffi, R., Cappelletto, E., & Di Maggio, R. (2015). Thermally treated clay sediments as geopolymer source material. *Applied Clay Science*, 107, 195–204. <https://doi.org/10.1016/j.clay.2015.01.027>

- Fu, R., Wen, D., Xia, X., Zhang, W., & Gu, Y. (2017). Electrokinetic remediation of chromium (Cr)-contaminated soil with citric acid (CA) and polyaspartic acid (PASP) as electrolytes. *Chemical Engineering Journal*, 316, 601–608. <https://doi.org/10.1016/j.cej.2017.01.092>
- FUNDAÇÃO COPPETEC-UFRJ. (1996). *Estudo da Contaminação e Disposição dos Rejeitos de Dragagem das Lagoas de Jacarepaguá, Camorim, Tijuca e Marapendí, na Cidade do Rio de Janeiro*.
- FUNDAÇÃO COPPETEC-UFRJ. (1998). *Estudo técnico para dragagem da lagoa da Tijuca e disposição dos seus rejeitos. Relatório III- Relatório descritivo apresentando os aspectos geotécnicos e de contaminação por metais pesados da disposição do sedimento em solo bem como conclusões e recomenda*.
- Garcia-Blas, N., Jimenez-Relinque, E., & Castellote, M. (2022). Surfactants in electrokinetic remediation of sediments to enhance the removal of metals. *Journal of Soils and Sediments*, 22(11), 2853–2864. <https://doi.org/10.1007/s11368-022-03299-5>
- GARVAN, F. L. (1964). Metal Chelates of Ethylenediaminetetraacetic Acid and Related Substances. In *Chelating Agents and Metal Chelates* (pp. 283–333). Elsevier. <https://doi.org/10.1016/B978-0-12-395499-2.50013-X>
- Gidakos, E., & Giannis, A. (2006). Chelate Agents Enhanced Electrokinetic Remediation for Removal Cadmium and Zinc by Conditioning Catholyte pH. *Water, Air, and Soil Pollution*, 172(1–4), 295–312. <https://doi.org/10.1007/s11270-006-9080-7>
- Gidudu, B., & Chirwa, E. M. N. (2020). The combined application of a high voltage, low electrode spacing, and biosurfactants enhances the bio-electrokinetic remediation of petroleum contaminated soil. *Journal of Cleaner Production*, 276, 122745. <https://doi.org/10.1016/j.jclepro.2020.122745>
- Gregolec, G., Roehl, K. E., & Czurda, K. (2005). Chapter 8 Electrokinetic techniques. In *Trace Metals and other Contaminants in the Environment* (Vol. 7, Issue C, pp. 183–209). Elsevier Masson SAS. [https://doi.org/10.1016/S0927-5215\(05\)80012-8](https://doi.org/10.1016/S0927-5215(05)80012-8)
- Hahladakis, J. N., Latsos, A., & Gidakos, E. (2016). Performance of electroremediation in real contaminated sediments using a big cell, periodic voltage and innovative surfactants. *Journal of Hazardous Materials*, 320, 376–385. <https://doi.org/10.1016/j.jhazmat.2016.08.003>
- Han, D., Wu, X., Li, R., Tang, X., Xiao, S., & Scholz, M. (2021). Critical Review of Electro-kinetic Remediation of Contaminated Soils and Sediments:

Mechanisms, Performances and Technologies. *Water, Air, & Soil Pollution*, 232(8), 335. <https://doi.org/10.1007/s11270-021-05182-4>

Hortellani, M. A., Sarkis, J. E. S., Abessa, D. M. S., & Sousa, E. C. P. M. (2008). Avaliação da contaminação por elementos metálicos dos sedimentos do Estuário Santos - São Vicente. *Química Nova*, 31(1), 10–19. <https://doi.org/10.1590/S0100-40422008000100003>

INEA. (2020). *Boletim De Qualidade Das Águas Da Região Hidrográfica II-Guandu Boletim De Qualidade Das Águas Da Região Hidrográfica II - Guandu (Cont .)* (Issue 3, p. 5). <http://www.inea.rj.gov.br/wp-content/uploads/2020/02/Boletim-IQA-RH-II-2020-N1.pdf>

International Organization for Standardization. (1994). *Soil quality- Determination of the specific electrical conductivity* (11265 ISO; pp. 1–8).

International Organization for Standardization. (2020). *Particle size analysis - Laser diffraction methods* (ISO 13320). International Standard published. <https://www.abntcolecao.com.br/pdfview/viewer.aspx?Q=Qmx1ZjdWb1lZdGNTNE83NlpPYjBCM0VJWFMyQm5BMTBJQkFJekduUVRPND0=>

Kanbar, H. J., Ammami, M.-T., & Benamar, A. (2024). Insights into processes and consequent metal(loid) behavior in dredged estuarine sediments upon electrokinetic treatment. *Environmental Challenges*, 15, 100880. <https://doi.org/10.1016/j.envc.2024.100880>

Kanbar, H. J., Zein-Eddin, A., Ammami, M.-T., & Benamar, A. (2023). Electrokinetic remediation of estuarine sediments using a large reactor: spatial variation of physicochemical, mineral, and chemical properties. *Environmental Science and Pollution Research*, 30(55), 117688–117705. <https://doi.org/10.1007/s11356-023-30271-8>

Kettle, S. F. A. (1996). *Physical Inorganic Chemistry* (Vol. 4, Issue 1). Springer Berlin Heidelberg. <https://doi.org/10.1007/978-3-662-25191-1>

Kim, K.-J., Kim, D.-H., Yoo, J.-C., & Baek, K. (2011). Electrokinetic extraction of heavy metals from dredged marine sediment. *Separation and Purification Technology*, 79(2), 164–169. <https://doi.org/10.1016/j.seppur.2011.02.010>

Król, A., Mizerna, K., & Bożym, M. (2020). An assessment of pH-dependent release and mobility of heavy metals from metallurgical slag. *Journal of Hazardous Materials*, 384(October 2019), 121502. <https://doi.org/10.1016/j.jhazmat.2019.121502>

Linares, C. F., González, W., Pérez, J., Ocanto, F., & Cardozo, X. (2013). Adsorción de urea y p-cresol mediante el uso de arcillas caolinitas

- venezolanas. *Avances En Química*, 8(2), 65–71.
www.saber.ula.ve/avancesenquimica
- Lockwood, D. J. (2012). *Electrophoretic Deposition of Nanomaterials* (J. H. Dickerson & A. R. Boccaccini, Eds.). Springer New York.
<https://doi.org/10.1007/978-1-4419-9730-2>
- Ma, Y., Li, X., Mao, H., Wang, B., & Wang, P. (2018). Remediation of hydrocarbon–heavy metal co-contaminated soil by electrokinetics combined with biostimulation. *Chemical Engineering Journal*, 353(April), 410–418.
<https://doi.org/10.1016/j.cej.2018.07.131>
- Madejová, J. (2003). FTIR techniques in clay mineral studies. *Vibrational Spectroscopy*, 31(1), 1–10. [https://doi.org/10.1016/S0924-2031\(02\)00065-6](https://doi.org/10.1016/S0924-2031(02)00065-6)
- Mankins, J. C. (2009). Technology readiness assessments: A retrospective. *Acta Astronautica*, 65(9–10), 1216–1223.
<https://doi.org/10.1016/j.actaastro.2009.03.058>
- Maqbool, T., & Jiang, D. (2023). Electrokinetic remediation leads to translocation of dissolved organic matter/nutrients and oxidation of aromatics and polysaccharides. *Science of the Total Environment*, 876.
<https://doi.org/10.1016/j.scitotenv.2023.162703>
- Masi, M. (2017). *Electrokinetic remediation of heavy metal-contaminated marine sediments: experiments and modelling* [University of Pisoa].
<https://doi.org/10.13131/unipi/etd/01122017-120456>
- Masi, M., Iannelli, R., & Losito, G. (2016). Ligand-enhanced electrokinetic remediation of metal-contaminated marine sediments with high acid buffering capacity. *Environmental Science and Pollution Research*, 23(11), 10566–10576. <https://doi.org/10.1007/s11356-015-5563-7>
- Masterplan. (2013). *Relatório Ambiental Simplificado das Obras de Recuperação Ambiental do Complexo Lagunar de Jacarepaguá Capítulo III – Diagnóstico Ambiental da Área de Influência*.
- Masterplan. (2015). *Estudo de Impacto Ambiental das Obras de prolongamento do enrocamento (molhe) existente na entrada do Canal da Joatinga e as melhorias da circulação hídrica do Complexo Lagunar de Jacarepaguá-IV Diagnóstico ambiental*.
- Mohamadi, S., Saeedi, M., & Mollahosseini, A. (2019). Enhanced electrokinetic remediation of mixed contaminants from a high buffering soil by focusing on mobility risk. *Journal of Environmental Chemical Engineering*, 7(6), 103470. <https://doi.org/10.1016/j.jece.2019.103470>

- Moura Ribeiro, N. (2019). *Prospecção tecnológica*. <http://www.profnit.org.br/pt/livros-profnit/>
- Osman, K. T. (2014). Soil degradation, conservation and remediation. In *Soil Degradation, Conservation and Remediation* (1st ed.). Springer Netherlands. <https://doi.org/10.1007/978-94-007-7590-9>
- Osman, K. T. (2018). Management of Soil Problems. In *Management of Soil Problems* (1st ed.). Springer International Publishing. <https://doi.org/10.1007/978-3-319-75527-4>
- Ottosen, L. M., Christensen, I. V., Rørig-Dalgård, I., Jensen, P. E., & Hansen, H. K. (2008). Utilization of electromigration in civil and environmental engineering—Processes, transport rates and matrix changes. *Journal of Environmental Science and Health, Part A*, 43(8), 795–809. <https://doi.org/10.1080/10934520801973949>
- Page, M. M., & Page, C. L. (2002). Electroremediation of Contaminated Soils. *Journal of Environmental Engineering*, 128(3), 208–219. [https://doi.org/10.1061/\(ASCE\)0733-9372\(2002\)128:3\(208\)](https://doi.org/10.1061/(ASCE)0733-9372(2002)128:3(208))
- Pal, D., & Hogland, W. (2022). An overview and assessment of the existing technological options for management and resource recovery from beach wrack and dredged sediments: An environmental and economic perspective. *Journal of Environmental Management*, 302(PA), 113971. <https://doi.org/10.1016/j.jenvman.2021.113971>
- Pansu, M., & Gautheyrou, J. (2007). *Handbook of Soil Analysis Mineralogical, Organic and Inorganic Methods* (Physical-Verlag, Ed.).
- Perminova, I. V., & Hatfield, K. (1993). Remediation Chemistry of Humic Substances: Theory and Implications for Technology. In *Use of Humic Substances to Remediate Polluted Environments: From Theory to Practice* (Vol. 49, Issue 5, pp. 3–36). Springer-Verlag. https://doi.org/10.1007/1-4020-3252-8_1
- Rahman, Z., Jagadheeswari, Mohan, A., Tharini, Selvendran, & Priya, S. (2021). Electrokinetic remediation: An innovation for heavy metal contamination in the soil environment. *Materials Today: Proceedings*, 37(Part 2), 2730–2734. <https://doi.org/10.1016/j.matpr.2020.08.541>
- Ramadan, B. S., Sari, G. L., Rosmalina, R. T., Effendi, A. J., & Hadrah. (2018). An overview of electrokinetic soil flushing and its effect on bioremediation of hydrocarbon contaminated soil. *Journal of Environmental Management*, 218, 309–321. <https://doi.org/10.1016/j.jenvman.2018.04.065>

- Reddy, K. R., & Cameselle, C. (2009). Electrochemical Remediation Technologies for Polluted Soils, Sediments and Groundwater. In K. R. Reddy & C. Cameselle (Eds.), *Journal of the Society of Mechanical Engineers* (Vol. 98, Issue 917). John Wiley & Sons, Inc. <https://doi.org/10.1002/9780470523650>
- Ribeiro, A. B., & Mateus, E. P. (2016). *Electrokinetics Across Disciplines and Continents* (A. B. Ribeiro, E. P. Mateus, & N. Couto, Eds.). Springer International Publishing. <https://doi.org/10.1007/978-3-319-20179-5>
- Rozas, F., & Castellote, M. (2012). Electrokinetic remediation of dredged sediments polluted with heavy metals with different enhancing electrolytes. *Electrochimica Acta*, 86, 102–109. <https://doi.org/10.1016/j.electacta.2012.03.068>
- Rulkens, W. (2005). Introduction to the Treatment of Polluted Sediments. *Reviews in Environmental Science and Bio/Technology*, 4(3), 213–221. <https://doi.org/10.1007/s11157-005-2167-6>
- Saini, A., Bekele, D. N., Chadalavada, S., Fang, C., & Naidu, R. (2020). A review of electrokinetically enhanced bioremediation technologies for PHs. *Journal of Environmental Sciences*, 88, 31–45. <https://doi.org/10.1016/j.jes.2019.08.010>
- Sapsford, D., Cleall, P., & Harbottle, M. (2017). In Situ Resource Recovery from Waste Repositories: Exploring the Potential for Mobilization and Capture of Metals from Anthropogenic Ores. *Journal of Sustainable Metallurgy*, 3(2), 375–392. <https://doi.org/10.1007/s40831-016-0102-4>
- Sharma, S., Tiwari, S., Hasan, A., Saxena, V., & Pandey, L. M. (2018). Recent advances in conventional and contemporary methods for remediation of heavy metal-contaminated soils. *3 Biotech*, 8(4), 216. <https://doi.org/10.1007/s13205-018-1237-8>
- Siegel, F. R. (2002). Heavy Metals Mobility / Immobility. In *Environmental Geochemistry of Potentially Toxic Metals* (pp. 45–59).
- Song, Y., Ammami, M.-T., Benamar, A., Mezazigh, S., & Wang, H. (2016). Effect of EDTA, EDDS, NTA and citric acid on electrokinetic remediation of As, Cd, Cr, Cu, Ni, Pb and Zn contaminated dredged marine sediment. *Environmental Science and Pollution Research*, 23(11), 10577–10586. <https://doi.org/10.1007/s11356-015-5966-5>
- SONG, Y., BENAMAR, A., MEZAZIGH, S., & WANG, H. (2018). Citric Acid-Enhanced Electroremediation of Toxic Metal-Contaminated Dredged Sediments: Effect of Open/Closed Orifice Condition, Electric Potential and

- Surfactant. *Pedosphere*, 28(1), 35–43. [https://doi.org/10.1016/S1002-0160\(18\)60003-7](https://doi.org/10.1016/S1002-0160(18)60003-7)
- Souri, A., Kazemi-Kamyab, H., Snellings, R., Naghizadeh, R., Golestani-Fard, F., & Scrivener, K. (2015). Pozzolanic activity of mechanochemically and thermally activated kaolins in cement. *Cement and Concrete Research*, 77, 47–59. <https://doi.org/10.1016/j.cemconres.2015.04.017>
- Stevenson, F. J. (1994). *Humus Chemistry: Genesis, Composition, Reactions* (2 nd). John Wiley & Sons.
- Tang, J., He, J., Tang, H., Wang, H., Sima, W., Liang, C., & Qiu, Z. (2020). Heavy metal removal effectiveness, flow direction and speciation variations in the sludge during the biosurfactant-enhanced electrokinetic remediation. *Separation and Purification Technology*, 246(February), 116918. <https://doi.org/10.1016/j.seppur.2020.116918>
- Teixeira, M., Cesar, R., Abessa, D., Siqueira, C., Lourenço, R., Vezzone, M., Fernandes, Y., Koifman, G., Perina, F. C., Meigikos dos Anjos, R., Polivanov, H., & Castilhos, Z. (2022). Ecological risk assessment of metal and hydrocarbon pollution in sediments from an urban tropical estuary: Tijuca lagoon (Rio de Janeiro, Brazil). *Environmental Science and Pollution Research*, 0123456789. <https://doi.org/10.1007/s11356-022-22214-6>
- Tian, Y., Boulangé-Lecomte, C., Benamar, A., Giusti-Petrucciani, N., Dufлот, A., Olivier, S., Frederick, C., Forget-Leray, J., & Portet-Koltalo, F. (2017). Application of a crustacean bioassay to evaluate a multi-contaminated (metal, PAH, PCB) harbor sediment before and after electrokinetic remediation using eco-friendly enhancing agents. *Science of The Total Environment*, 607–608, 944–953. <https://doi.org/10.1016/j.scitotenv.2017.07.094>
- Touhami, K., Chihaoui, R., Nefoussi, A. M., & Mouli, M. (2024). Investigation of the potential use of dredged dam sediments as supplementary cementitious materials. *Construction and Building Materials*, 422, 135730. <https://doi.org/10.1016/j.conbuildmat.2024.135730>
- Viadero, R. C., Reed, B. E., Berg, M., & Ramsey, J. (1998). A Laboratory-Scale Study of Applied Voltage on the Electrokinetic Separation of Lead from Soils. *Separation Science and Technology*, 33(12), 1833–1859. <https://doi.org/10.1080/01496399808545908>
- Virkutyte, J., Sillanpää, M., & Latostenmaa, P. (2002). Electrokinetic soil remediation — critical overview. *Science of The Total Environment*, 289(1–3), 97–121. [https://doi.org/10.1016/S0048-9697\(01\)01027-0](https://doi.org/10.1016/S0048-9697(01)01027-0)

- Wang, Y., Li, A., & Cui, C. (2021). Remediation of heavy metal-contaminated soils by electrokinetic technology: Mechanisms and applicability. *Chemosphere*, 265(xxxx), 129071. <https://doi.org/10.1016/j.chemosphere.2020.129071>
- Wen, R., Yang, X., He, S., Wu, J., Ge, H., Chi, Z., Shi, Y., Wang, S., Gerson, A. R., & Pi, K. (2023). Enhanced washing of cadmium and lead from polluted river sediment using horizontal electroosmosis. *Journal of Environmental Chemical Engineering*, 11(1), 109157. <https://doi.org/10.1016/j.jece.2022.109157>
- Yeung, A. T., & Gu, Y.-Y. (2011). A review on techniques to enhance electrochemical remediation of contaminated soils. *Journal of Hazardous Materials*, 195, 11–29. <https://doi.org/10.1016/j.jhazmat.2011.08.047>
- Zhang, K., Dai, Z., Zhang, W., Gao, Q., Dai, Y., Xia, F., & Zhang, X. (2021). EDTA-based adsorbents for the removal of metal ions in wastewater. *Coordination Chemistry Reviews*, 434, 213809. <https://doi.org/10.1016/j.ccr.2021.213809>
- Zheng, D., Liang, X., Cui, H., Tang, W., Liu, W., & Zhou, D. (2022). Study of performances and microstructures of mortar with calcined low-grade clay. *Construction and Building Materials*, 327. <https://doi.org/10.1016/j.conbuildmat.2022.126963>